VEHICLE LUNARIZATION STUDY

U.S. ARMY M-274 'MULE' VEHICLE

VOLUME-II

PART 2, APPENDIX

BY

DEPARTMENT of THE ARMY

OFFICE, CHIEF of ENGINEERS

ARMY MATERIEL COMMAND

FOR

NATIONAL AERONAUTICS and SPACE ADMINISTRATION

WASHINGTON, D.C.

APRIL 1966

VEHICLE LUNARIZATION STUDY

U.S. ARMY M-274 "MULE" VEHICLE

FINAL REPORT

VOLUME II

PART 2 - APPENDIX

Prepared By

DEPARTMENT OF THE ARMY
Office, Chief of Engineers

and

Army Materiel Command

Prepared For

National Aeronautics and Space Administration
Office of Manned Space Flight
Washington, D.C.

April 1966

PREFACE

This is the final report of a study conducted for the purpose of determining if it would be feasible to modify a current military cargo type vehicle to operate in the lunar environment with a reasonable degree of confidence.

The study was requested by the Office of Manned Space Flight, National Aeronautics and Space Administration and was conducted by personnel from the Office of the Chief of Engineers; Headquarters, Army Materiel Command; Army Automotive Tank Center; and Engineer Research and Development Laboratories.

The military vehicle selected for modification analysis was the Army M-274 vehicle which is a 4 x 4, 1/2 ton, weapons carrier. This versatile vehicle is known more commonly as the "Mule". This vehicle was subjected to three orders of modification. The first modification was the minimum changes necessary to provide a modified vehicle having a capability consistent with the study criteria and at minimum cost. The second and third modifications were made to provide for comparison modified vehicles with increased capability for lunar surface mobility.

The Report is presented in two volumes, Volumes I and II. Volume II consists of two parts. Part I consists of the technical discussions concerned with vehicle modifications, development program schedules and cost estimates. Part 2 consists of study criteria and supplementary material developed to assist in the details of vehicle modification. Volume I is a separate summary which presents in less detail the material contained in Volume II - Part 1.

CONTENTS

VOLUME I - SUMMARY

VOLUME II - Part 1, TECHNICAL DISCUSSION

CONTENTS (Cont'd)

CONTENTS (Cont'd)

CONTENTS (Cont'd)

CONTENTS (Cont'd)

VOLUME II - Part 2, APPENDIX

CONTENTS (Cont'd)

CONTENTS (Cont'd)

CONTENTS (Cont'd)

CONTENTS (Cont'd)

Page Intentionally Left Blank

ILLUSTRATIONS

VOL. II - PART 1, TECHNICAL DISCUSSION

ILLUSTRATIONS (Cont'd)

ILLUSTRATIONS (Cont'd)

ILLUSTRATIONS (Cont'd)

ILLUSTRATIONS (Cont'd)

Page Intentionally Left Blank

Page Intentionally Left Blank

TABLES

PART 1 - TECHNICAL DISCUSSION

PART 2 - APPENDIX

TABLES (Cont'd)

APPENDIX 1.0
STUDY GUIDELINES AND CONSTRAINTS

1.0 STUDY GUIDELINES AND CONSTRAINTS

1.1 Apollo Applications Program System Configurations

The Apollo Applications Program (AAP) system includes three basic vehicle classes: the launch vehicle, the spacecraft Command and Service Modules (CSM) and derivatives of the Lunar Excursion Module (LEM).

1.1.1 Saturn V Launch Vehicle

The Saturn V launch vehicle shown in Figure 1-1 will be capable of placing a payload of about 43,000 Kg (95,000 lbs) into an earth-moon trajectory. Its payload capability for synchronous earth orbits is about 26,000 KG (57,250 lbs) at 0° inclination. The Saturn V has three propulsive stages - the S-IC, the S-II and the S-IVB - and an Instrument Unit. Each propulsive stage has its own instrumentation and safety systems, and receives guidance and control commands from the Instrument Unit (IU).

The S-IC stage is powered by five F-1 engines, burning liquid oxygen and RP-1 (kerosene) fuel to provide a nominal sea-level thrust of thirty-three million newtons (7.5 million pounds). The S-II stage is powered by five J-2 engines, burning liquid oxygen and liquid hydrogen to provide a thrust of four and one half million newtons (1,000,000 lbs) in vacuo.

The IU is a three segment, cylindrical, unpressurized structure, which houses the instrumentation concerned with vehicle performance from liftoff to insertion of the S-IVB/IU and spacecraft into earth orbit.

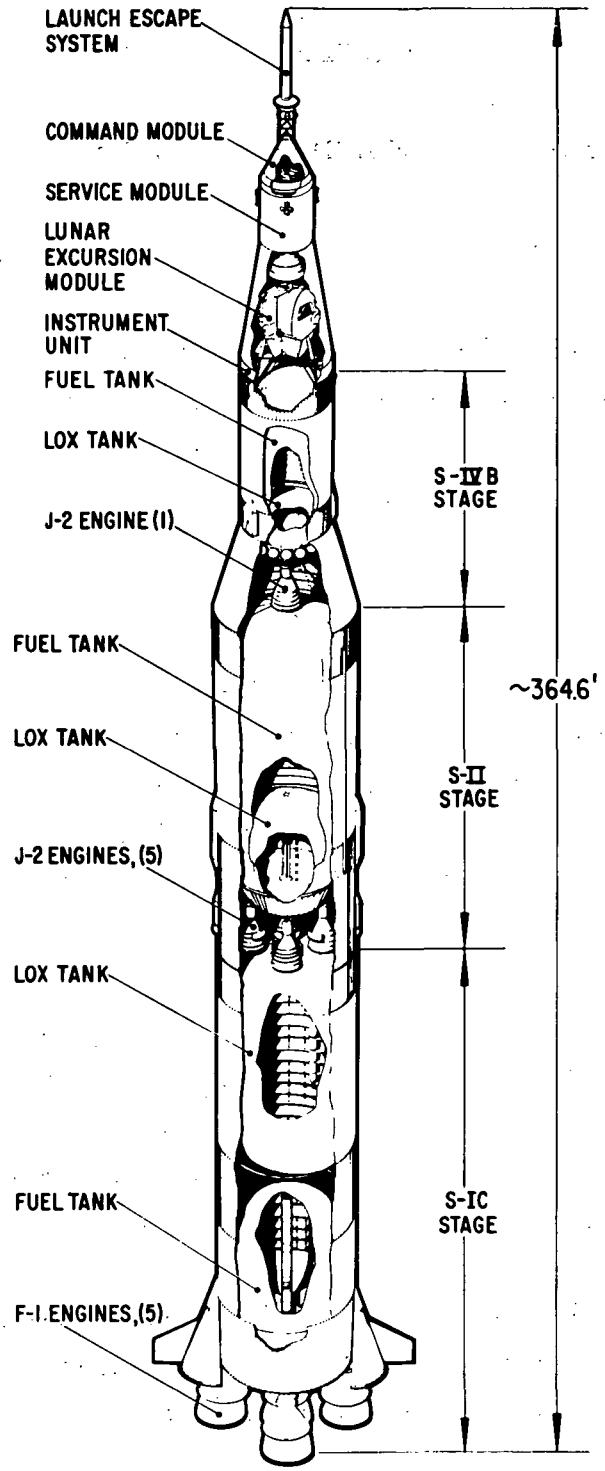

Figure 1-1. Apollo Program Saturn V Transportation System

The AAP configuration provides the capability of a second burn for the S-IVB stage and extends vehicle performance functions of the IU through both the second burn and the spacecraft transposition phase immediately following.

1.1.2 Spacecraft

The spacecraft for the Apollo Application Program will consist initially of the basic Apollo Spacecraft. Subsequently, it may consist of an extended Command and Service Module (XCSM) and one of several possible Lunar Excursion Module (LEM) derivatives, as described separately.

1.1.2.1 Extended CSM. The extended CSM is that developed for the Apollo lunar landing mission and modified to provide for extended duration missions. The modifications are primarily in the Service Module.

1.1.2.1.1 Command Module—The Command Module (CM) will contain crew support systems, displays, control equipment requiring direct access by the crew, and all systems needed for earth entry and landing. The CM is divided into three basic compartments: (1) the crew compartment, (2) the forward compartment, and (3) the aft compartment.

The crew compartment, which comprises the major portion of the CM, is a 345 millibar, oxygen pressurized (5 psia), three-man cabin that maintains a habitable environment for the crew during space flights. It contains spacecraft controls and displays, observations windows, food, water, sanitation, and survival equipment.

The forward compartment is located at the apex of the conical shaped crew module. This compartment is unpressurized, and the center portion is occupied by a 76 cm (30 inch) diameter tunnel to permit the crew to debark from the spacecraft during flight. The major portion of the remaining area is occupied by the earth-landing system.

The aft compartment is an area located around the lower rim of the conic body. This area also is unpressurized and not accessible to the crew. It contains the reaction control motors, impact attenuation equipment, instrumentation and consumable storage.

The exterior of the Command Module is designed to provide shielding against the heat of reentry. The ablative covering varies from 4.35 cm (1.71 inch) in regions of high heat load to 84 mm (0.33 inch) in low heat load regions.

1.1.2.1.2 Service Module—The Service Module (SM) is an unmanned, unpressurized vehicle which contains stores and systems which do not require direct crew accessibility. This module contains the propulsion utilized for midcourse correction and for insertion into and from lunar orbit, fuel cells which provides spacecraft power, radiators for spacecraft cooling, and oxygen and hydrogen supplies. The SM remains attached to the CM throughout the space flight; however, it is separated from the CM just prior to earth reentry and is not recovered.

The modifications in the SM can provide for additional fuel cells and cryogenic storage in the electrical power system and for additional reactants for attitude stabilization.

1.1.3 LEM Derivatives

LEM derivatives and modifications of the basic LEM as developed for the extended Apollo manned lunar landing mission. The basic LEM is described below, followed by a discussion of its principal derivatives.

1.1.3.1 Basic LEM. The basic LEM is designed to carry two men and the required equipment from lunar orbit to the lunar surface, to provide support for the astronauts while on the lunar surface, and to return the men and lunar samples

to the CSM in lunar orbit. It consists of two stages: (1) the descent stage, which provides the braking and hover capability needed for landing, and (2) the ascent stage for return to lunar orbit.

The descent stage is the unmanned portion of the LEM. It consists of that equipment necessary for landing on the lunar surface and serves as a platform for launching the ascent stage after completion of the lunar stay. The landing gear is attached externally to it.

The ascent stage houses the two crewmen during lunar operations. It provides a pressurized oxygen environment, food, water, communications equipment, and environmental control for the crew for a period up to 45 hours. It has the necessary propulsion and guidance to return the crew from the lunar surface to rendezvous in lunar orbit with the CSM. It remains in lunar orbit, when the CSM departs from it for the return to earth.

1.1.3.2 LEM-Taxi. The LEM-Taxi is a modified basic LEM vehicle, which is intended to deliver the crew to the LEM-Shelter for extended lunar surface missions. The Taxi must wait in a quiescent mode until the crew is ready to return, and then transport them into orbit for rendezvous with the XCSM.

The mass difference between the LEM-Taxi and changes to the basic LEM are relatively minor, and result from the removal of scientific equipment and TV, and the addition of meteoroid shielding and insulation.

1.1.3.3 LEM/Shelter. The LEM/Shelter (LEM/S) is a derivative of the LEM that provides living and working accommodations for astronauts during lunar surface missions. It is intended to be delivered into lunar orbit as in a normal Apollo mission, then to be landed unmanned on the lunar surface. It must remain in a stored condition until the crew arrives a few weeks or months later. After

arrival, the crew is intended to transfer from the LEM-Taxi to the Shelter for periods up to 14 days. The Shelter will also contain equipment necessary for the lunar operations.

The descent stage of the basic LEM is unmodified, and the ascent stage is modified for unmanned landing, pre-usage storage, support of two men for 14 days, and delivery of experimental equipment. The major mass changes are the removal of ascent propulsion and the increase in the environmental control system and electrical power system capability.

1.2 Mission Definitions and Constraints

1.2.1 Overall Mission Definition

The overall mission for the AAP lunar surface exploration consists of three phases, lunar surface delivery, lunar surface operations, and the return to earth by the astronaut personnel, which are carried out in the steps as outlined below:

- Lunar Surface Delivery: The AAP lunar surface mission presently planned requires two separate spacecraft launch and delivery operations. For both operations the spacecraft are injected through an earth parking orbit into a lunar transfer trajectory by the Saturn V launch vehicle. Near the moon, the SM brakes the spacecraft into a lunar parking orbit. In the first delivery operation, the LEM/Shelter is delivered. After the LEM/Shelter separates from the CSM, the LEM/Shelter is remotely landed on the lunar surface and the CSM returns to earth. In the second delivery operation, the astronaut exploration team is delivered to the lunar surface. The LEM-Taxi separates from the CSM and lands while the CSM remains in lunar orbit. Up to ninety days delay might be incurred between the launchings.

- Lunar Surface Operations Phase: During the presently planned fourteen-day mission, the astronauts will operate out of the LEM/Shelter. Primary mission tasks will include exploration traverses and the deployment of scientific instrumentation. These tasks will be conducted at the shelter and on limited sorties away from the shelter using either a rolling or flying mobility device. At the end of the fourteen-day period, the astronauts will place the LEM/Shelter and support equipment in a dormant mode and return to the LEM-Taxi.
- Return to Earth: Rendezvous with the CSM is made using the LEM-Taxi ascent stage. The CSM is then used to return to an earth parking orbit orbit for a subsequent landing using the CM.

1.2.2 Mission Constraints

Though the total payload delivery capability of the LEM/Shelter depends primarily on the storage time required between its delivery and that of the astronauts in the LEM-Taxi, a nominal mass allowance of 1135 Kg (2,500 lbm) has been set for the mobility vehicle and scientific packages for mission planning purposes. Preliminary payload allocations of this total have been established that, provide for incorporation of scientific instrumentation and experiment support equipment, and up to 680 Kg (1,500 lb mass) for a mobility device to extend the radial effectiveness of the mission. This mobility device is the subject considered in this study. Specific mission constraints are as follows:

- The mass of the vehicle without cargo and operator, but fully fueled, will not be more than 680 Kg (1,500 lbm).
- The vehicle must be capable of carrying two astronauts, one as the vehicle operator, and the other as an alternate payload. This sets the minimum cargo mass at 145 Kg (320 lbm). A maximum cargo carrying capability of 320 Kg (704 lbm) is desired.
- The vehicle should be capable of speeds of at least 4.8 km/hr, 3 mph (statute) in level soft soils ($K\phi = 0.5$, $n = 0.5$) and 8 km/hr, 5 mph

(statute) on level compacted soils ($K\phi = 3$, $n = 1.00$), and must be capable of operation over as wide a range of lunar surface soil conditions as possible. As a minimum requirement, the mobility and power system must be sized such that the vehicle is capable of traversing slopes of up to 15 degrees with the soil characteristics ($K\phi$ and n) and frequency distribution as specified for that range in The Engineering Lunar Model Surface (ELMS).

- Operational sorties will be 6 hours in length. The Apollo Portable Life Support System (PLSS) will be used to furnish the astronaut with oxygen and water. For 3 to 4 hours, depending on metabolic demand, one PLSS will be required. To enable the astronaut to complete the sortie, a second PLSS must be carried in an accessible position on the vehicle.
- The operational radius of the vehicle will be limited to radio line-of-sight distance between the LEM/Shelter and the suited astronaut on the surface. For this study this radius has been established as 6 km. The linear traversing distance per sortie within this circular area will be a maximum of 24 km (15 miles). Total operational travel for a 14-day mission will be a maximum of 240 km (150 miles).
- The vehicle must be capable of operation at least during the lunar day (14 earth days time) in the lunar equatorial regions. Systems must be capable of withstanding the extremes of the space and lunar environment for at least 21 days (3 days transit and a minimum of 18 days for the combined storage and operational phase) but preferably for 107 days (3 days transit time, 90 days storage time, and 14 days operating time), to provide for the time lapse between launch operations.
- Vehicle reliability shall be 0.9 (80% confidence).

1.2.3 Design Constraints

In addition to the Mission Constraints which comprise the primary restraints on the design of a lunar surface mobility vehicle, based on the definition of the mission and consideration of other mission parameters such as human capabilities in protective garments, packaging, mission safety, et al, the following design constraints have been established.

1.2.3.1 Payload Packaging and Transport Design Constraints.

- The vehicle structure and systems shall be capable of resisting the loads (including vibration and acoustical) associated with the handling, transportation, launch, and cis-lunar transfer and an 8-g landing load of the vehicle; and also those associated with the operational use of the vehicle for a two-week period.
- The vehicle must be carried above the LEM/S descent stage between the shelter and adapter. Definitions of the payload volume, volume configuration and other factors are given in the following-listed NASA drawings and notes:
  (1) Dwg. No. SK 10-9004 - LEM Shelter Adapter Area - Free Volume - Payload Envelope. This 1/20th scale drawing shall serve as the basic guideline for defining space between the LEM/Shelter and surrounding hardware systems which is available for other payload elements.
  (2) Dwg. No. SK 10-9000 - General Arrangements - Lunar Excursion Module - Ascent Stage. This 1/20th scale drawing provides additional information on the physical size and description of the ascent stage.
  (3) Dwg. No. SK 10-90001 - Assembly Layout - Payload - Saturn V. This 1/40th scale drawing provides additional information on the entire area where a LEM/Shelter and associated payloads would be installed.
  (4) LED-280-10000 - LEM General Arrangement - (Additional information on LEM.)
  (5) LTM-280-25103 - Ascent Stage Structural Arrangement and LDW-280-21600 - Descent Stage Structural Arrangement - (Information on structure which may be useful in defining structural interfaces.)
  (6) SHE-LEM Mode A, sheets 1 and 2, and SHE-LEM Mode C, sheets 1 and 2 - (General information on two proposed revisions of LEM to provide a shelter. Mode A has more extensive modifications than Mode C.)

- The vehicle structure must include provisions for mounting on the LEM/Shelter and for attaching the system to a suitable off-loading mechanism.

1.2.3.2 Power System Design Constraints.

- The vehicle power system must furnish all power required on each sortie. Refueling or recharging of batteries from the LEM/Shelter system at the completion of each sortie is permissible; however, mass equivalents of fuel used for this purpose must be provided for from the maximum vehicle mass allowed (680 Kg).
- Power (thermal or electrical) required for thermal control of the vehicle and its systems during transit and storage will be furnished by the LEM/Shelter or an auxiliary power supply of the SNAP variety. Passive thermal control techniques will be used to the maximum extent possible.
- A central means for control and monitoring of all power generating, distribution, and control elements, and their functions (start-up, shut-down, system status, etc) will be included.

1.2.3.3 Bio-Engineering Design Constraints.

- All payload systems shall be compatible with the capabilities and limitations of the man/suit/PLSS combination - particularly with respect to dexterity limitations as defined in Table 1-1, and Figure 1-2.
- A single pressure-suited crewman shall be able to perform all essential functions associated with unloading, checkout, resupply, start-up, traveling, and maneuvering of the vehicle.
- The vehicle shall be designed to adequately accommodate a single pressure-suited crewman with additional space allotted for a second pressure-suited crewman. The anthropometric size and mass of the crewman will range between the 5th percentile, 59 kg (130 lb) mass to 95th percentile, 88.5 kg (195 lb) mass. Seating parameters are characterized in Figure 1-3.

TABLE 1-1

MAXIMUM PERFORMANCE REQUIREMENTS FOR THE ELEMENTARY BODY MOVEMENTS FOR INTRAVEHICULAR AND EXTRAVEHICULAR SUIT WEAR VENTED AND AT 255 MILLIBARS GAGE (3.7 psig)

Movements	Range of Movements (In Degrees)
A. NECK MOBILITY	
Flexion (forward-backward)	120
Flexion (left-right)	30
Rotation (abduction-adduction)	45
B. SHOULDER MOBILITY	
Adduction	45
Abduction	125
Laterial - Medial	150
Flexion	170
Extension	50
Rotation (X-Z Plane):	
Down-Up	150
Rotation (Y-Z Plane):	
Laterial Rotation	35
Medial Rotation	110
C. ELBOW MOBILITY	
Flexion - Extension	155
D. FOREARM MOBILITY	
Supination (palms up)	130
Pronation (palms down)	75
E. WRIST MOBILITY	
Flexion (adduction)	85
Extension (abduction)	65
Flexion (backward)	35
Extension (forward)	50
F. TRUNK - TORSO MOBILITY	
Trunk Rotation (abduction-adduction)	70
Torso Flexion (laterial - medial)	50
Torso Flexion (forward)	80
Torso Flexion (backward)	25

Table 1-1 (Cont'd)

Movements	Range of Movements (In Degrees)
G. HIP MOBILITY	
Abduction (leg straight)	45
Adduction (knee bent)	30
Abduction (knee bent)	35
Rotation (sitting): Lateral	30
Rotation (sitting): Medial	30
Flexion	115
Extension	35
H. KNEE MOBILITY	
Flexion (standing)	120
Rotation (medial)	35
Rotation (laterial)	35
Flexion (kneeling)	160
J. ANKLE MOBILITY	
Extension	40
Flexion	50
Abduction	30
Adduction	30

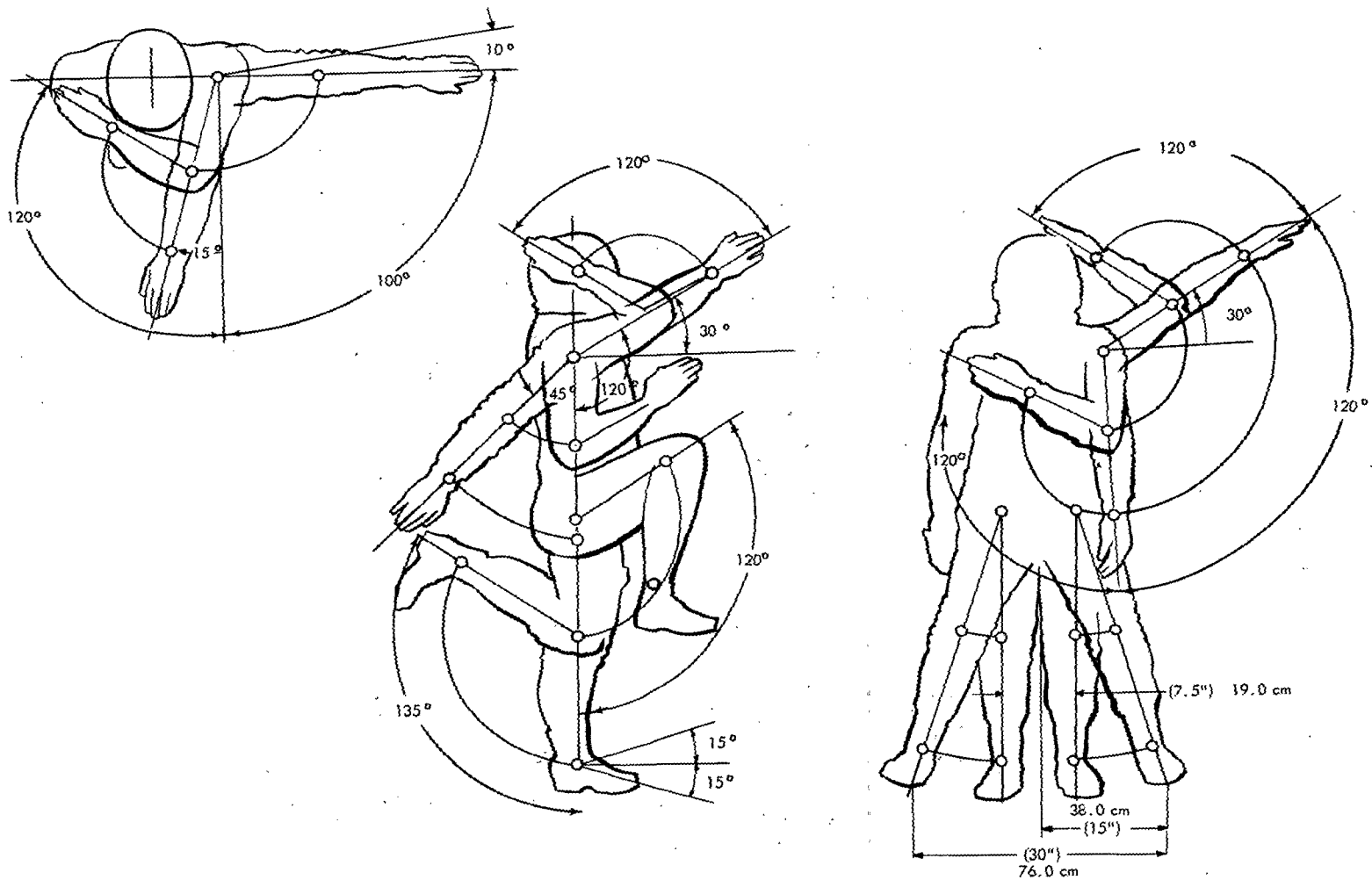

Figure 1-2. Space Suit Assembly Mobility

LIMITS FOR SEATED POSITIONS SHOWN FOR THE LUNAR SURFACE VEHICLE WITH MAN IN PRESSURE SUIT AT 240 MILLIBARS (3.5 PSI) AND CONTROL HANDLES 38 CM (15") FROM BODY CENTER-LINE

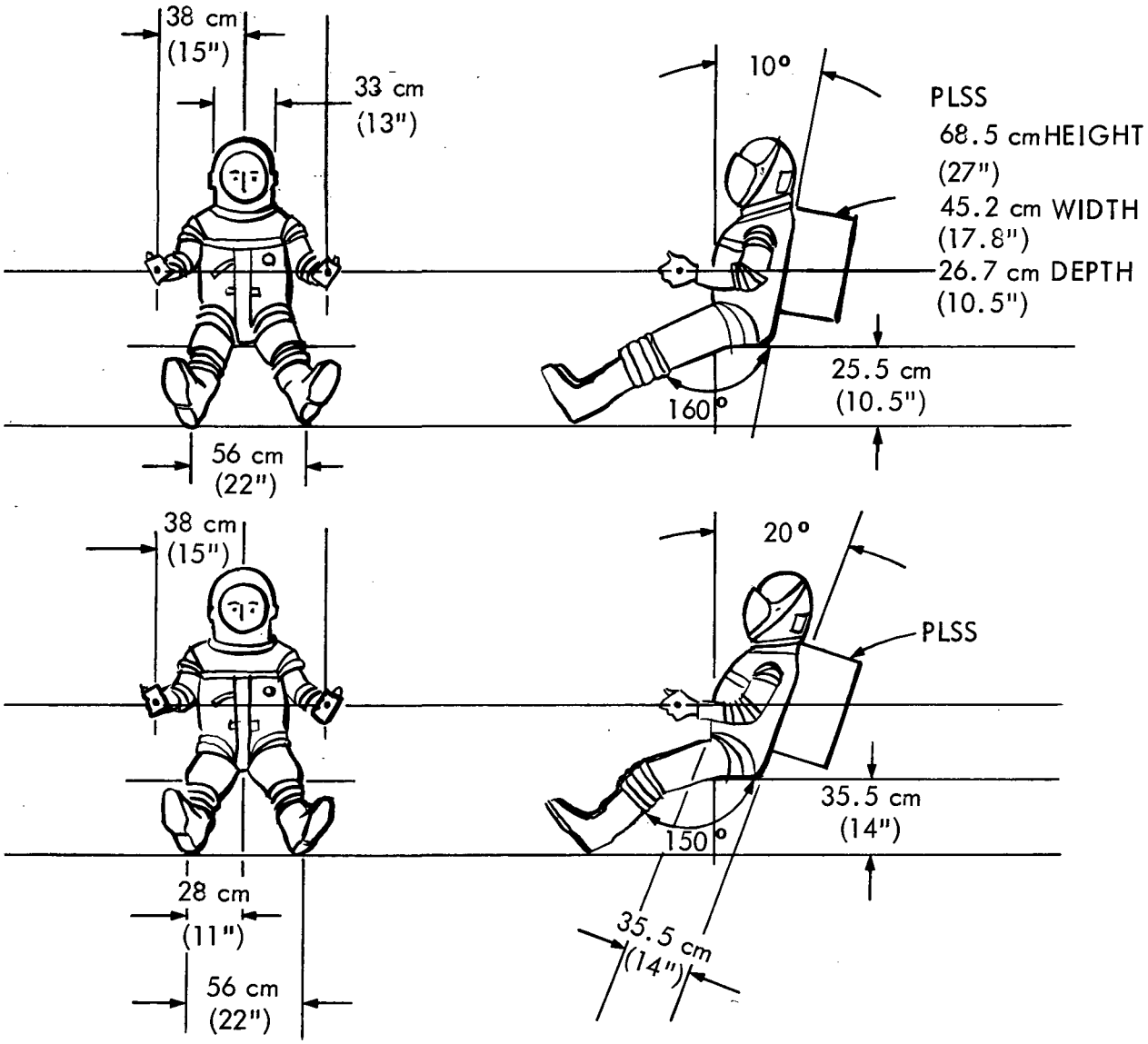

Figure 1-3. Crew Seat Dimensions for Lunar Surface Vehicle

- The vehicle will be designed to enable a single astronaut to load and unload cargo. In addition, it will be so designed as to permit easy boarding and dismounting by the suited astronaut.
- The vehicle will include a support and restraint system that will accommodate the crew when wearing a pressurized space suit and the portable life support system (PLSS), and will provide adequate protection against all anticipated acceleration vectors.
- The vehicle design must provide for protection of the crew against debris which may be thrown off by the locomotion system. A roll bar should be added to the vehicle to protect the crew in the event of vehicle roll-over, which shall not permit deep sinkage into soft soils.
- The PLSS will provide also for all communication facility and will have mass of 286 kg (63 lbs). The PLSS total metabolic support capacity is 1410 metabolic watt-hours (1215 kg cal or 4800 Btu). The normal metabolic support rate may vary between 352 metabolic watts (304 kg cal/m or 1200 Btu/hr) to 470 metabolic watts (404 kg cal/hour or 1600 Btu/hr). The PLSS in use may be stowed during vehicle operation immediately behind the seated operator. The spare PLSS must be stowed such that it is immediately available for use.
- The mass of the pressure suit, complete with PLSS, will be 57 kg (125 lbs), hence the maximum mass allowance for man with suit and PLSS will be 145 kg (320 lbs mass).

1.3 Lunar Environment

The environmental characteristics of the moon set out the fundamental constraints for any operation or item of equipment intended for application on the lunar surface. Insofar as this lunar surface mobility vehicle study is concerned, certain of these environmental characteristics are more significant than others. The more significant characteristics include essential lack of atmosphere and concommitant lack of attenuating properties with respect to thermal radiation, and the surface characteristics

which are so important to the assessment of vehicle mobility and the design of mobility systems. Other characteristics, such as high-energy particle bombardment and its biophysical effects, are by defintion of the study scope ignored. They are considered elsewhere in the NASA Apollo Applications Program, in the mission definition, and in the design of the astronauts' protective clothing and equipment. In this section, the environmental characteristics of the moon are defined, so as to establish a model of the environment.

1.3.1 Lunar Atmospheric Pressure

- The gas pressure at the surface of the moon is estimated to be less than 10^{-13} times the earth's mean sea level pressure of 1.01325 bars or therefore is $\simeq 1.01325 \times 10^{-8}$ newtons/m^2 (14.7×10^{-13} psi).
- There may be pockets of gases of molecular weight over 60, especially argon as a decay product from potassium, radon from uranium, and possibly, xenon from uranium^{238}.
- Density of the atmosphere - 10^{10} molecules/cm^3.
- Temporary local atmospheres might have higher densities.

1.3.2 Lunar Gravitational Acceleration

The acceleration of gravity on the lunar surface is 1.6241 m/sec^2(5.3283 ft/sec^2). The corresponding terrestrial value is 9.80665 m/sec^2 (32.174 ft/sec^2) or the lunar gravitational acceleration is about 1/6 of that experienced on earth.

1.3.3 Solar Electromagnetic Radiation at the Lunar Surface

The intensity of the solar radiation on the lunar surface varies as the square of the distance of the surface point of interest from the sun. At the mean earth orbital distance, this intensity is 1396 watts/m^2; however, values of 1400 watts/m^2 and 2.0 calories/cm^2 minute are generally accepted. This "solar constant" correlates to an apparent solar photosphere black body temperature of 5800°K. Because of

a band of ultraviolet radiation in the observed solar spectrum of greater intensity than indicated by a 5800°K black body spectral distriubtion curve, a black body temperature of 6000°K is generally assumed for evaluation or prediction of the solar spectral distribution. The actual spectral quality of solar radiation in space is still the subject of scientific conjecture. (Ref: Thekaehara, M.P., Survey of the Literature on the Solar Constant and the Spectral Distribution of the Solar Radiant Flux, NASA SP-74, Washington, D. C.) Use is made, generally, of the 6000°K black body curve for analysis of the solar spectral quality, to show:

Wave Length	Spectral Type	Percent of Total Radiated Power
Below 1,000 Å	Far ultraviolet and x-ray	10^{-4}
1,000 Å to 2,000 Å	Far ultraviolet	0.02
2,000 Å to 3,800 Å	Near ultraviolet	7.5
3,800 Å to 7,000 Å	Visible	41.5
7,000 Å to 10,000 Å	Short infrared	22.0
10,000 Å to 20,000 Å	Medium infrared	23.0
20,000 Å to 100,000 Å	Long infrared	6.0

X-Ray Flux

20 Å to 100 Å	6×10^{-8} watts/cm^2
8 Å to 20 Å	2×10^{-10} watts/cm^2
2 Å to 8 Å	5.5×10^{-11} watts/cm^2

During periods of solar activity, variation in x-ray flux of one or two orders of magnitude may occur.

1.3.3.1 Solar Illumination.

13.4 lumens/cm^2 or 1.34×10^5 lumens/m^2 at the lunar surface. The brightness of the sun is 200,000 candles/cm^2.

1.3.4 Earth's Radiation

This consists of the Earth's thermal radiation plus the Earth's albedo radiation. The amounts of energy from these two sources arriving at the lunar surface are small when compared with direct solar radiation or illumination.

1.3.4.1 Earth's Thermal Radiation. This is approximated by the radiation from a black body at 288°K between 8μ and 12μ, and by a black body at 218°K for longer wave lengths. The total energy is approximated by the radiation from a black body at 248°K. See Figure 1-4.

1,3.4.2 Earth's Albedo Radiation

Earthlight on the moon from the earth is at its minimum at the time of full moon. This corresponds to the time of new earth, as viewed from the moon. The amount of light increases as the earth reaches the full earth position (new moon). Illumination by this source would only be of importance during the 14-day lunar night. Minimum illumination during this period occurs at sunrise and sunset when the earth is at quarter phase (one-half disc). Investigators have concluded that all earthlit surface features on the moon from full-earth to quarter-earth have surface brightnesses above the eye threshold. The mean illumination of the moon by the earth changes with the phases of the earth as follows:

0	(Full disc illumination)	13.5 lumens/m^2
30°		9.3 lumens/m^2
60°		5.6 lumens/m^2
90°		2.8 lumens/m^2
120°		1.1 lumens/m^2
150°		0.2 lumens/m^2

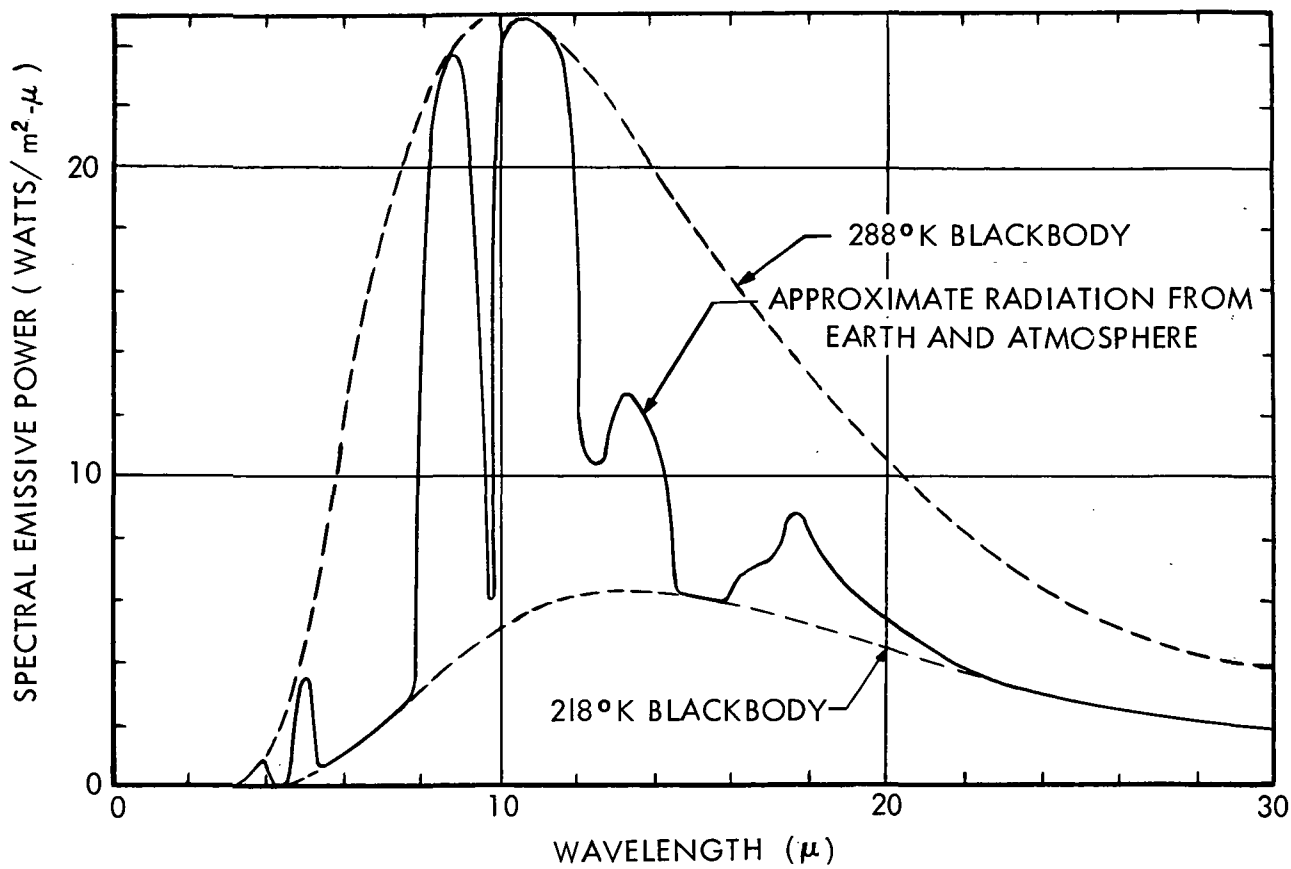

Figure 1-4. Spectral Emissive Power Curve

1.3.5 Lunar Surface Characteristics

In this environmental model the basic surface characteristics concern surface temperature, surface thermal inertia, albedo, and soil characteristics at the surface, and surface thermal radiation.

1.3.5.1 Lunar Surface Temperature. Temperatures for a complete lunation are given in Figures 1-5 and 1-6. E. Pettit and S. B. Nicholson have given the maximum surface temperature at the sub-solar point on the full moon to be 407°K (134°C, 273°F) and the surface temperature at new moon to be 120°K (-153°C, -243°F).

At present, the maximum temperature used by most investigators is 390°K (117°C, 243°F). This is at the sub-solar point on the full moon.

The temperature decreases from the center of the lunar disc toward the limb at full moon, and also toward the terminator at other times.

The current best value for the minimum lunar temperature is 104°K (-169°C, -272°F). This occurs at lunar midnight on the side of the moon directly opposite to the sub-solar point.

The temperature variation on the moon's surface is thus about 290°C or 520°F.

Subsurface temperature - a constant value of 230°K (-40°C) at the depth of 1 meter below the surface.

1.3.5.2 Parameters Determining Thermal Inertia at the Lunar Surface.

Thermal conductivity - k	= 4×10^{-3} to 3×10^{-6} cal/cm/sec/°c
Density - ρ	= 1.5 to 3.5 gm/cm^3
Specific heat - c	= 0.2 cal/gm/°c
Thermal inertia - $\frac{1}{\sqrt{kpc}}$	= value of this appears to be 1,000

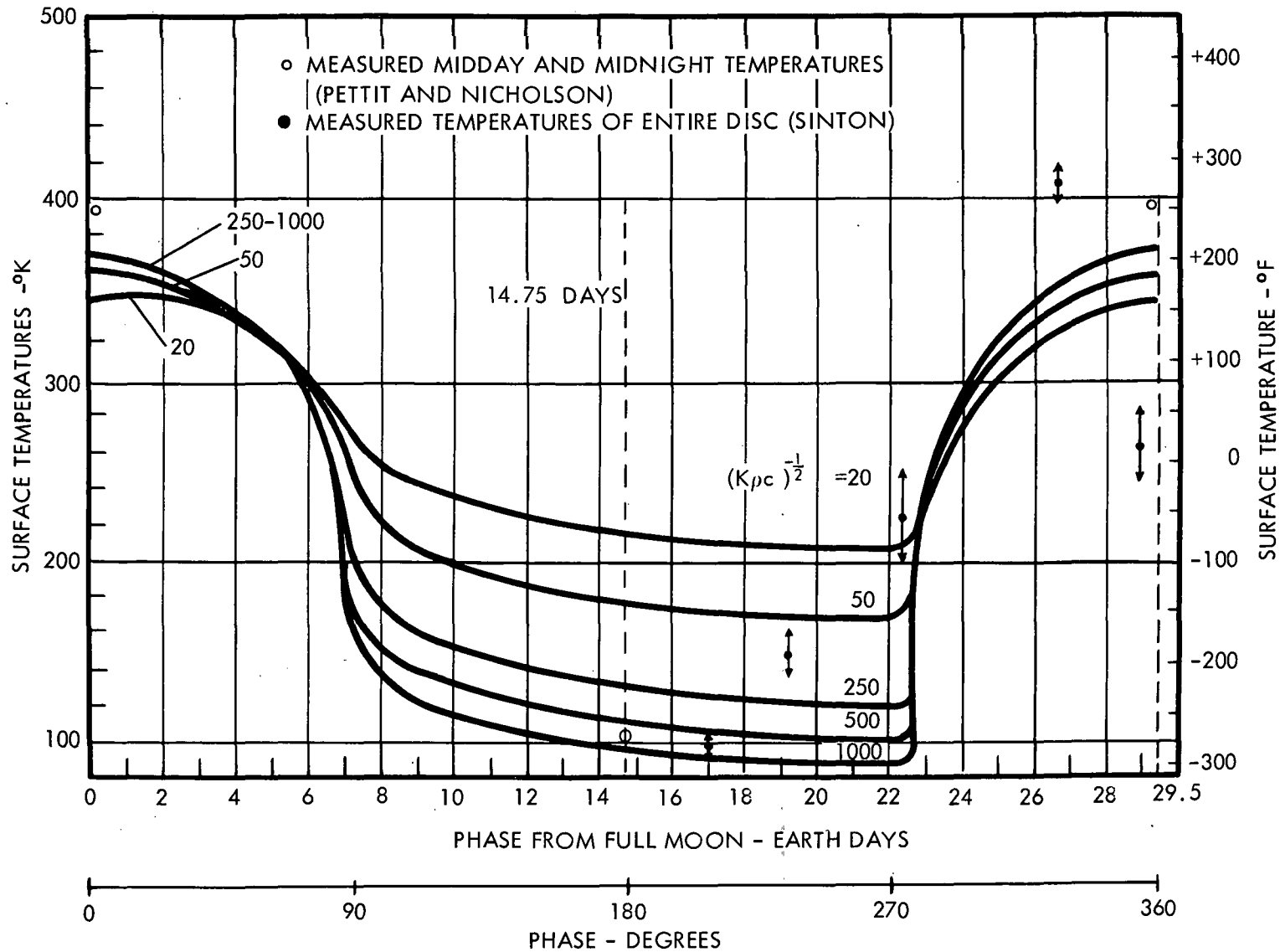

Figure 1-5. Lunar Surface Temperature Variations, Phase-Temperatures

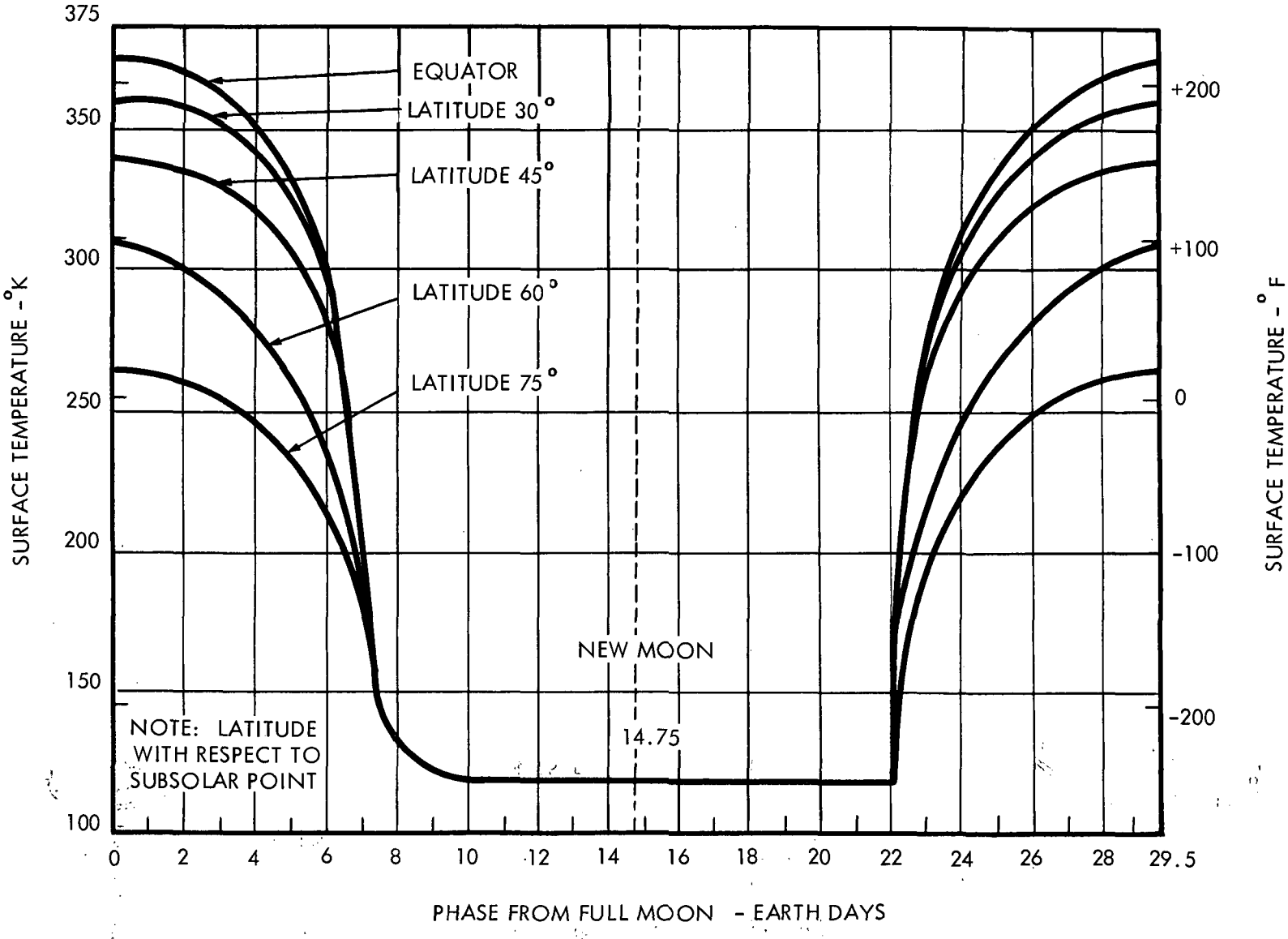

Figure 1-6. Lunar Surface Temperature Variations, Phase-Latitude-Temperatures

Average Maria Model

(The maria may be regraded as a vesicular solid of high porosity and low permeability having the following properties):

$k = 0.5 \times 10^{-4}$ to 4.0×10^{-3} cal/cm/sec/°c

$\rho = 1.8$ to 2.1 gm/cm^3

$c = 0.2$ cal/gm/°c

(For a dust cover of 1 mm to 1 meter in depth over the maria the thermal properties of this layer will be):

$k = 10^{-5} \times 10^{-6}$ cal/cm/sec/°c

$\rho = 1.5$ to 1.8 gm/cm^3

$c = 0.2$ cal/gm/°c

1.3.5.3 Lunar Surface Albedo (Spherical or Visible)

Site	Fraction of Visible Radiation Reflected
Average maria normal	0.065
Average continent normal	0.105
Average	0.072
Overall Values	
Maximum value	0.183
Minimum value	0.051

1.3.5.4 Primary Soil Characteristics and Engineering Constants—The lunar soil varies greatly in granular gradation dependent on locations. Overall, the soil particle size distribution is mainly composed of fine sizes, i.e., sand and silt-size granules with only a small percentage of cobbles and boulders. In the highlands, the grain-size distribution is skewed toward the coarse granules, ranging from cobbles to boulders and monolithes.

Stratification of the granules takes place due to the infall of secondary ejecta and sputtering caused by corpuscular radiation.

The maria is a flat plain with the surface layer consisting of fine granules in the topmost layer. The sub-surface characteristics vary from coarse-grained layers of variable thickness to thin layers of fine granules.

Engineering characteristics of the soil stated as study constraints are cited in Section 2.2.2.

1.3.5.5 Lunar Surface Thermal Radiation. The temperature and reflecting power of the lunar surface depends upon the phase and altitude of the sun above the horizon. A study of the thermal radiation on the moon was conducted by Pettit and Nicholson on the 100-inch reflector of the Mt. Wilson Observatory. The results of the measurements are given by Figure 1-7. The dotted line is the theoretical distribution of the radiation assuming the moon is a smooth sphere. It is $E = Eo \cos \theta$ (lambert's Law).

However, the distribution of planetary heat over the lunar disc actually follows the formula:

$$E = Eo \cos^{2/3} \theta$$

where E = measured energy

Eo = radiated energy from the sub-solar point

θ = angle between the normal to the point and the line of direction to the sun

The irregularities of the lunar surface produce a greater heating at the edges of the lunar disc at full moon than would occur for a smooth body. This is illustrated in Figure 1-8 which is an expansion of Figure 1-7.

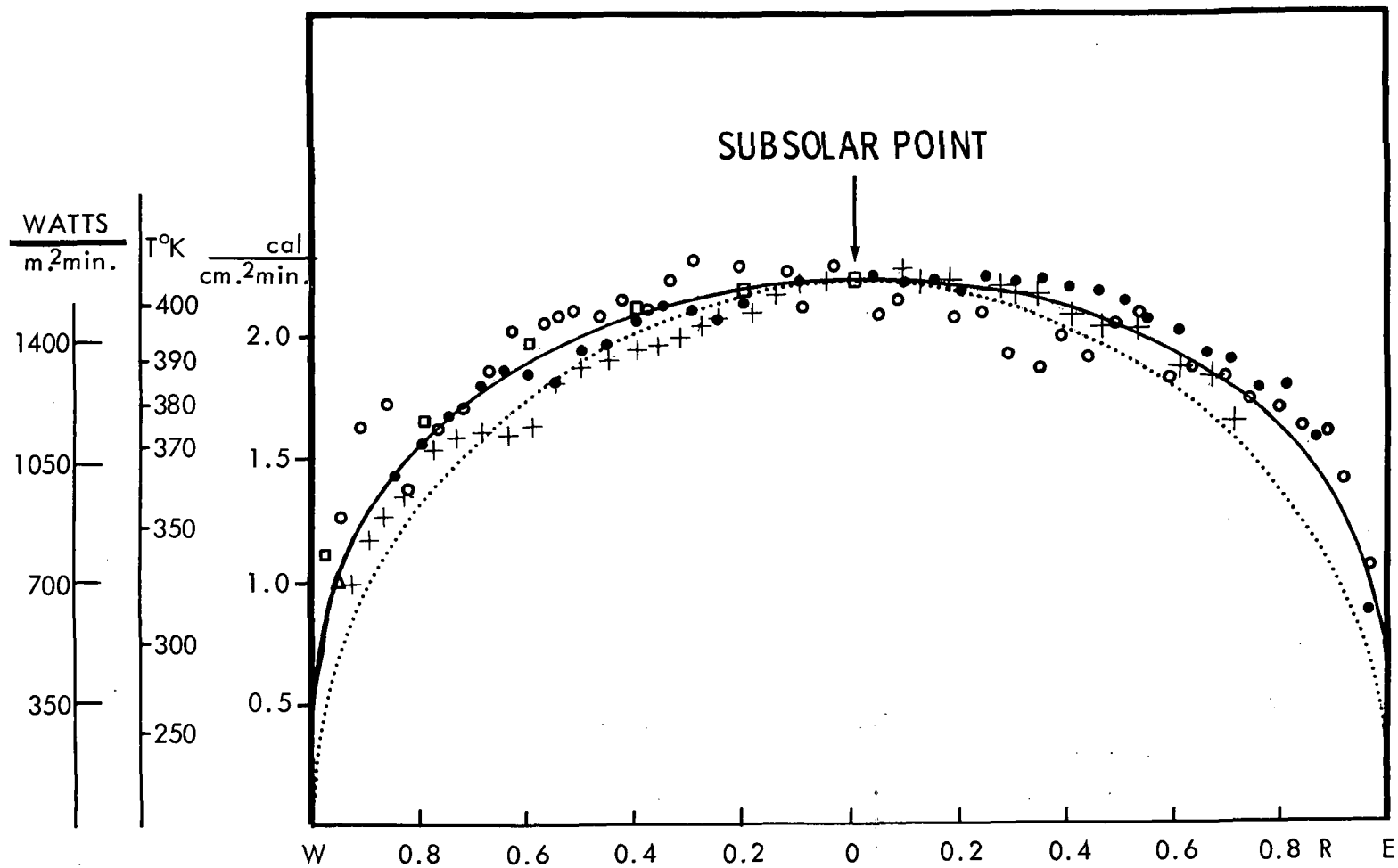

Figure 1-7. Distribution of Proper Radiation of Moon

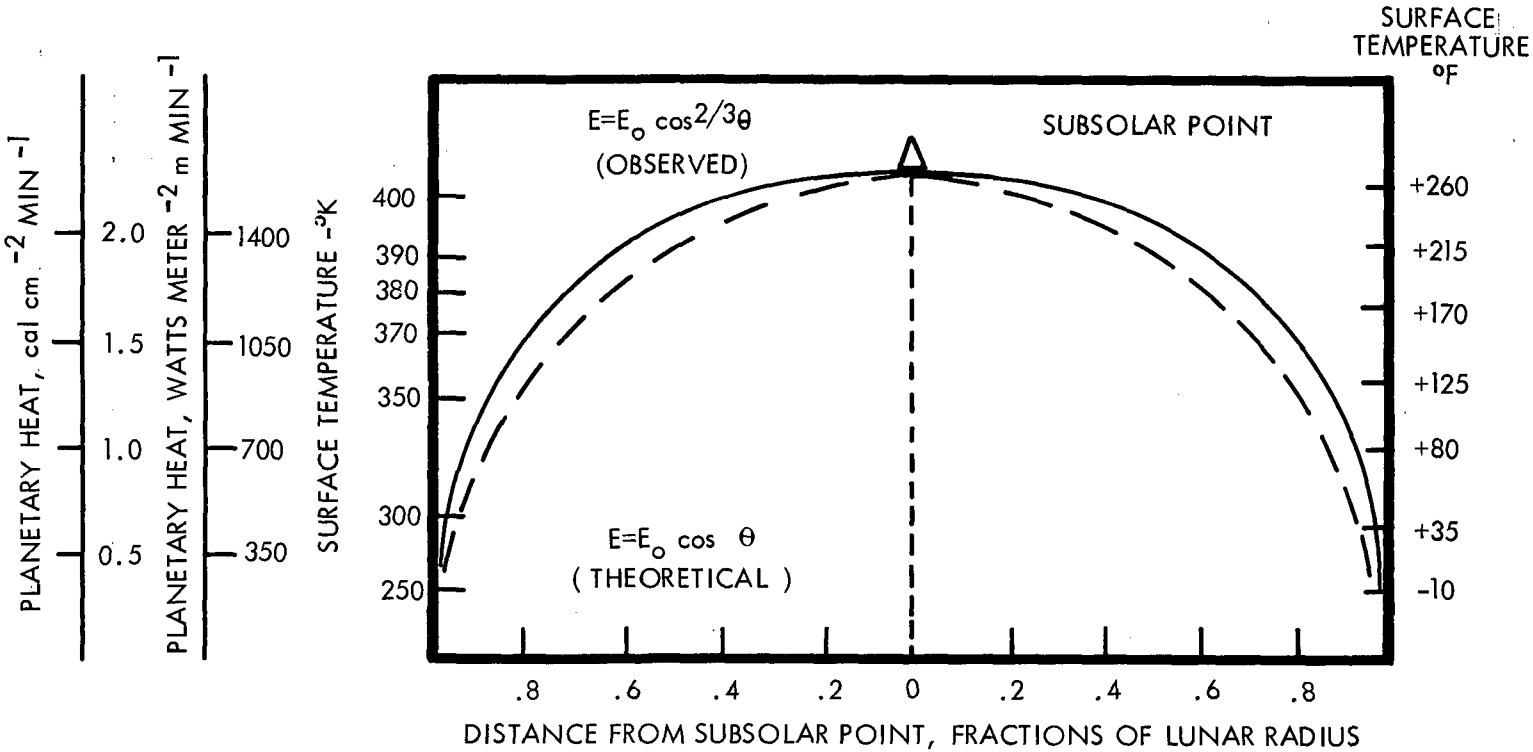

Figure 1-8. Emitted Planetary Heat Distribution About Subsolar Point of Full Moon

Using the figures above, the diagram of lunar isotherms is derived, as shown in Figure 1-9.

1.3.6 Meteoroid Flux and Erosion at the Lunar Surface

1.3.6.1 Meteoroid Flux. Meteoroid Flux is the number of meteoroids of a given mass and greater which pass through a unit area in unit time.

Photographic and radar methods are used for determining the flux of the large-size meteoroids, while various measuring devices carried by rockets and satellites determine flux rates for the smaller meteoroids. Data reduction to give useful distribution tables involves assumptions of density, luminous efficiency, etc. Other uncertainties are also involved, so that meteoroid observations have resulted in influx rates which may vary by several orders of magnitude. Figure 1-10 shows two curves which bracket the actual meteoroid distribution in space. Actual distribution varies with time and location in space. The following relationships may be used:

$$\phi = K/M$$

where ϕ = the flux in particles/unit area/unit time, having a mass greater than M

K = a constant

M = the meteoroid mass

The number of meteoroids increases as their mass decreases. Structures may be penetrated by particles with masses greater than 10^{-4} grams at the kinetic energy associated with the meteoroidal velocity range of 11 to 72 km/sec. Particles larger than 10^{-4} grams are considered "puncture size" meteoroids. Erosion of exposed surfaces may occur from micrometeoroid particles (masses less than 10^{-4} grams).

The velocities of the small mass particles probably lie near the lower velocity limit.

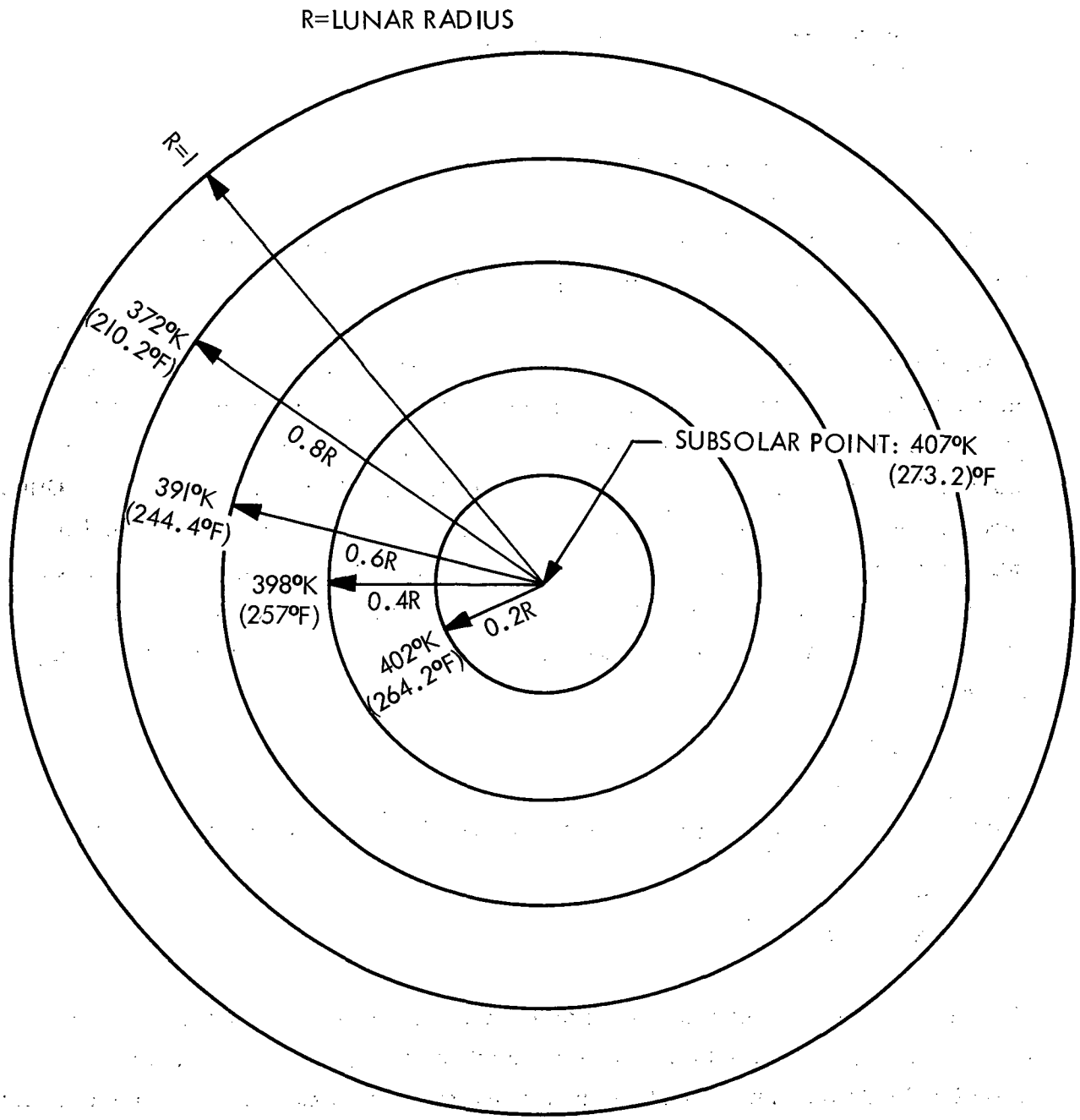

Figure 1-9. Lunar Isotherms

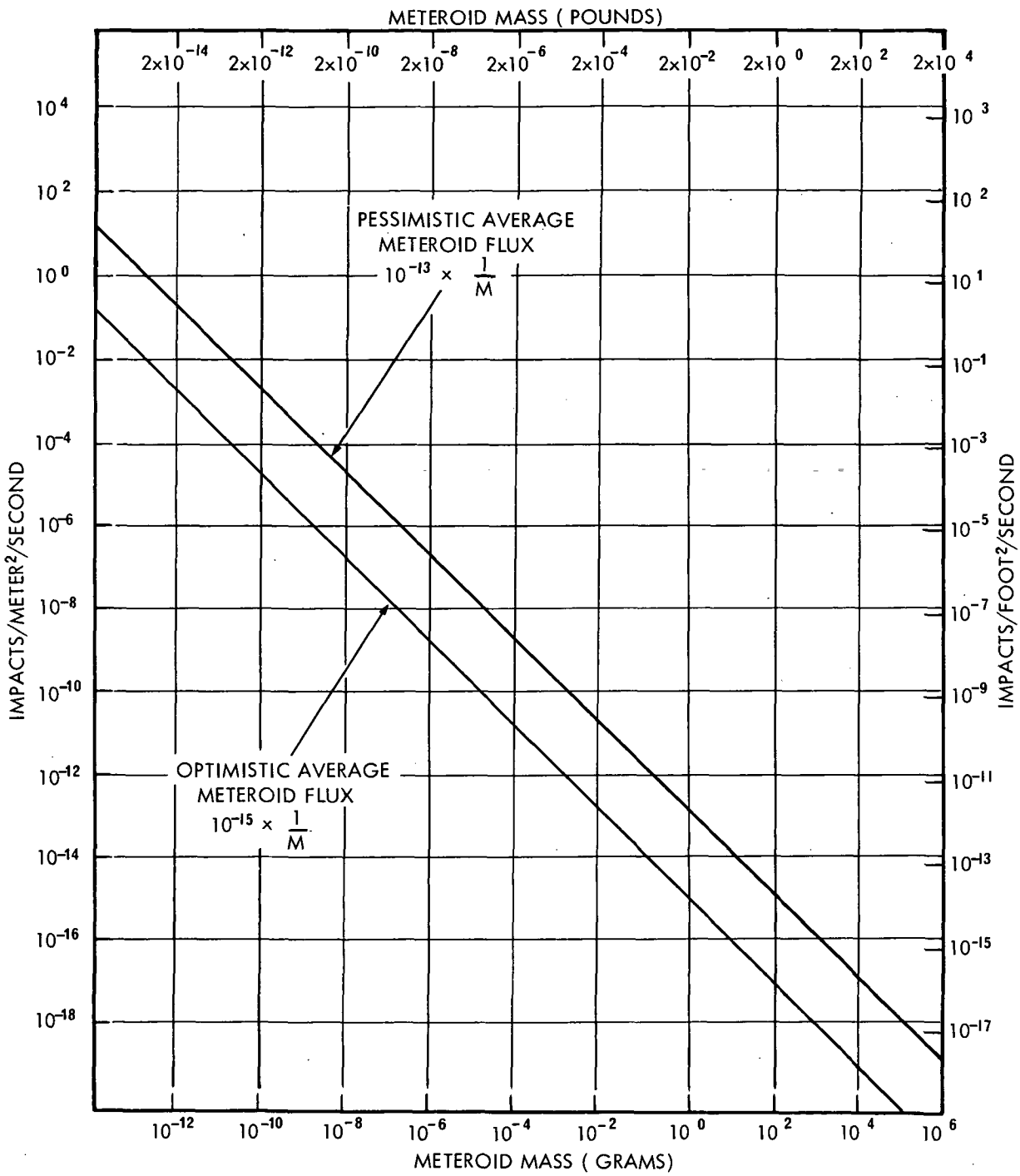

Figure 1-10. Meteoroid Frequency - Function of Mass

Whipple (1961) estimates an average velocity of 15 km/sec for particles up to $10^{-7.7}$ grams mass and 28 km/sec for particles greater than $10^{-2.5}$ grams.

A cumulative mass distribution curve for the vicinity of the moon is given by McCracken and Dubin and is shown in Figure 1-11. Flux rates of particles with mass m and larger are plotted against particle mass. The flux rate is given in particles/ meter^2/sec.

Visual magnitude is related to the particle mass by assuming that a meteoroid with a mass of 1 gram and a speed of 30 km/sec will produce a meteor with a visual magnitude of zero.

Flux of secondary ejecta may be 10^4 to 10^5 times the incident meteoroid flux. Secondary ejecta possess velocities considerably lower than impacting meteoroids and do not seem to be a hazard to space station or structures. However, erosion damage may greatly increase.

1.3.6.2 Meteoritic Dust Erosion Rates. The following estimate for light metal erosion by meteoritic dusts may be used in lieu of specific experience values:

Depth Rate for Aluminim or Magnesium	1.5×10^{-3} cm/sec

For comparison:

Corpuscular sputtering rate for the same metal is	2×10^{-13} gm/cm^2-sec

1.3.7 Lunar Magnetic Fields

According to the Lunik 2 (USSR) probe, the total lunar magnetic field is less than 6×10^{-4} gauss.

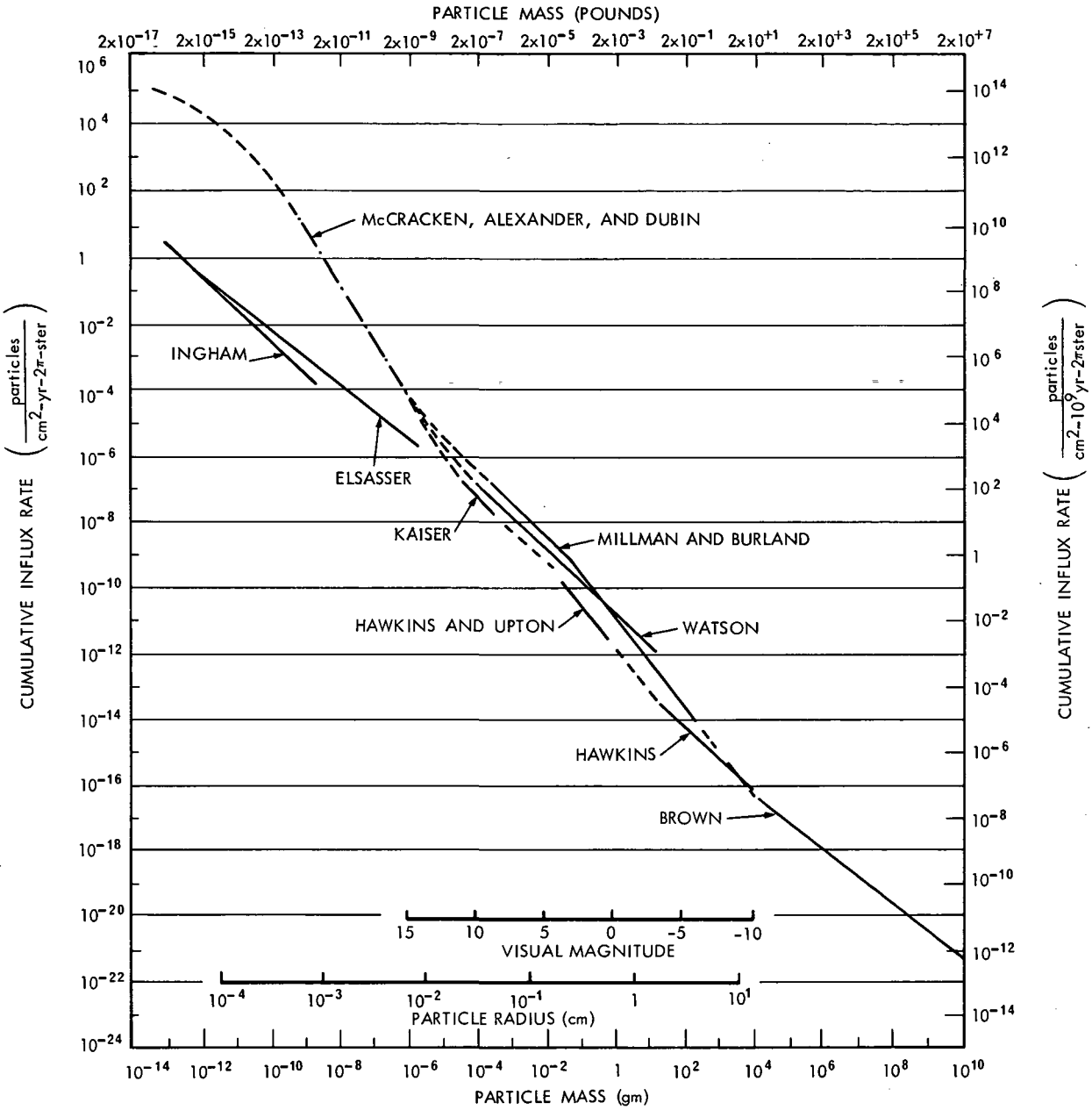

Figure 1-11. Meteoroid Mass Distribution - Vicinity of Moon

Kopal says that the moon's surface magnetic field strength should be less than 10^{-2} gauss because the observed solar corpuscular-induced surface luminescence would be nonexistent if a 10^{-2} gauss field were present.

The magnetic field of the moon has been estimated at about 1.4×10^{-6} gauss by many investigators.

1.3.8 High Energy Particulate Matter Influx and Radio-Activity on the Lunar Surface

The particulate radiation on the lunar surface may be broken down into four categories which are differentiated by the source of the radiation effects:

- Galactic Cosmic Influx
- Solar Particle Influx (high energy and solar wind)
- Natural Surface Radioactivity
- Induced Surface Radioactivity

The flux rates, dosage rates and energy ranges of the above types of radiation are given in the following subsections.

1.3.8.1 Galactic Cosmic Radiation.

Composition:	~85% protons (H^+)
	~14% alpha particles (He^{++})
	~1% nuclei of elements LI-FE
Flux at sunspot minimum:	~4 protons/cm^2-sec (isotropic)
Integrated yearly rates:	~1.3×10^8 protons/cm^2
Flux at sunspot maximum:	~2.0 + 0.3 protons/cm^2-sec (isotropic)
Integrated yearly rate:	~7×10^7 protons/cm^2
Energy Range:	~40 Mev to 10^{13} Mev
Predominate Energy:	~10^3 to 10^7 Mev
Integrated Dosage:	~6 to 20 rads/year
(Independent of shielding)	~0.7 to 2.3 millirads/hour

1.3.8.2 Solar Particle Influx. There are two classes of solar particle influx. The most critical concerns the high-energy atomic nuclei associated with solar flare events. In the absence of solar flare effects there is a continuous flux of particles designated as the "solar wind."

1.3.8.2.1 High Energy Solar Particles—

Composition: Predominatly of protons (H^+) and alpha particles (He^+)

Integrated yearly flux:

For energy > 30 Mev	$J \simeq 6 \times 10^9$ protons/cm^2	near solar flare maximum
	$J \simeq 1 \times 10^9$ protons/cm^2	near solar flare minimum
> 100 Mev	$J \simeq 1 \times 10^9$ protons/cm^2	near solar flare minimum
	$J \simeq 1 \times 10^9$ protons/cm^2	near solar flare minimum

Where J = the number of protons/cm^2-year. The maximum dosage with a shielding of 5 gm/cm^2 = $\sim$100 rad per flare, skin dosage.

Distribution of the particles can be considered to follow an inverse square law.

Solar flares occur cyclically with a period of eleven years and are more probably at solar maxima than at solar minima; that is, when sunspot activity is at its greatest. The sunspot activity follows a cycle with approximately a period of eleven years. Although flares are 5 to 10 times as probable at the solar maxima than at solar minima, this bears no relation to the size of the event. Some of the largest flares have occurred during periods of minimum solar activity. It is not possible to predict the size of a flare beforehand.

The worst years for flares will be 1967, 1968, and 1969 (180 flares are predicted for 1968.) Years with fewer events will be 1972 and 1973.

The probability, P, of encountering a flare of total integrated flux J, with energies greater than 30 Mev in one day is as follows:

J (E 30 Mev)	P
10^7	0.0113
5×10^7	0.0073
10^8	0.0058
5×10^8	0.0038
10^9	0.0023
5×10^9	0.0003

The energy spectrum shifts during any given flare because of the difference in transit time between low-energy and high-energy protons. Therefore, the low-energy end of the spectrum tends to build up as the event progresses.

1.3.8.2.2. Solar Wind—This is a continuous flux of particles (protons and/or electrons) coming from the sun while it is in its quiet state. The distribution of the particles follows an inverse square law with the sun as a joint source. There is still considerable controversy regarding origin, flux and energy characteristics of the solar wind. The following estimates are given:

Mean Density:	1.0 A.U. = $\sim$ 20 hydrogen atoms/cc
Mean Flux:	1.0 A.U. = $\sim$ 2×10^8 hydrogen atoms/cm^2-sec

Mean velocity of the solar wind from 0.5 A.U. to 1.75 A.U. is 450-500 km/sec. Energies are around 1 kev.

1.3.8.3 Natural Surface Radioactivity. There is probably some natural radioactivity on the lunar surface caused by trace quantities of naturally occurring radioactive elements. If the distribution of elements is the same as the earth, the elements will be U^{238}, thorium and potassium 40.

	Dosage Rate
Differentiated moon (acidic rocks in crust)	0.3 to 2.0 millirem/week
Non-differentiated moon (basaltic)	0.7 to 0.5 millirem/week
Surface covered with meteoritic material	0.3 to 0.20 millirem/week

These dosage rates are too small to be a hazard to man and materials.

1.3.8.4 Induced Surface Radioactitivy. Some activation of the moon's surface by bombardment as particles is believed to occur. This is the result of the processes of spallation, fission, fragmentation and capture. The induced radioactivity is a result of the de-excitation and decay of the resulting nuclei together with the leakage of certain fragments, particularly neutrons.

Calculations of rates of flux of induced neutrons and gamma rays are as follows:

Flux Rate	0.02 neutrons/cm^2-sec
	0.60 gamma/cm^2-sec
Dosage Rates (using assumed energy spectra)	
Neutrons	0.12×10^{-3} rem/week
Gammas	0.37×10^{-3} rem/week

These dosage rates are again too small to be of significance to men and materials especially over the 14-day period.

1.3.8.5 Units for Measurement of Radiation, Radioactivity and Radiation Biological Effectivity.

1 rad (radiation absorbed dose = 100 ergs (10^{-5} joule) of absorbed energy per gram of any absorbing material).

1 millirad (1 m rad) = 1/1000 of a rad

The Rem (roentgen equivalent man) equals the absorbed dose in rads times the RBE factor (relative biological effectiveness), where the RBE is the ratio of the absorbed dose in rads of x-rays of 200 erg of energy which produces a specific biologic effect, to the absorbed dose in rads of the ionizing radiation which produces the same effect.

1 gamma = 10^{-5} gauss

APPENDIX 2.0

2.0 MATERIALS

2.1 General Lunar Environmental Effects on Materials

2.1.1 Lunar Atmospheric Pressure

The atmospheric pressure at the lunar surface is so low, that it may more readily be expressed as a concentration of atoms or molecules per unit volume, specifically:

$$\sim 3.5 \times 10^{3} \text{ molecules/cubic centimeter at } 0\,^{\circ}\text{C}$$

The mean free path of molecules between collisions at these conditions is: $\sim 1.6 \times 10^{9}$ meters, or 1,600,000 kilometers which is roughly 1,000 lunar radii.

Corresponding values in the terrestrial atmosphere are 2.5×10^{19} molecules per cubic centimeter at 25 °C with a mean free path of 6.6×10^{-6} cm.

2.1.1.1 Physical Principles Involved. Gas pressure is the force effected per unit area against a bounding surface by the collisions of gas molecules, atoms or ions, having velocities determined by the thermal (kinetic) energy distributions. Therefore, pressure is a function of the system temperature and the concentration of the molecular, atomic, or ionic species present.

Pressure is one of the most important lunar environmental parameters to be considered. The effects of the reduced pressure environment include:

- Loss of ability to transfer heat by convection. Heat transfer by convection essentially vanishes at the pressure range of ca. 10^{-2} microbars (10^{-4} to 10^{-5} mmHg and below).

- Corona discharge and electric arc-over in electrical equipment. Arc-over is a phenomenon important at pressures down to ca. 10^{-2} microbars (10^{-5} mmHg).
- Loss of aerodynamic damping. Air-damping of vibrations is effective down to pressures of about one microbar (10^{-3} mmHg).
- Loss of mobility in flexible internally pressurized systems.

Operation of soft, pressurized garments in a low pressure environment must be verified. Exterior to the suit, pressure of a few millibars are sufficiently low to examine the low pressure effect of mobility in such systems.

In addition, the direct effect of the lack of gas pressure (i.e., molecular bombardment) on materials in space is two-fold. First, it enhances escape of material molecules or atoms following the Langmuir effect.* Secondly, it does not permit build-up of gas molecule layers on solid surfaces. This is required for lubrication, or prevention of seizure on surface sliding contact. Tests show that at least 10^{-5} microbars (10^{-8} mmHg) pressure is required for a reasonably rapid build-up of the gas layers. The five decade pressure range of about 1.3×10^{-5} down to 1.0×10^{-10} microbars is then of particular interest for materials effects studies.

Hence, for practical purposes, we should consider pressures under 10^{-5} microbars or 10^{-11} bars for materials evaluation. Higher pressures are used in simulating gross effects, such as soft pressure suit performance, etc.

In discussing pressure levels of interest in space environments the most convenient unit probably will prove to be the unit of 1 bar** defined as 10^6 dynes per square centimeter or 10^5 newtons/square meter***. Coincidently, one bar so defined is nearly one terrestrial atmosphere pressure at mean sea level as shown in Table 2-1 (i.e., ca. 0.987 atmospheres). A microbar is 1 dyne/cm^2 pressure.

---

*$dm/dt = 4.37 \times 10^{-2} P \sqrt{M/T}$ = loss rate in vacuo where m = gms/cm^2, t = seconds, P = millibars partial pressure at T°K, M = molecular wt., and T = °K.

**The American Vacuum Society has adopted the unit of the Torr, 1 mmHg. However, the millibar is the unit used by the U. S. Weather Bureau

***Newtons/square meter, in the preferred "MKS" system of International Units (IS).

Table 2-1

ATMOSPHERIC PRESSURES DEFINED

Designation	Definition
Physical Atmosphere*	1.01325×10^5 newtons/meter^2 or 1.01325×10^6 dynes/centimeter^2
Bar	1×10^5 newtons/meter^2 or 1×10^6 dynes/centimeter^2
Technical Atmosphere**	9.80665×10^4 newtons/meter^2 or 1 Kilogram-force/centimeter^2 or 0.980665×10^6 dynes/centimeter^2

*equivalent to 14.7 lbs-force/square inch
**used in metric engineering technology

Table 2-2

PRESSURE UNITS USED

UNIT	EQUIVALENT UNITS				
	Bar	Millibar	Microbar	mmHg (Torr)	Micron Hg (Millitorr)
Bar	1	1,000	10^{6}	750.06	7.5006×10^{5}
Millibar	10^{-3}	1	1,000	0.75006	7.5006×10^{2}
Microbar	10^{-6}	10^{-3}	1	7.5006×10^{-4}	0.75006
mmHg (Torr)	1.33322×10^{-3}	1.33322	1.33322×10^{3}	1	1,000
Micron (millitorr)	1.33322×10^{-6}	1.33322×10^{-3}	1.33322	10^{-3}	1

For historical reasons, since the mercury manometer was used to measure intermediate pressures, the unit millimeter of mercury (mmHg) has been widely used, and has been (practically speaking) designated as the Torr (after Torricelli). However, the Torr has been defined as 1/760 standard atmosphere. Since the standard atmosphere differs exactly 1 part million from 760 millimeters mercury, this difference exists between the mmHg and Torr units. Units used in low pressure technology are interrelated as shown in Table 2-2.

Low pressure regimes may then be characterized in three-decade ranges as follows:*

ILP	Intermediate low pressure range - 1 bar to 1 millibar
LP	Low pressure range - 1 millibar to 1 microbar
VLP	Very low pressure range - 1 microbar to 1 nanobar
ULP	Ultra low pressure range - 1 nanobar to 1 picobar
ELP	Extreme low pressure range - 1 picobar to 1 femtobar
SELP	Sub-extreme low pressure range - 1 femtobar (10^{-9} microbar) and below

Below the femtobar pressure range, it would be more convenient to give the particle (ion) count per cubic meter as an equivalence of the measure of pressure.

The problem of low pressure environmental effects depends, as pointed out above, upon the nature of the specific effect. Assuming no sliding surfaces are concerned, pressure of a millibar would be sufficiently low to evaluate gross lunar environmental pressure effects on suit mobility. Otherwise, pressures in the range of nanobars down to picobars must be used to define this environmental parameter.

---

*Note that:
1 bar ≡ 750 mmHg
1 millibar $\simeq$ 0.750 mmHg
1 microbar $\simeq 7.5 \times 10^{-4}$ mmHg or 0.750 microns Hg
1 nanobar $\simeq 7.5 \times 10^{-7}$ mmHg
1 picobar $\simeq 7.5 \times 10^{-10}$ mmHg
1 femtobar $\simeq 7.50 \times 10^{-13}$ mmHg

2.1.2 Pressure Effects on Materials

Under the reduced atmospheric pressure on the lunar surface, volatile components of materials may be lost. Layers of absorbed gases on the surfaces of materials will also be removed. The volatilization of materials may result in the following effects: (1) loss of bulk material; (2) change in composition of bulk material; (3) loss of thin coatings, such as thermal control surfaces; (4) change in frictional properties of metals; (5) change in optical transmission of plastics or glasses. The loss of bulk material may result in a reduction of structural strength.

Conservative rates of evaporation indicate, however, that there should be no problem due to evaporation of metals, either to structural metals or to those used in bearing and gear applications. It is possible that alloys with volatile elements, i.e., zinc and cadmium, may change composition due to a greater vaporization rate of some component. Zinc and cadmium will sublime readily at lunar temperatures and cannot be used as platings on other metals. This will be of no consequence in a short time application, however. Evaporation rates are higher for plastics and the loss of the plasticizer may take place with subsequent change in the physical properties. Plastics formed from pure materials have lower vapor pressures and will be more stable. It is possible that plasticizers may redeposit on surfaces to impair functioning, i.e., surfaces of electrical contacts, or on thermal or electrically conducting surfaces.

Evaporation losses of oils and greases may cause severe effects such as an increase in friction and cold welding. Bearing surfaces would either have to be sealed or pressurized to maintain low coefficients of friction. If this is not practical, methods of boundary lubrication must be used, such as molybdenum disulfide films.

Ceramics, such as oxides may change emissivity characteristics because of a loss of water vapor or other gases. Chemical conversion coatings on metals are mostly oxides and phosphates and these are generally more stable in low atmospheric pressures than the metal bases. Sublimation or composition changes may change electrical properties. Glasses may devitrify at high temperatures to change optical transmission characteristics.

2.1.3 Temperature

The high temperatures which can be reached on the lunar surface, up to about 416°K (289°F) will tend to increase the evaporation rates of metals and plastic materials. This will be of no significance to metals with which we will be concerned. Many polymer materials can also be found that can withstand these temperatures.

Embrittlement of metals and unreinforced plastics takes place at low temperatures. Reinforced plastics may show an increase in impact, tensile and compressive strength but may become too brittle to be used. Many elastomers and rubbers will not withstand temperatures below about 228°K (-49°F).

Thermal radiation increases the thermal agitation of atoms and molecules so that reactions initiated by ultraviolet radiation or nuclear radiation proceed at greater rates. Moderate temperatures will produce some reversible effects on polymers such as melting and glass transitions but higher temperatures can produce permanent damage. Decomposition stability is determined by the basic structure of the polymer.

2.1.4 Nuclear Radiation

NASA, MSC has obtained a solar flare radiation model for long term missions in space based on probability treatments of observations made by observers over several years. This model calls for a 1% probability of a total integrated flux, over a period of two years of about 10^{11} particles/cm^2. This would correspond to a total dose of a about 10^5 rad. Damage thresholds for most materials are well above this level.

Several types of damage to materials takes place in materials due to particle radiation. Atoms may be displaced from their equilibrium positions to form interstitial-vacancy pairs. Regions of localized heating occur along the paths of the primary and secondary particles and resultant thermal stresses set up during heating and cooling generate dislocations in the material. Large numbers of atoms may be displaced from equilibrium at the end of the paths of the particles and melting and turbulent flow takes

place. Ionization effects and electronic excitation occur along the particle paths. The latter effect is insignificant in metals but in non-metals, coloration, bond-rupture and luminescence can take place. Atomic displacement is the chief damage mechanism to metals and semi-conductors and is of some importance in glasses and ceramics. Ionization, or electron removal is of prime importance to plastics, elastomers, oils and greases, glasses and ceramics. The intensity of displacement reactions occurring in a given material drops with increasing proton energy but increases with increasing electron energy. The amount of ionization is determined by the total amount of incident energy of both protons and electrons.

All effects described depend to a great extend on the ambient temperature, melting point of the materials, mechanical and thermal history, and the total radiation dose. Estimates of effects on specific materials can be evaluated by using data from nuclear reactor studies of neutron and gamma ray fluxes. Gamma rays produce mainly ionization and fast neutrons produce mainly displacement reactions. Metals are undamaged by gamma rays and extremely high neutron fluxes are needed to cause appreciable damage to structural properties. It is believed that comparable proton doses would be needed for the same effects. Nuclear radiation effects on organic materials are more severe, especially on polymer films and elastomers. The latter, however, will most likely have some sort of shielding and not be as exposed as structural plastics may be. It has been estimated that as little shielding as 1 mg/cm^2 (2.05×10^{-3} lb/ft^2) will shield out most of the solar flare protons. Even the most sensitive polymers will suffer no damage if shielded by 1 g/cm^2 (2.05 lb/ft^2).

2.1.5 Ultraviolet Radiation

Radiation of wavelengths less than 3,000 Å is likely to have detrimental effects on organic polymers because of the susceptible carbon-to-carbon framework of these materials. Cross-linking and chain scission are the main types of reactions taking place. Chain-scission causes weight loss and internal porosity effects. Excessive cross-linking is generally harmful to elastomers because of the loss of flexibility. It will cause cracking and crazing in structural plastics. Metals and alloys will not

be damaged by solar photons although a static charge may occur because of photo-electric emission of electrons. There will be no permanent changes in engineering properties of semi-conductors. Inorganic insulators may have thin layers of their surfaces damaged with a possible increase in surface electrical conductivity.

Excitation or ionization in inorganic materials from short ultraviolet wavelengths releases electrons from their normal positions in the lattice. If they become trapped and do not return, color centers may be formed. These centers may absorb visible or ultraviolet wavelengths and color changes will occur in the material. Transparent optical materials such as glasses tend to darken as may certain pigments such as titanium dioxide. The latter, used in white paints for thermal control surfaces, tends to turn yellow on exposure.

2.1.6 Meteoroids

Meteoroids are believed to originate from either asteroids or comets. Asteroids are responsible for about 10% of the particles in space. They are of a stony composition, with densities averaging about 3 gm/cc (187 lb/ft^3). Some of these particles ($\sim$10%) are metallic, with densities of 8 gm/cc (499 lb/ft^3). Most meteoroids are of cometary origin and are apparently of very low average density. Estimates of the density of these particles vary from 0.01 to 0.30 gm/cc (.021 to .615 lb/ft^3) and the average estimated density is 0.05 gm/cc (.103 lb/ft^3).

Flux of micrometeoroid particles near the Earth is higher than it is at distances of several earth radii. Calculations of erosion rates at low satellite altitudes give a value of about 200 Å/yr. Away from the Earth, less than 1 Å/yr is lost from exposed surfaces. Analysis of meteorites which have landed on the Earth, show that erosion of these bodies by smaller meteoroids and other particles while they were far from Earth was less than 30 Å/yr. and probably less than 1 Å/yr. It has been concluded that erosion due to small meteoroids will result in negligible amounts of material loss and structural damage will not result. Optical properties of mirrors, windows and lenses and surface emissivity values may be affected by this amount of erosion, however. An erosion rate of 200 Å/yr would require about 4 years to degrade an optical surface.

Metal surfaces may undergo cratering and puncturing when struck by larger particles, which would be encountered much less frequently than the small meteoroids. Spallation may also take place in structures. This effect is produced as a result of the shock wave from the impact which passes through the metal from the outer surface to the inner surface. This causes pieces of the inner surface to be ejected at high velocities. Estimates of probability of penetration vary greatly because of uncertainties in the mass and the frequency of encounter of meteoroids.

A study by Bjork treats the problem of meteoroid penetration as a compressible hydrodynamic flow problem. Crater depth is found to be proportional to projectile diameter and the cube root of the impact velocity. Meteoroid encounters must be assumed to be random events occurring at some average rate over a period of time. The survival probability of a satellite depends upon exposure time and the damaging hit rate; i.e., the meteoroid flux that will penetrate the satellite skin. Survival probability then depends upon the total surface area, the structural material properties, meteoroid characteristics, and time of exposure. The required thickness of vehicle skin material may be calculated for any particular survival probability. Bjork has calculated skin thickness of aluminum as a function of surface area and time of exposure for three survival probabilities. This is shown in Figure 2-1.

Structural damage may be reduced or eliminated by the use of meteoroid bumpers. A bumper is merely a thin wall which is placed in front of the main wall of the vehicle and separated from it by about an inch or more. Impacting meteoroids will tend to shatter upon penetrating the thin wall, which absorbs most of the kinetic energy. The fragments are dispersed and the impact against the main wall is spread out and reduced.

2.2 Specific Component Effects

2.2.1 Metals

2.2.1.1 Wheels. The major change in the wheel makeup most likely will be a change from the rubber tire to a metal one and a design change in the general shape of the present wheel to accomodate this change.

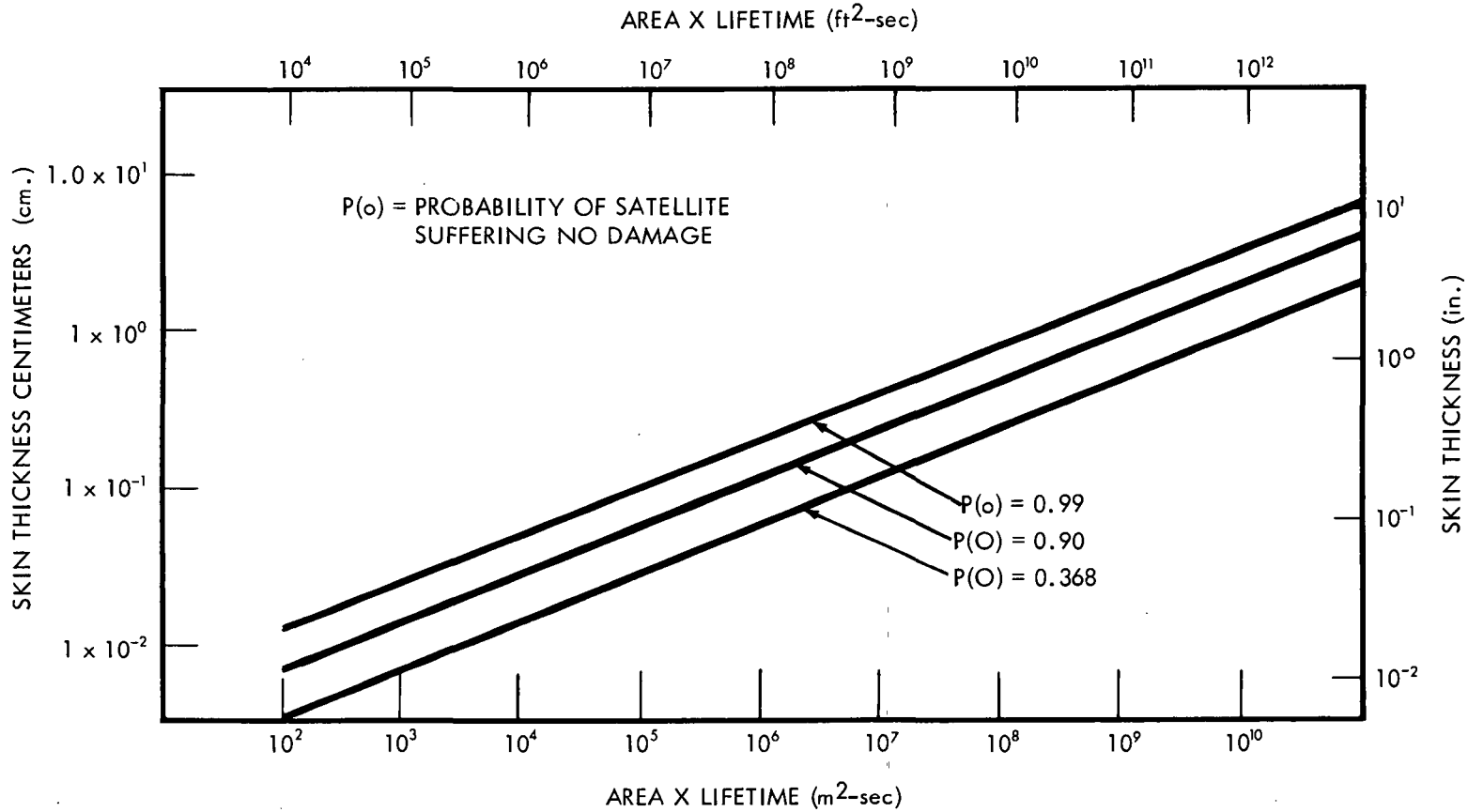

Figure 2-1. A1. Thickness Required for Material Protection

An aluminum alloy will be a good material to use for the wheel as some of the aluminum alloy series have good low temperature properties; such as increase in the tensile strength and good resistance to impact. Use of the aluminum as the strengthening members will save on weight. A simple circular tire of an austenitic stainless steel would be tough enough and have enough shock resistance to withstand the severe abrasion of the lunar soil. Another possible metal to use as the tire material may be titanium. Titanium alloys have strengths comparable to steels but their weights are only about 50% that of steel alloys.

For structural materials, in general, the following metals and their alloys should be used: (1) Magnesium, (2) Aluminum, (3) Beryllium, (4) Titanium and (5) Steel. Evaporation from these metals will not present any problem. Pure magnesium is the only metal which should not be over-exposed. If the useful temperature limit of a metal is defined as that temperature for which evaporation is less than 0.0102 cm/year (0.004 in/yr), then the maximum useful temperature of magnesium would be 472 °K (390 °F). Since the maximum lunar daytime temperature is 390 °K (243 °F), there is no need to be concerned about using magnesium as a structural material.

As far as creep rupture and fatigue of metals in the hard vacuum is concerned, there should be no worries because experiments have shown that metals are stronger in a vacuum than at normal atmospheric pressure. Reduction in strength from that found in a high vacuum has been attributed to the decrease of surface energy accompanying gas absorption, which lowers the work required for crack propagation. Also, if a crack develops in a normal atmosphere, gas molecules penetrate the crack and react with the new surface. The reaction product may be more voluminous than the original metal, a wedging action develops, which further strains the crystal structure and promotes crack propagation.

The very small loss of metal atoms from the surface of the magnesium-aluminum alloys will be even less significant than it would be for pure magnesium metal, since the loss rate of magnesium from the alloy is proportional to the atomic percent of magnesium in the alloy. The loss is of no significance as far as structural strength is

concerned but may become important because of changes in the absorptivity and emissivity characteristics of the surface. Metals generally have low thermal emittance values, often less than 0.03, but oxidized and painted surfaces have high ones, sometimes exceeding 0.90. Evaporation of this layer could drastically change the emittance value of the surface with a resultant drastic change in the heat balance of the vehicle as a whole. The oxide and paints would evaporate more slowly than the base metal and also would serve to slow down evaporation of the metal, since metal ions would have to diffuse through the oxide layer before being lost into space.

Certain grades of titanium and certain titanium alloys have excellent low temperature properties. Titanium and its alloys increase in hardness with decreasing temperature. The tensile properties of wrought, commercially pure titanium shows similar increases. It is neither brittle nor notch sensitive at low temperatures. The lower the temperature the higher the V-notch Charpy impact strength of high purity titanium (down to 77°K [-321°F]). Weld strength of some titanium alloys is quite good at low temperatures. The wrought austenitic stainless steels have good strength, ductility, and resistance to notch impact at temperatures down to at least 78°K (-320°F). They are satisfactory construction materials at room temperature and they increase in strength consistently with lower temperature without changing much in ductility and toughness.

Recommendations are that wheels may be made of the cast magnesium alloy used now in the terrestrial vehicle, or an aluminum alloy such as 6061 T6. Rubber tires will not be used but will be replaced by tires of stainless steel; such as stainless steel 347 (niobium-stabilized 18-8). This stainless steel should resist the severe abrasion effect of the lunar soil.

2.2.1.2 Metallic Tires. Tires might be constructed of a fabric "woven from metallic threads such as aluminum. This fabric would need to be supported in some fashion. Such supporting means might be: (1) spring metal ribbing, (2) filling of the tire cavity with a foamed metal such as aluminum, (3) filling of the cavity with a plastic foam, i.e., polystyrene, polyethylene, etc., or (4) an inner tube of a plastic which could be inflated with a gas or liquid.

2.2.2 Lubrication

2.2.2.1 Lubrication Materials

2.2.2.1.1 Oils and Greases. Oils and greases are the most commonly used lubricants and are easily available. They offer a number of advantages: (1) they are easily applied and renewed; (2) a wide range of properties is available; (3) they remove frictional heat; (4) they offer good protection against corrosion; (5) they provide seals against dirt; and (6) they are inexpensive. Disadvantages are: (1) at high temperatures, they have viscosities which are too low to lubricate well, they will evaporate and will decompose, while at low temperature, their viscosities are too high; (2) in the lunar vacuum, they will evaporate, causing the formation of hard residues, which will not lubricate and may jam systems. Since oils are complex mixtures, evaporation can leave residues which have lower viscosities than the original mixture; (3) oils can migrate away from the critical area to be lubricated; and (4) the radiation stability of petroleum oils and polyphenyl ethers is less than that of inorganic lubricants, such as laminar solids and soft metals. However, it does not appear that radiation will limit the use of oils and greases over a period of several years. General changes, due to radiation, in oils and greases are as follows: (1) in oils, viscosity increases. In greases, a marked drop in consistency occurs initially and then polymerization takes place and the grease becomes solid; (2) volatility of both oils and greases increases, foaming tendencies increase, flash point drops and gases are released; (3) acidity and corrosiveness increase for both oils and greases, (4) oxidation stability and heat conductivity decrease; and (5) the tendency towards coking increases in both.

In the lunar vacuum, the loss of oil from the base material of the grease will cause the grease to eventually thicken and form a hard residue which will jam gears and bearings. Oils with low vapor pressures and low evaporation rates would seem to be the best choices for the purpose but good lubricating qualities must also be considered. Evaporation of oils is more rapid at first when the most volatile components are lost. The less volatile components then evaporate more slowly.

A number of studies on lubrication of oils and greases by several laboratories have been made. The tests were made on ball bearings operating under vacuum conditions. Silicone greases and oils proved to be the most satisfactory lubricants in these tests. In one set of tests conducted at 436°K (325°F) and at 1.33×10^{-6} millibar (10^{-6} mm Hg), ball bearing lives were determined. Speeds of 11,500 rpm were attained. General Electric Versilube F-50 silicone fluid, G-300 silicone grease and Shell Apiezon T high-vacuum grease performed well under these conditions. In other tests at 383°K (230°F) and 1.33×10^{-7} millibar (10^{-7} mm Hg), GE Versilube F-50 silicone oil and G-300 silicone grease were the best materials tested.

Tests at Lockheed Missile and Space Company showed that the longest run of all materials tested was achieved by GE Versilube F-50 silicone oil. The operation was continuous at 8,000 rpm and between 1.33×10^{-6} millibar (10^{-6} mm Hg) and 5.32×10^{-7} millibar (4×10^{-7} mm Hg). These ball bearings operated for 4574 hours before failure. GE Versilube G-300, which is GE F-50 silicone oil in a lithium-base soap, was the best grease tested.

2.2.2.1.2 Solid Lubricants. Wheel bearings will be exposed to the environment and use may be made of laminar solids as lubricating surfaces. These are used in a variety of ways as follows: (1) as loose powders or dispersions in volatile carriers, (2) as burnished films, (3) as bonded films, (4) as oil and grease additives and (5) impregnated into porous solids.

These solids have a number of advantages over oils and greases. With extreme loads, fluid lubricants tend to be squeezed out from between the surfaces to be lubricated but the laminar solids do not. They shear more easily at high loads, so that they are more suitable for higher pressure applications. At low speeds, stick-slip action and cold-welding are likely to occur with oils and greases because asperities penetrate the lubricating film. This does not happen with the solid lubricants. Laminar solids have better thermal stability as they do not thin out at high temperature or become viscous at low temperatures. They would be better in dusty environments where complete sealing is

not practical. They can be used for inaccessible areas where relubrication with oils and greases is not possible. Laminar solids will be especially good where a part is used only intermittently and undergoes long idle periods. These solids also have better stability to nuclear radiation than do oils and greases.

These solids have the disadvantage of not being renewable unless the part is disassembled and rebuilt. They cannot carry away frictional heat and methods of application of the solids must be very carefully controlled to obtain the best services. Coating application methods may limit design.

Molybdenum disulfide is one of the best lubricants that is available. Films of MoS_2 on metal surfaces give coefficients of friction in the range of 0.04 to 0.10. This is about one-half that of graphite for similar films. MoS_2 is very effective in vacuum, while graphite is not. Oxidation resistance of MoS_2 is very good as it does not begin to oxidize until a temperature of 647°K (705°F) is reached.

There are a number of methods of forming bearings of MoS_2. MoS_2 may be simply rubbed onto the metal to form an adherent film without using any binding material. A strong metal-to-sulfur bond holds the film in place. For longer life, organic or inorganic bonding agents should be used, although coefficients of friction are higher. Steel is generally used for a substrate since it is quite hard. The harder the substrate, the lower is the coefficient of friction. The hardest of the two surfaces should have the MoS_2 film. Film conditions and other factors which affect the life of bonded MoS_2 films are: binder material, ratio of binder to MoS_2 curing method, film thickness, buffing and run-in. Sodium silicate, metallic-type and ceramic-bonded films are used. Resistance to wear drops off rapidly below a film thickness of $.6 \times 10^{-4}$ cm (1.5×10^{-4} in) (0.15 mil). A properly applied film would be between $.6 \times 10^{-4}$ cm (1.5×10^{-4} in) and 2×10^{-4} cm (5×10^{-4} in) (0.15 to 0.5 mil) thick. Films must be cured and organic materials volatilized. This film must be run-in before use by slowly rotating the parts and removing dislodged particles. In many cases, lubricating oil may be used with a MoS_2 film to reduce the coefficient of friction. Wear lives depend on the binder used and its resistance to radiation and other effects.

Plastic and powder metallurgy materials may be impregnated with MoS_2 to form gears, bearings, cams, etc. Plastics have a lowered coefficient of friction when impregnated. Teflon, Nylon and sintered bronzes blended with MoS_2 are all commercially available.

MoS_2 can be dispersed in oils and greases as additives. These are available commercially.

At elevated temperatures (above 672°K [750°F]), PbO is used as a lubricant. The coefficient of friction is 0.20 to 0.30 at room temperature. PbO may be bonded with SiO_2 to form coatings for metals.

2.2.2.1.3 Miscellaneous Lubricants. Soft metals such as silver and gold can be used as thin films over hard base metals. Friction is low when these metals are used because the area of real contact between the mating parts is small and the film metals have a low shear strength to reduce the formation of strong welded junctions. These metals, along with lead, indium and barium have low vapor pressures up to high temperatures (1075°F). They are more resistant to radiation damage than organic materials. Silver and gold have good chemical stability up to high temperatures. Barium is reactive. Lead and tin are moderately stable. All conduct electric currents. Seizure of bearings is less likely if the two surfaces are of dissimilar metals and have little solubility in each other.

Plastics can be used in friction applications such as in gears, bearings, cams and rollers. Nylon and Teflon are two commonly used plastics. These materials have good friction charactertistics, have little tendency to cold-weld, have good impact strength, absorb vibrations and are light in weight. Teflon retains its mechanical properties at temperatures at which oils and greases are too viscous for use. They are also less volatile in a hard vacuum. Plastics, however, dissipate heat less readily than metals, are weaker than metals, cannot stand the same extremes of temperature as metals can and have higher rates of thermal expansion. Radiation stability is poorer than that of metals.

In general, oils and greases are recommended where bearing surfaces are shielded from the vacuum environment but bonded MoS_2 coatings or a dispersion of MoS_2 in a grease should be used for exposed applications.

2.2.2.2 Bearing Lubrication. Lubricants will vary as to the particular application and environmental conditions experienced. Environmental parameters of importance are vacuum and radiation. Operating conditions that will determine the selection of the proper lubricant will be: (1) speed, (2) load, (3) temperature, (4) duty cycle (whether continuous or intermittent action) and (5) the type of motion (sliding, rotating, etc.).

2.2.2.2.1 High Load, Low Speed. Bearings with balls or rollers of plastics, such as Nylon, Delrin or Lexan may be used. For applications where speeds are less than 100 rpm these plastics offer certain advantages. They are lighter, do not tend to brinell the races as much as metals do and they eliminate the need for lubrication to prevent cold welding. If steel ball bearings are used, Versilube G-300 silicone grease may be used but bearings should be double shielded to minimize evaporation losses. Specific applications would be wheel bearings, needle bearings, and the constant velocity universal joints.

2.2.2.2.2 Moderate Load, Moderate Speed. This would apply to the drive train and bearings. As stated in section 2.2.2.3, MIL-L-7808 may be used. Use of labyrinth seals minimizes evaporation. Metal gears and bearings should be used because of higher speeds. Wear resistance of plastics would not be as good.

2.2.2.2.3 Light Load, Low Speed. For sliding surfaces exposed to vacuum solid lubricants such as MoS_2 or Teflon bonded onto the hard metal substrate may be used. MoS_2 may also be burnished onto the metal surface. Phenolic laminates, Nylon and Delrin may also be used and, as stated, do not need to be lubricated to prevent cold welding. These plastics are strong and resist wear. Parts made by powder metallurgy

impregnated with MoS_2 or oil may also be used. Steels require a phosphate treatment before burnishing with MoS_2.

2.2.2.2.4 Heavy Load, Sliding. An example of this is the steering gear mechanism. This will be exposed to vacuum. Recommended lubricant will be a dispersion of MoS_2 in grease such as Molykote Type G. Other lubricants here could be bonded solid MoS_2, which is compatible with a grease or oil plus a low volatility oil. A typical bonded solid film lubricant is Electrofilm 4856, and may be used with MIL-G-7118 or MIL-L 25336. Electrofilm 77-S may be used as a bonded solid film lubricant without any oil added. Dispersions of MoS_2 in grease such as Molykote Type G might be used.

2.2.2.3 Lubrication of Transmission and Drive Train. Bearings for gears and motors can generally stand some torque increase before the drive actually stalls and sometimes until the bearings actually freeze. Actual selection of the best lubricant may be difficult as several materials may be able to accomplish the purpose equally well. The material selected will have to be checked by service tests under simulated conditions.

High-speed gears and bearings transmitting moderate to heavy loads are used on turbine drive units for liquid propellant pumps. Speeds on these units are greater than 10,000 rpm and a temperature range of 230°K to 347°K (-45° to 165°F) is normal. Recommended lubrication for these units would be a low volatility oil. Labyrinth seals minimize evaporation. Metal gears and bearings are needed in this application. Oils recommended for use are MIL-L-7808 Type 1 or 2 for light loads or MIL-L-25336 for heavier loads. This type of lubrication should be sufficient for the transmission of the lunar surface vehicle.

Lubricants for this type of operation are MIL-L-7808 or MIL-L-25336 type oils. MIL-L-7808 oils have the following characteristics:

- Viscosity at 372°K (210°F) is 3.0×10^{-6} meter^2/sec (3.0 centistokes) at 311°K (100°F) is 1.1×10^{-5} meter^2/sec (11.0 centistokes) (minimum values)
- Specific gravity 0.9 to 1.1
- Pour Point 214°K (-75°F) - (max.)
- Flash point 478°K (-400°F) - (min.)
- Foaming tendency is nil

These oils perform well in vapor phase coking tests and rider gear scuffing tests.

They are inert to steels, copper and titanium.

2.2.3 Organic Materials

Most organic materials are composed of long chain polymeric compounds which break down in vacuum into smaller, more volatile components. The decomposition of the polymer occurs throughout the bulk of the material and is determined by the particular monomer involved, the molecular weight and by branching and cross-linking of the polymer. Loss does not depend on the surface area but on the total volume or weight as the decomposition is the rate limiting process and not diffusion. The molecular weights of the break down products are not well established and equilibrium decomposition pressures are not known for most compounds. Langmuir's equation, which gives the rate at which molecules leave a surface into a vacuum, cannot be used for plastics as it is used for metals and inorganic materials. Experimental data must be undertaken directly upon the particular polymer concerned. Tables of the data obtained are expressed in terms of the temperatures at which a weight loss of 10 percent per year would occur. A weight loss of 1 or 2 percent will not, in general, produce any significant changes in engineering properties of a plastic. A weight loss of 10 percent, on the other hand, might be accompanied by a considerable change in engineering properties. In some cases, plasticizer loss of less than 10 percent can cause radical changes, such as embrittlement.

Decomposition of polymers can be accelerated if certain addition agents are present in the material. Catalysts, plasticizers and mold lubricants all tend to lower the stability of polymers in a vacuum.

In an area of wide temperature extremes, the possibility exists that organic materials may evaporate from warm areas and redeposit by condensation in cool areas. They may alter electrical or heat conduction properties of the affected surfaces. Protective coatings may be applied to the plastic to prevent this.

High energy particles, such as protons and electrons, can damage organic materials to a definite depth or range, which is expressed in terms of the grams/cm^2 through which they will penetrate. If energies are high, ranges will be great. Three types of damage mechanism take place: ionization, excitation and atomic displacement. Ionization, or electron removal, occurs in plastics, elastomers, oils and greases, glasses and ceramics. Electron interaction with the material causes some production of x-ray photons. These photons, in turn, cause radiation damage. Nearly all of the energy of the protons, electrons and the x-ray photons ends up as ionization energy. Low-energy particles cause more intense damage than the high energy particles because ionization effects are distributed over a smaller volume of material. Ionization damage is expressed in energy absorbed per mass of material. The common unit used is the rad (100 ergs/gram). Atomic displacement damage occurs in metals and semiconductors. Whereas, ionization is the loss of an electron by an atom or molecule caused by collision with a high energy particle, excitation results when the electron gains energy from the collision without itself being ejected. When excited electrons return to their original energy states or when an electron is captured by an ion, chemical bonds are ruptured by the absorbed energy. This results in: (1) chain-scission, in which molecular bonds are broken, (2) polymerization, in which the ends of molecules become active and join together to make long chains, and (3) cross-linking, when molecules link up laterally, instead of end to end as they normally would. All of these processes may occur simultaneously. The energy threshold for ionization is about 20 ev. for electrons and photons, and 1,000 A ev. for protons, where A is the atomic weight of the atoms ionized. The energy threshold for displacement reactions is about 8,000

A ev. for electrons and photons and 7 A ev. for protons. Protons, therefore, tend to cause more damage.

Ultraviolet radiation can cause damage to organic materials. Organic materials will receive ionization dosages of 10^{12} to 10^{15} erg/gm-yr from sunlight of 100 to 1,000 Å wavelength in surface layers 10^{-4} to 10^{-7} cm ($.4 \times 10^{-4}$ to $.4 \times 10^{-7}$ inches) thick. All polymers will suffer damage to certain properties from this amount of radiation. Optical absorption and surface electrical conductivity may increase and insulating properties of materials may be damaged. There will most likely be no changes in dimensions and mechanical properties, since damage is confined to a thin surface layer. Electronic excitation produced by solar wavelengths of 1000 to 3000 Å will also produce significant property changes to greater depths. If the total irradiation, 5×10^{11} erg/cm^2-yr below 3000 Å, is spread over a depth of 10 cm., then the excitation dose would be 5×10^{10} erg/gm-yr. This is enough to damage most organic materials.

The absorption of ultraviolet by polymeric compounds in the lunar vacuum will have the following effects: (1) random chain breaking, (2) cross-linking, (3) breaking off of side chains, and (4) shortening of chains by scission. Both the cross-linking and chain-scission reactions are activated by the formation and interaction of free radicals. The chain breaking or decomposition causes loss of mechanical strength and elastic deflection. Apparently oxygen catalyzes the effect of ultraviolet on plastics, thereby accelerating the decomposition process. In vacuum, the decomposition process will be less important. In the lunar environment, heating of the material by absorption of infrared rays will tend to aid the decomposition process, however. Cross-linking will be of more importance on the lunar surface. This will tend, at first, to strengthen and increase the mechanical hardness of polymers but eventually embrittles them until surface flaking and fracturing takes place. Reduction of elasticity in elastomers will be a detrimental effect. As mentioned, thermal radiation has the effect of increasing the thermal agitation of the atoms and molecules in the lattice but does not in itself rupture chemical bonds. Reactions which have been started by ultraviolet radiation will proceed at accelerated rates. Sunlight above 3000 Å is not likely to damage engineering materials even though it produces excitation, since this is the sunlight

encountered on the surface of the earth. Materials which could not withstand this exposure would be of no engineering significance.

Plastics for structural use consist of a thermosetting resin binder and a woven or random fiber reinforcement in a mat or laminated form. The order of importance of the above-mentioned environmental factors on degradation of structural plastics is as follows: (1) nuclear radiation, (2) ultraviolet radiation, (3) high vacuum, and (4) thermal radiation.

Tests with various dosages of nuclear radiation have been made on these materials. Radiation is from nuclear reactors and consists of neutrons and gamma radiation. Polyester, epoxy, phenolic, and silicone glass fabric laminates have been evaluated at dosages up to 10^{10} rad. Results show that the mechanical properties of these materials were not significantly affected at dosages up to 8.7×10^{8} rad. This is for gamma radiation in air. For degradation dosages, it was found that the order of decreasing radiation stability is: (1) Phenolic, (2) Epoxy, (3) Polyester, (4) Silicone, Heat resistant Epoxy (Epoxy-phenolic) and (5) Heat resistant Polyester (Triallylcyanurate). Electric properties were not altered by these tests. Flexural strengths of phenolic glass fabric laminates subjected to irradiation at 500°F were about twice those subjected to heat alone up to 4.15×10^{7} rad. Slight improvements in strengths are noted at higher temperatures with the epoxy-phenolic (heat resistant) laminates. After exposure to ultraviolet light (2500-4000 Å) at an intensity of 2 cal/cm^2-min (0.14 w/cm^2) and 1.33×10^{-6} millibars (10^{-6} mm Hg) for periods up to 500 hours, no significant changes were noted in polyester (P-43), epoxy (Epon 815) or phenolic (CTL-91-LD) glass fabric laminates. Higher dosage resulted in weight loss and decrease in mechanical properties. Polyester, epoxy, and phenolic glass laminates will perform satisfactorily at ultraviolet intensities in space for periods in excess of 500 hours. Bulk properties remain the same and only the surface will degrade. Order of decreasing stability is: (1) Phenolic, (2) Epoxy, and (3) Polyester.

Thermal radiation has some effect on these materials by assisting in the degradation processes initiated by ultraviolet and nuclear radiation. Order of decreasing strength

retention at elevated temperatures for organic resins would be: (1) Phenolics, (2) Silicones, (3) Epoxy-phenolics, (4) Triallylcyanurates, (4) Epoxies, and (5) Polyesters.

Experiments in the range of 1.33×10^{-4} to 1.33×10^{-6} millibars (10^{-4} to 10^{-6} mm Hg) and at temperatures up to 400°F on epoxy, phenolic, polyester and silicone impregnated glass and asbestos materials have been compared to tests of the same materials under the same temperature conditions but at atmospheric pressure. Conclusions are that aging in vacuum at elevated temperature does not produce as severe effects on mechanical properties of these materials as high temperature aging in air.

Several studies of the effects of nuclear radiation on non-structural plastics and elastomers have been made. Mylar, styrenes and polycarbonates seem to be the most stable. Next in order of stability are low-density polyethylene and plasticized polyvinyl chlorides. High density polyethylene is next, and polytetrafluorethylene is the least stable to gamma irradiation. Table 2-3 shows a number of commercial polymers in order of decreasing stability to nuclear irradiation. Test results show that materials react differently when irradiated in the presence of air as compared to irradiation in a vacuum. Oxygen apparently speeds up degradation in some polymers but has no observed effect upon others.

Electrical conductivity of most polymers is greatly increased by exposure to nuclear high energy radiation. If the radiation is insufficient to cause chemical changes, the material assumes its normal conductive state when the radiation source is removed. Volume resistivity, dielectric strength and arc resistance undergo little change in most polymers until mechanical properties are altered by high doses.

Stability of polymers to ultraviolet radiation is related to the dissociation energies of the types of chemical bonds involved in the particular compound. Most functional groups absorb radiation in the 2000-4000 Å region but the carbon-hydrogen, carbon-halogen and carbon-carbon bonds absorb in the 1000-2000 Å range. Polymers will undergo surface damage. Experiments indicate that degradation depends upon oxygen in the atmosphere and that this process will be lessened in the lunar environment.

Table 2-3

APPROXIMATE ORDER OF STABILITY OF COMMERCIAL POLYMERS

Commercial Polymer	Nuclear Energy For Appreciable Damage (rad)	Comments
Polystyrene	10^9	Cross-links but distorts under load at 80°C
Silicone (aromatic)		Cross-links
Polyethylene		Cross-links
Epoxy polymers	10^8	
Melamine-formaldehyde polymers		
Urea-formaldehyde polymers		
Mylar		
Natural Rubber (polyisoprene)		Cross-links
Silicone Elastomers (aliphatic)	10^7	Cross-links
Polypropylene (isotatic)		Cross-links
Polycarbonates (aromatic, Lexan)		
Polyvinyl chlorides		Degrades via scission
Nylons		Cross-links
Synthetic Rubbers		
Kel-F	10^6	Degrades via scission
Polyurethanes		
Polymethacrylates		Degrades via scission
Polyacrylates		Cross-links
Teflon	10^5	Degrades via scission

However, cross-linking will still take place in vacuum with subsequent brittleness and shrinkage effects. Tests show that deterioration of Polyethylene, Teflon, Nylon, Mylar and Acrilan is faster for short wavelength ultraviolet than it is for long wavelength ultraviolet.

Thermal effects on polymers are determined by the energies needed to rupture primary valence bonds. The characteristics of the decomposition depend upon the basic structure of the polymer not upon the impurities. The magnitude of the rates and the activation energies are sensitive to trace impurities. Tests have been conducted to determine the temperature that will give a 10% weight loss per year at 1.33×10^{-6} millibars (10^{-6} mm Hg) pressure for common polymers. Some of these materials breakdown to yield only the monomer, while others give a range of decay products of varying molecular weights. See Table 2-4.

As far as vacuum effects are concerned, most polymers will lose some surface material as the result of exposure. This will vary with the temperature. Polymers that have a negligible amount of moisture and do not require plasticizers will perform well under vacuum conditions.

2.2.4 Seals

Four main factors which affect seals and gaskets are: (1) contact with reactive fluids, (2) nuclear radiation, (3) high vacuum and (4) solar radiation.

Contact with chemically reactive fluids produces deterioration and decomposition of organic polymer seals depending upon the particular chemical system in contact with the seal and the temperature. Properties such as hardness, permeability, tensile strength, weight, etc. may be altered by the chemical contact. Resultant contamination of the contained fluid system may take place. Nuclear radiation results in: (1) cross-linking which produces rigidity and brittleness in seals, (2) chain-scission which produces softening and flow and (3) depolymerization. Particular effects depend upon the type of chemical in the seal. High vacuum tends to volatilize the basic polymer plus

Table 2-4

APPROXIMATE DECOMPOSITION TEMPERATURES OF POLYMERS IN 1.33×10^{-6} MILLIBARS VACUUM

Polymer	Estimated Temperature For 10% Weight Loss Per Year (°F)	°K
Polysulfide	100	311
Polyurethane	150 - 300	339 - 422
Nylon	80 - 340	300 - 444
Butyl Rubber (isobutylene-isoprene)	250	394
Polystyrene (not cross-linked)	270 - 420	405 - 489
Natural Rubber	380	466
Silicone Elastomer (methyl)	400	478
Mylar (Dacron)	400	478
Polystyrene (cross-linked)	440 - 490	500 - 528
Polyethylene (low density)	460 - 540	511 - 555
Polypropylene	470	516
Polyethylene (high density)	560	566
Teflon	730	661
Phenyl Methyl Silicone Resin	740	666

any plasticizers, antioxidants and fillers. Hardening, crazing and cracking will result from loss of plasticizer. Decomposition by formation of low molecular weight fragments takes place throughout the bulk of the material. Decomposition is the most effective rate-limiting process and not the diffusion of the polymer fragments to the surface. In thicker materials (0.12 cm), diffusion will limit weight loss. Higher temperature will accelerate the evaporation rate. Ultraviolet radiation causes degradation reactions in polymers. The main types are cross-linking and chain-scission. As mentioned, chain scission causes weight loss and porosity effects and cross-linking strengthens materials, but produces loss of flexibility.

Since organic polymers have inherent limitations, seals are being developed from composite (inorganic-organic) materials and from metals. Advantages are: (1) wider temperature range (33°K to 922°K), (2) they are not appreciably affected by nuclear radiation and (3) they are more resistant to propellants and synthetic lubricants. Weights and leakage rates are comparable to elastomer seals. Metallic seals such as aluminum or stainless steel can withstand high doses of radiation but will not really be needed for a short duration mission.

Buna-N (high nitrile) can withstand 5×10^7 rad and a temperature range of 219°K to 394°K (-65° to +250°F) and should prove satisfactory for hydraulic systems. TFE Teflon and TPE Teflon (filled and unfilled) can also be used for seal materials. Although Teflon cannot stand as much radiation as the other elastomers it has a larger useful temperature range 200°K to 283°K (-100° to +50°F). Buna N (high nitrile), Hycar, IF-4-(FBA) and Vyram are all satisfactory as far as compatibility with MIL-L-7808 is concerned.

Neoprene can withstand 5×10^7 rad and has a useful temperature range of 219°K to 394°K (-65° to +250°F). Kel-F can withstand 10^6 rad and has a useful temperature range of 200°K to 450°K (-100° to 350°F).

Viton fluororubber, Teflon, butyl rubber and Buna-N have all performed well as seals under continuous service in vacuum systems operating up to 1.33×10^{-8} millibars (10^{-8} mm Hg) and up to 422°K (300°F).

Teflon (TFE), Kel-F and Viton fluororubber exhibit the best high temperature stability and would be recommended for use in the lunar vehicle.

2.2.5 Wire and Insulation

Hughes Aircraft Company has investigated several types of wire and wire insulation for use in the lunar environment. The tests included subjecting wire and wire insulation to flexing at 80°K (-315°F). Polyethylene, neoprene, vinyl and silicone insulators were found to be unsuitable because of brittleness. Other tests included outgassing rate, high-temperature stability and current capacity.

Conclusions reached as a result of these tests indicated: (1) ordinary copper wire and alloy 63 are both suitable for use. Alloy 63 has 10% less conductivity but much greater life under flexing tests at room temperature and pressure, (2) Surok, which is an FEP Teflon coated with a modified polyimide lacquer seemed to be the best insulation in terms of outgassing, high-temperature stability and weight. TFE Teflon and Surok insulations did not crack when bent through 180 degrees at 80°K (-315°F). Alloy 63 operated for 830 cycles before breaking, while ordinary copper operated for 594 cycles before breaking. In a test where current through the wire was increased while in a vacuum of 1.33×10^{-8} millibars (10^{-8} torr), Surok did not outgas until a temperature of 533°K (500°F) was reached, while TFE Teflon did not outgas until 575°K (575°F) was reached.

Aluminum has a lower density than copper and a resistivity which is only slightly higher so that it appears that aluminum could possibly be used in wiring applications. Recommendations are to use ordinary copper wire with FEP Teflon insulation.

2.2.6 Optical Materials

The effects of micrometeorite bombardment on structural materials such as metals and laminated plastics is expected to be small and merely a thin outer layer of material will be degraded. This will not impair the function of these materials. However, such

an abrasion could seriously affect the functioning of glasses or plastics used in mirrors or on meters on the dashboard. These materials must transmit or reflect light and a roughened surface can impair this function. Windows, the rear view mirror, and other glass parts must be protected by means of visors or sheets of shielding material, which would be removed during use.

Glasses, such as optical lenses, tend to develop color centers after intense nuclear and solar radiation. Some cerium type glasses have been developed to resist long exposure to gamma radiation fields. Vycor, fuzed silica, arsenic trisulphide or selenium glasses all remain stable in external applications, in satellites, up to a year at 2300 statute miles altutude. Vidicon and image-orthicon types of satellite cameras now use cerium glass lenses. High purity fuzed silica is more resistant than fuzed silica of ordinary purity.

Recommendations for protection of glass surfaces is to use visors as permanent fixtures or shielding plates as removable fixtures when the vehicle is not in use. Glass should be of boro-silicate glass with cerium doping as this should hold up well in the lunar environment although shields will be needed for micrometeorite protection.

2.2.7 Fabric Materials

Polymer materials used in films or fibers for purposes such as covers for seats will be subject to: (1) nuclear radiation, (2) volatilization, and (3) ultraviolet radiation. Plasticizers, unreacted monomers or polymerization catalysts in the materials will all volatilize in vacuum, especially at higher temperatures. They also tend to accelerate decomposition of the polymer itself. Losses take place throughout the bulk of the material and not just at the surface. This tends to produce porosity effects.

High energy radiation produces several effects in polymeric materials. Molecular changes in these materials are as follows: (1) chain-scission, (2) cross-linking, (3) modifications of side-groups and (4) any combination of these reactions. Some polymers tend to harden because of cross-linking or further polymerization but others may

soften and become tacky because of chain-scission and depolymerization. The relative rates of the two main reactions, i.e. chain-scission and cross-linking, will determine what the final physical properties will be.

Fiber materials of Nylon 66, Dacron or glass, can be used. No significant loss of material in vacuum will take place in the Nylon or Dacron if plasticizers are not used. Lifetimes are long as regards nuclear radiation (up to two years) but some decomposition may take place because of ultraviolet radiation. Glass fibers should not be affected by either vacuum or radiation up to a two-year period. Any of these materials can be used for the lunar surface vehicle.

2.2.8 Nonmetallic Tires

See Section 7.0, paragraph 7.3.1 Vol II - Part 1, TECHNICAL DISCUSSION, for a discussion on the rubber pneumatic tire.

2.2.8.1 Standard Rubber Pneumatic Tire. The tire on the M-274 light weapons carrier is a 4-ply, flotation type, all service, cross-country tire. The size is 7.50 x 10.

Tires in general use on commercial and private vehicles are made of natural or synthetic rubbers. Natural rubber is prepared by coagulating the latex of the Hevea brasiliensis tree. Exposure to air and sunlight will tend eventually to make rubber products hard and brittle. Dry heat up to 322°K (120°F) has little deteriorating effect. At temperatures of 455° to 477°K (360° to 400°F), natural rubber begins to melt and becomes sticky; at higher temperatures, it becomes entirely carbonized.

Synthetic rubbers used are GR-S, which is a butadiene-styrene copolymer and butyl which is formed by the copolymerization of isobutylene with a very small proportion of butadiene or isoprene. The particular types of rubber used in tires for military applications are not specified as such but specifications as set forth in MIL-T-467259 must be adhered to by tire manufacturers. These specifications state that the total rubber hydrocarbon content of the tires must be at least 75% if natural rubber is used and that this total must be at least 87% if the total rubber hydrocarbon content is synthetic

rubber. The government does not specify that natural rubber or any specific type of synthetic rubber be used. The remaining weight is made up of the vulcanizing agent which may be sulphur or sulphur-bearing organic compounds. Other materials used in tires would include carbon black and organic vulcanization accelerators.

Natural rubber is preferred for use in treads of tires since its resistance to abrasion is excellent, and its resistance to tearing is very good. Resilience and tensile properties are excellent. GR-S (butadiene-styrene) is used alternately for tire treads but more generally is used for the sidewalls. Tensile properties, resistance to abrasion and resilience of GR-S are listed as being good but its resistance to tearing is considered to be poor. Permeability to gases for both natural rubber and GR-S is low. Butyl rubber is used mostly for fabrication of inner tubes since its permeability to gases is lower than the corresponding values for GR-S and natural rubber.

Other commonly used synthetic rubbers are neoprene, nitrile rubbers, thiokol or polysulphide rubbers, silicone rubber and the polyurethane rubbers.

Neoprene is formed by polymerization of chloroprene, a derivative of acetylene. Nitrile rubber is a copolymer of butadiene and acrylonitrile and its manufacture is similar to the process of making GR-S rubber from butadiene and styrene.

Table 2-5 gives some of the important properties of natural and synthetic rubbers. As can be seen from this table, the limiting factor for natural rubber and the synthetic rubbers used in conventional tires, when considered for use in the lunar environment is the temperature at which they become brittle. The lunar sunset temperature on the dark side of a vertical cylindrical radiator will be approximately 178 $^{\circ}$K (-140 $^{\circ}$F). The value at sunrise will be less than this. Permanently shadowed areas on the lunar surface should also have temperatures near this value. Tire temperatures will drop because of thermal radiation to these dark areas if the tire is allowed to remain in the same position for any extended period of time.

Table 2-5

PROPERTIES OF NATURAL AND SYNTHETIC RUBBER

Material	Cold Brittle Point			Resistance to Abrasive Wear	Ball Rebound (1.9 cm Steel Ball Dropped 100 cm on Sample 1.9 cm Thick) (%)			Resistance to Flexing	Tensile Strength (Based on Original Section) 298°K (25°C)		Tear Resistance (Crescent Test)		Permeability to Gases
	°K	°F	°C		253°K	293°K	373°K		kg/cm^2	n/cm^2	kg/cm	n/cm	
Natural, cis-isomer (Hevea)	219	-65	-54	Excellent	12	45	71	Excellent	315	3089	125	1226	Fairly low
Butadiene-styrene (GR-S)	213	-76	-60	Good	13	37	47	Good	380	3727	65	637	Fairly low
Neoprene (poly-chloroprene)	233	-40	-40	Very Good	8	35	67	Good	245	2403	75	735	Low
Butyl (isobutylene) diolefin copolymer	233	-40	-40	Good	15	9	50	Excellent	210	2059	75	735	Very low
Silicone (dimethyl siloxane)	193	-112	-80			43			56	549	8	78	
Nitrile (butadiene-acrylonitrile)	235	-36.4	-38	Good	13	33	63	Good	280	2746	50	490	Fairly low
Polyurethane (Adiprene) 90A	205	-90	-68	Excellent[1]				Good	3515	3447	17	167	
95A	205	-90	-68	Excellent[1]				Good	4922	3826	28	275	
75D	208	-85	-65	Excellent[1]				Good	5624	5516	21	206	

[1]Outwears ordinary rubbers in actual service by as much as 8 to 1.

Stability of natural and synthetic rubbers towards the lunar environment, in general, can be determined from Tables 2-6 and 2-7.

If we use the calculated total radiation dosage of 10^5 rad over a two-year period, calculated on the basis of a 1% probability, we can see that none of these elastomers will be damaged in this time interval.

The upper operating temperature limit on automobile tires has been determined as 405°K (270°F). This figure is for special racing tires and is the internal tire temperature.

2.2.8.2 Adiprene Tire. E. I. DuPont de Nemours and Company has developed a polyurethane rubber called Adiprene. This material has a range of hardness values which lies in an intermediate position on the hardness scales for elastomers and plastics. In effect, it bridges the gap in hardness values between these two classes of materials. For this reason it can be used as a tire material. Adiprene is tough and durable, having outstanding abrasion resistance and high impact strength. Its resilience is maintained with changing temperature far better than it is with other rubbers through the range from 283° to 380°K (50 to 225°F). Low temperature impact resistance is good and cold brittle temperatures reach about 205°K (-90°F) for the standard compounds. Special compositions can be made which retain some flexibility at temperatures as low as 186°K (-125°F). It has been successfully used at cryogenic temperatures in handling non-oxidizing liquefied gases. Products made from Adiprene are very stable under high vacuum conditions. They exhibit extremely low weight losses in standard outgassing tests. The desirable properties of Adiprene do not extend into higher temperatures, however. Above +373°K (212°F), this material loses tensile strength, elongation increases and elastic modulus decreases. Resistance to tearing decreases at these temperatures.

Some tire manufacturers have made pneumatic tires of Adiprene rubber. These tires are made of cast material and have operated successfully in passenger cars for 8045 to 11,265 km (5000 to 7000 miles). Polyurethane does not hold to the fabric material

Table 2-6

STABILITY OF NATURAL AND SYNTHETIC RUBBERS
PRESSURE—TEMPERATURE—STRENGTH RELATIONSHIPS

Material	Test Conditions Pressure Temperature			Property Change (%)		Temperature Required for a 10% Weight Loss Per Year	
	(mm Hg)	°F	°K	Tensile Strength	Elongation	°F	°K
Natural, cis-isomer (Hevea)	1×10^{-6}					380	466
Butadiene-styrene (GR-S)	10^{-5}					460	511
Neoprene (poly-chloroprene)	5×10^{-4}	300	422	+34.2	- 6.8	200	366
Butyl (isobutylene diolefin copolymer)	8.4×10^{-4}	300	422	- 7.7	-11.9	250	394
Silicone (dimethylisoxane)	1.2×10^{-4}	450	505	0	-10.2	400	477
Nitrile (butadiene-acrylonitrile)	1.2×10^{-3}	300	422		- 7.8	300-450	422-505
Polyurethane (Adiprene)						150-300	339-422

Table 2-7

STABILITY OF NATURAL AND SYNTHETIC RUBBERS RADIATION STABILITY

Material	Radiation Dosage For Threshold Damage (rad)	Maximum Dosage (rad)	Maximum Service Temperature	
			°F	°K
Natural, cis-isomer (Hevea)	2×10^6	5×10^8	225	380
Butadiene-styrene (GR-S)	$\sim 2 \times 10^6$	1.5×10^7	250	394
Neoprene (polychloroprene)	2×10^6	1×10^7	250	394
Butyl (isobutylene-diolefin-copolymer)	2×10^6	4×10^6	300	422
Silicone (dimethylsiloxane)	1.3×10^6		600	589
Nitrile (butadiene-acrylonitrile)	2×10^6	1×10^8	300	422
Polyurethane (Adiprene)		1×10^9	200	366

used in conventional tires. Cast tires are used for low speed, highly-loaded applications, i.e., fork lift trucks.

Adiprene is a trademark of E. I. DuPont de Nemours and Company but other polyurethanes are being manufactured. Neothane and Elastothane are other polyurethanes which may possibly be used in tire manufacture. Ethylene-propylene rubber has also been used.

2.2.8.3 Terra-Tire. A recently developed tire is the so-called "terra-tire," which is manufactured by the Goodyear Tire and Rubber Company. This is a low-pressure tire which is capable of a wear life of 724 km (405 miles) at a temperature of 394°K (250°F) while traveling at a speed of 4.8 km/hr (3 mph). This tire is made completely of the butadiene-styrene copolymer. A gain of approximately 50% in wear time may be achieved if this tire is compounded of 50% of polybutadiene and 50% styrene. Plasticizers are normally incorporated into the manufacture of the terra-tire. Soft soil tire pressure is 2 psi and average tire pressure for all types of soil is about 3.85 psi. As may be noted from Table 2-5, the cold brittle point is 213°K (-76°F, -60°C). Loss of resilience will occur as this temperature is approached, with eventual embrittlement.

2.2.9 Thermal Control

Thermal control of the lunar surface vehicle will develop because of the need to maintain various components within the operable limits of each. That is, batteries, solar cells, gears, bearings and oils all have particular ranges of peak operating efficiency. The thermal environment of the vehicle will be such that provision will most probably need to be made for the maintenance of components at their operating temperatures.

The vehicle will exchange thermal energy with its environment solely by means of thermal radiation. It can receive energy from the following sources: (1) earth thermal radiation; (2) earth albedo radiation; (3) solar radiation; (4) lunar thermal radiation, and (5) lunar albedo radiation. The first two sources mentioned will probably not be significant.

Two methods of temperature control are available, i.e., passive and active control. Passive control employs no power or moving parts and employs geometrical design and proper materials selection. Methods generally employed are: (1) the use of materials with the desired radiation properties; (2) proper geometrical design; (3) use of materials with proper thermal conductivity; (4) use of materials as heat sinks and (5) use of self-thermostatic surfaces. Active control is gained by using a feedback system of control employing temperature as the controlled variable. This means using a temperature-induced physical change in a material (i.e., expansion or contraction of metals). Methods employed are: (1) thermostats and heaters; (2) bimetallic strips to control shutter systems; (3) fluid transport refrigeration systems; (4) variable thermal resistance techniques; (5) thermoelectric cooling. Active systems can correct for changes in environment of the vehicle or changes in the energy absorption and emission rates of the vehicle itself. Passive control is unable to do this.

Three radiation characteristics are of utmost importance in the thermal control of vehicles and their components. These are: (1) the solar absorptance or the percentage of radiant solar energy absorbed by the surface of the material (α), (2) the infrared emittance or the percentage of radiant energy emitted by a given surface when compared to black body emission at the same temperature (ϵ) and (3) the ratio of these two quantities (α/ϵ). The infrared emittance determines energy losses by radiation from materials. The α/ϵ ratio is an index of the relative amount of incident solar radiation retained by the surface materials and can be used to estimate the equilibrium temperature of the surface. Determination of α and ϵ values for materials are made by calorimetric measurements or from reflectance measurements. The calorimetric measurements are based on the fact that if a body absorbs solar energy and emits radiant energy characteristic of its temperature, then its final equilibrium temperature is directly proportional to the α/ϵ. When the source of solar energy is removed, the temperature of the body approaches the temperature of the environment at a rate determined by its emittance and the Stefan-Boltzmann Law.

Radiative response of materials is determined by a very thin upper layer of the surface. Surface roughness and profile have an effect on radiative behavior. A surface

with a micro-profile of one micron appears rough to incident visible solar radiation but smooth to infrared radiation. Surface roughness leads to multiple reflectances and increased absorption. Radiation characteristics may be controlled by changing the surface profile. Methods involved include mechanical polishing or lapping, deposition of finely divided particles on the surface or control of the size of pigment particles and dispersions in film-forming paints. If large quantities of heat are to be dissipated so that the body remains at a relatively low temperature, materials with very low α/ϵ ratios are needed. α/ϵ ratios of 0.3/0.9 or 0.32 with reflectances of 70 percent are available with many white paints. Lockheed Missiles and Space Company is engaged in research on materials with various α/ϵ for use as solar concentrators and solar collectors. The goal of this research in thermal control surfaces is to obtain four basic surfaces as follows: (1) solar absorber, (2) solar reflector, (3) flat absorber and (4) flat reflector. Any desired radiation characteristics can be obtained by appropriate mosaic combinations of the four basic surfaces. LMSC has developed an inorganic paint called LP-40A. This is a lithium aluminum silicate pigment in a potassium silicate vehicle and has an α of 0.12 and an ϵ of 0.95. Another paint (LP-10A) is a zirconium silicate pigment in a potassium silicate base. This paint has an α of 0.13 and an ϵ of 0.90. Both of these materials degrade no more than 20% when exposed to the equivalent of 600 hours of solar radiation in space. Surfaces covered with laminates of cork tiles have exhibited values of α from 0.07 to 0.12 and ϵ values of about 0.90. This type of coating is fragile and has a low thermal conductivity value, however. Work is continuing on investigations into materials with values of α down to 0.07 and values of ϵ better than 0.90. These should be fully developed with the next two to three years (by 1969). For the thermal control surfaces on the first vehicle modification, the value of α will be 0.12 and the value of ϵ will be 0.90. These values are within the current state-of-the-art.

Thicknesses of paints required for opacity are not great, being only 0.001 inches or less for some black paints (flat absorbers) and about 0.005 inches for some white paints.

As far as stability to vacuum conditions is concerned, inorganic compounds are generally more stable than organic ones. The inorganic paints are quite stable to

ultraviolet radiation, to heat, to long term vacuum environment and show good vibration resistance and thermal shock resistance. They exhibit good adhesion to the commonly used structural metals. Coatings are being developed based upon plastic polymer materials and on elastomers to provide flexible coatings. Also, some silicone-based coatings have been developed. For the greatest stability these paints should be fully cured and contain essentially no plasticizer or other volatile components. Ultraviolet radiation has a greater effect upon organic materials than inorganic materials; i.e., the paint vehicle, and the characteristic reactions of cross-linking and decomposition take place in them. Ultraviolet radiation generally affects solar absorptance α much more than infrared emittance and increases α's. Silicone-based materials are frequently the most stable of the organics. Inorganic pigments form color centers. White dielectric materials turn brown. Black surfaces are not significantly affected. Impurities in inorganic materials may be responsible for the color changes. Experiments with irradiation of thermal control surface specimens indicate that although these materials do undergo a change in α and ϵ values, these values reach a constant state after the passage of a certain amount of time.

Practical predictions of damage from nuclear radiation on the lunar surface would be extremely difficult to make. Estimates are that high tolerance materials are not needed. Inorganic materials for these applications may be expected to remain stable, neglecting other degrading influences. Organic materials would be susceptible to damage by low-energy electrons. Electrons and gamma rays would produce surface effects but protons will affect the bulk of the material. It is difficult to predict damage by protons and electrons from data obtained by gamma irradiation from nuclear reactors. However, a number of thermal control paints and pigments exposed to 10^7 rad of gamma irradiation at LMSC showed negligible changes in α/ϵ value.

The effects of impact damage due to meteoroids on the lunar surface are considered to be negligible up to a period of two years.

2.2.9.1 Thermal Insulation. Insulation is a means of providing a barrier to heat flow. There are three classical mechanisms of heat transport, namely, fluid convection, conduction and radiation. In the extreme low pressure of the lunar environment only the latter two mechanisms are of interest. To effect insulation with respect to the former of these two mechanisms, actual body to body contacts must be minimized, and extreme low atmospheric pressure is desirable with respect to the latter.

Two types of insulating materials are available which perform as desired in low pressure environments. One type comprises the opacified powders and the other type, consist of multiple layers of reflective foils, known as super insulation.

The multilayer insulations are composed of alternate layers of metal foil and sheets of fibers in the form of fluffy mats or thin sheets of paper. The fibers are used to separate the foils and are generally of glass; i.e., borosilicate glass or quartz. The number of layers per unit thickness of the super insulation can be varied over a fairly wide range with a resultant large variation in the thermal conductivity of this type of material.

The effectiveness of the multilayer insulators is more dependent upon degree of gas evacuation than are the opacified powders but, as seen in Table 2-8, the insulating effect is orders or magnitudes better than that of opacified powder types. Since the lunar environment includes extreme low pressure, good performance of multilayer insulations may be anticipated. Protection of the multilayers by light metal sheet overlayers may be required for mechanical abrasion and shock load protection in exposed applications anticipated in the lunar environment.

The effectiveness of the multilayer insulation stems from the formation of a cascade of surface temperatures corresponding to each of the individual foil layers. Since the rate of heat transport in a radiating system is a function of $T_r^4 - T_e^4$, i.e., the difference of the fourth powers of emitter and receiver temperatures, the closer the values of T_r and T_e, the lower will be the transport rate. This is critical since each layer pair can be considered a "cell" in a series system and hence the transport across the cell pair is a limiting value for the overall multilayer heat conductivity.

Table 2-8

ENGINEERING CHARACTERISTICS OF INSULATION MATERIALS

Type	Commercial Designation	Thermal Conductivity 20°K to 294°K watt-meters/m^2°K	Density kg/m^3
Powder	"Santocel A"	166.1×10^{-5}	96.1
Powder	"Perlite"	124.5×10^{-5}	128.1
Powder	"Linde CS-5"	31.1×10^{-5}	176.2
4-8 multilayer/cm	"Linde SI-12"	15.6×10^{-5}	40.0
6-12 multilayer/cm	"Linde SI-10"	11.2×10^{-5}	32.0
14-28 multilayer/cm	"Linde SI-44"	3.5×10^{-5}	75.0
20-39 multilayer/cm	"Linde SI-62"	3.1×10^{-5}	88.0
30-59 multilayer/cm	"Linde SI-92"	1.7×10^{-5}	120.1

2.3 HEAT TRANSPORT FLUIDS

The pumping power due to the pressure drop in one conduit is:

$$P = \frac{w\Delta p}{\rho} = \frac{4f}{2g_c} \cdot \frac{w^3}{\rho^2 A^2} \cdot \frac{L}{D}$$

where w = the flow rate
A = the free flow area of the conduit
D = inside diameter of the conduit
f = the Fanning friction factor
L = the length of the conduit
g_c = dimensional constant
ρ = the fluid density
Δp = the pressure drop for one-phase flow in a conduit

When heat is being transferred across the conduit wall, the flow rate can be given by the heat balance on the fluid side.

$$w = \frac{q}{C_p \Delta T}$$

where q = the heat absorbed
C_p = the specific heat at constant pressure
ΔT = the temperature change

and $$f = c_o R e^{-n} = c_o \left(\frac{\mu A}{Dw}\right)^n$$

where c_o and n are constants, and μ is the fluid viscosity, combining the above:

$$P = \frac{2 c_o 4^{2-n}}{g_c \Pi^{2-n}} \cdot \left(\frac{q}{C_p \Delta T}\right)^{3-n} \cdot \frac{\mu^n L}{D^{5-n} \rho^2}$$

for fixed q and ΔT

$$P = C_1 \frac{L}{D^{5-n}} \cdot \left(\frac{\mu^n}{C_p^{3-n} \rho^2} \right) = C_1 \frac{L}{D^{5-n}} \cdot (\Psi)$$

Since Ψ contains only properties of the fluid and the exponent n, this quantity can be used as a point for comparison of heat transport fluids in a specific application. In turbulent flow, with which we are concerned $n \simeq 0.25$ and

$$\psi = \frac{\mu^{0.25}}{C_p^{2.75} \rho^2}$$

Low values of ψ are desirable for heat transport fluids.

Coolants must be highly stable and nonvolatile at the selected operating temperature and must not undergo a change of state. Important desirable properties of coolants are chemical inertness, high dielectric strength, low toxicity, high flash point, and low freezing temperature. Use of flammable materials may cause a problem. In assessing this danger, flash temperature, explosion limits and vapor pressures, etc., are considered. The potential danger varies according to all of these properties. Ignition sources must be removed from any contact with leaking liquid or vapor. Flammable liquids with relatively high vapor pressures should not be considered. Problems are involved in assessing water solutions of flammable liquids. Many of these are good heat-transport fluids, i.e., 60% ethylene glycol/40% water. The latter is relatively safe because of low vapor pressures, high flash temperatures and vapor high in water content.

Toxicity will not be a problem because the vapors, if any, will leak into an open area and not into a closed cabin, where they might be inhaled.

Vapor pressure is chosen so that there is no vaporization at the highest working temperature and no cavitation in the pumping units. All equipment must be stressed to withstand this operating pressure. High pressures increase the weight penalty. For example, ammonia has excellent heat transport properties but high working pressures

require very heavy equipment. Fluids should be chosen having vapor pressures below the rated pressure of standard fittings 10.34 bars to 27.58 bars (150 to 400 psi).

Fluids of low viscosity should generally be used. Viscosity considerations are important when dealing with submerged motors and pumps to eliminate dynamic seals. A decrease in viscosity by an order of magnitude will reduce motor drag by about three times.

High dielectric strength is required to reduce corrosion due to galvanic action and also to simplify the design of fully submerged motors. Some motors are being developed which will operate in aqueous solutions.

Petroleum oils can be used in systems where temperatures do not exceed 448°K (374°F, 175°C). Oils oxidize and decompose rapidly at high temperatures. Impurities cannot be tolerated, as even small amounts of moisture can cause electrolysis and rapid corrosion of metals.

Series 200 silicone fluids should not be operated at temperatures greater than 323°K (121°F, 150°C) for optimum heat stability. These fluids differ only in viscosity. 500 and 700 series silicone fluids are blends of dimethyl and phenolmethyl fluids. They are stable to 473°K (392°F, 200°C) and are available in a wide range of viscosities. These fluids have a greater temperature range than hydrocarbons. Silicones are available in a wide range of viscosities. Dielectric constants and power factors are good to 100 Mc. Changes in dielectric constant and power factor with temperature are insignificant and thermal expansion coefficients are rather high. Silicate esters have useful temperature ranges of 223°K to 473°K (-50°C to 200°C, or -58°F to 392°F). Coolant 45 is compatible with most materials except silicones and they do not corrode the common metals. Water will seriously contaminate these systems.

Minnesota Mining and Manufacturing Company produces fluorochemical liquids which can be used over a high temperature range and have good dielectric characteristics. Convective heat transfer coefficients are higher than for other conventional coolants.

2.4 REFERENCES

2-1 AiResearch Manufacturing Company, Division of the Garrett Corporation, "Radiator Design for Space Vehicles," Los Angeles, California, 1963.

2-2 Allen, J. M., "Environmental Factors Influencing Metals Applications in Space Vehicles," Defense Metals Information Center, Battelle Memorial Institute, Columbus, Ohio, December 1960.

2-3 Baumeister, T., (Editor), "Mark's Mechanical Engineers' Handbook," McGraw-Hill Book Company, Inc., New York, 1958.

2-4 Broadway, N. J., King, R. W., Palinchak, S., "Space Environmental Effects on Materials and Components, Volume I, Elastomeric and Plastic Materials," Battelle Memorial Institute, Columbus, Ohio, April 1964.

2-5 Burriss, W. L., Johnson, A. L., "Thermal Management of Manned Lunar Capsules," AiResearch Manufacturing Company, Division of Garrett Corporation, Los Angeles, California, March 1963.

2-6 Douglas Aircraft Company, Inc., "Lunar Surface Vehicles," Report No. SM-42115, Santa Monica, California, June 1962.

2-7 E. I. DuPont de Nemours and Company, "Engineering Properties of Adiprene," Elastomer Chemical Department, Wilmington, Delaware.

2-8 Engineer Research and Development Laboratories, "Conference on Materials and Design for Low Temperature Service," Fort Belvoir, Virginia.

2-9 Hodgman, C. D. (Editor), "Handbook of Chemistry and Physics," Forty-Fourth Edition, Chemical Rubber Publishing Company, Cleveland, Ohio, 1962.

2-10 Jaffe, L. D., Rittenhouse, J. B., "Behavior of Materials in Space Environments," Jet Propulsion Laboratory, California Institute of Technology, Pasadena, California, November 1961.

2-11 Jaffe, L. D., "Effects of Space Environment upon Plastics and Elastomers," Jet Propulsion Laboratory, California Institute of Technology, Pasadena, California, November 1961.

2-12 Klass, P. J., "Survivability of Wire on Moon," Avionics Magazine.

2-13 Lad, R. A., "Survey of Materials Problems Resulting from Low Pressure and Radiation Environment in Space," Lewis Research Center, Cleveland, Ohio, NASA, Washington, D. C., November 1960.

2-14 Lockheed Missiles and Space Company, "Deployment Procedures, Lunar Exploration Systems for Apollo, Volume III, Appendix," Sunnyvale, California, February 1965.

2-15 Lockheed Missiles and Space Company, "Space Materials Handbook," edited by Goetzel, C. G., Singletary, J. B., Sunnyvale, California, January 1962.

2-16 McKellar, L. A., "Effects of the Spacecraft Environment on Thermal Control Materials Characteristics," Lockheed Missiles and Space Company, Sunnyvale, California, March 1962.

2-17 Matsch, L. C., "Advances in Multilayer Insulations," Linde Company, Division of Union Carbide Corporation, Tonawanda, New York, 1961.

2-18 Minnesota Mining and Manufacturing Company, "Technical Information Bulletin - 3M Brand Inert Fluorochemical Liquids," St. Paul, Minnesota, 1965.

2-19 National Aeronautics and Space Administration, "Materials for Space Operations," Office of Scientific and Technical Information, Washington, D. C., December 1962.

2-20 National Aeronautics and Space Administration, "Effects of Low Temperatures on Structural Metals," Technology Utilization Report, Washington, D. C., December 1964.

2-21 Sibert, M. E., "Technical Bulletin - Inorganic Coatings," Lockheed Missiles and Space Company, Palo Alto, California, 1965.

APPENDIX 3.0

3.0 TERRAIN ANALYSIS

3.1 Lunar Terrain

3.1.1 Introduction

Terrain information essential to a study of cross-country vehicle performance includes topography and trafficability. Topographic data needed are the slopes that have to be climbed or descended in traverses; the walls, crevasses, craters, and large obstacles that have to be detoured; and the surface roughness that affects wheel passage. Data needed for trafficability estimates are the engineering properties of soil at the wheel-soil interface that affect the mobility of vehicles.

3.1.1.1 Sources of Lunar Terrain Information. The lunar terrain information used in this analysis is based principally on three sources:

- NASA, 1964, Engineering Lunar Model Surface (ELMS); NASA, John F. Kennedy Space Center, Launch Support Equipment Engineering Division, Future Studies Branch (Reference 8).
- NASA, Ranger VII; Jet Propulsion Laboratory Technical Reports. Part I, 1964 and 1965, Photographs of the Moon (in three series); Part II, 1965, Experimenters' Analyses and Interpretations (Ref. 4-7, 12, 14, 15).
- Air Force, 1964, Ranger VII Lunar Charts RLC 1 through 5 (Ref. 3).

These reports, photographs and maps were used for source data because they cover marial regions of the moon in the equatorial belt, and because they contain the most detailed information yet available. The ELMS model was created for the purpose of evaluating vehicle performance and is specificially applicable to this study.

Equatorial marial areas are expected to be the most probable targets for manned landings on the lunar surface, at least for early landings. The part of the ELMS study used for this report is based on analysis of 10 marial traverses, of 100 km each, in marial areas in a southeastern extension of Oceanus Procellarum, between 10^{o}S and 10^{o}N of the lunar equator and between 310^{o} and 340^{o} longitude. The marial region explored by Ranger VII, now named Mare Cognitum, is 10^{o} south of the equator at longitude 340^{o}, approximately. Although there is no basis for predicting that all maria will be alike, these are the two areas for which data are available and furthermore the observations of these areas to date are mutually consistent.

Interpretations by the Ranger VII Experimenter Team were of great value both because each Team member studied the photographs in the light of a highly specialized background in lunar phenomena and because the Ranger VII photographs increased the resolution of surface features between 3 and 4 orders of magnitude over the resolution afforded by telescopes. Part II of the Ranger VII series includes articles by R. L. Heacock, G. P. Kuiper, E. M. Shoemaker, H. C. Urey and E. A. Whitaker, and a summary by the Experimenter Team as a group.

The series of Lunar Charts are shaded relief maps compiled in consultation with G. P. Kuiper from the television records of the six Ranger VII cameras. The charts were produced for NASA by the Aeronautical Chart and Information Center, Air Force. The series of five charts shows areas of decreasing size at increasingly larger scales:

RLC 1	Scale:	1:1,000,000
RLC 2		1:500,000
RLC 3		1:100,000
RLC 4		1:10,000
RLC 1		1:1,000 with insets at 1:350

The three principal sources of terrain data were supplemented by Schurmeier, H. M., Heacock, R. L., and Wolte, A. E., "The Ranger Missions to the Moon" in the January 1966 issue of Scientific American. This article included a computer-generated contour map of the last usable Ranger VIII photograph, and a profile along a line near

TABLE 3-1

Slopes, Lunar Model (Modified from ELMS Table 4-1)

TERRAIN PROFILES FOR A REPRESENTATIVE
24.14 km (15 mile) TRAVERSE
ON THE LUNAR MARIA SURFACE

Slope (degrees)	% of Traverse	Total Distance	$K\phi$	n	ϕ
0	11.0	2.655 km (1.6 mi.)	0.5	0.5	32^{o}
-1^{o}	13.0	3.138 km (2.0 mi.)	0.5	0.5	32^{o}
$+1^{o}$	9.5	2.293 km (1.4 mi.)	0.5	0.5	32^{o}
-2^{o}	12.8	3.089 km (1.9 mi.)	0.5	0.5	32^{o}
$+2^{o}$	11.7	2.824 km (1.7 mi.)	0.5	0.5	32^{o}
-3^{o}	5.5	1.328 km (0.8 mi.)	0.5	0.5	32^{o}
$+3^{o}$	10.5	2.534 km (1.6 mi.)	0.5	0.5	32^{o}
-4^{o}	3.0	0.724 km (0.5 mi.)	0.5	0.5	32^{o}
$+4^{o}$	7.0	1.690 km (1.0 mi.)	0.5	0.5	32^{o}
-5^{o}	3.0	0.724 km (.5 mi.)	1.0	0.75	32^{o}
$+5^{o}$	4.5	1.086 km (.7 mi.)	1.0	0.75	32^{o}
-7.5^{o}	1.8	0.434 km (.3 mi.)	1.0	0.75	32^{o}
$+7.5^{o}$	1.2	0.269 km (.2 mi.)	1.0	0.75	32^{o}
-10^{o}	.6	0.145 km (.1 mi.)	3.0	1.0	32^{o}
$+10^{o}$	1.2	0.270 km (.2 mi.)	3.0	1.0	32^{o}
-12.5^{o}	0.72	0.182 km (.1 mi.)	3.0	1.0	32^{o}
$+12.5^{o}$	0.48	0.126 km (.1 mi.)	3.0	1.0	32^{o}
$-15.0^{o}+$	1.55	0.384 km (.2 mi.)	3.0	1.0	32^{o}
$+15^{o}+$	0.95	0.241 km (.1 mi.)	3.0	1.0	32^{o}
	100.00	24.14 km (15.0 mi.)			

$K\phi$ = Modulus of soil deformation due to frictional ingredients of soil ($lb/inch^{n+2}$)
n = A dimensionless factor reflecting stratification of soil
ϕ = Angle of friction (between soil grains), degrees.

the center of this photograph which shows total relief of about 3 meters (11 feet) in a 137 meter (450 foot) traverse, and individual crater depths of about 1 meter (3 feet). Ranger VIII explored an equatorial marial area in the Sea of Tranquility about 3^{o}N latitude and 25^{o} longitude. The authors speak of the similarity of topography in the Ranger VII and Ranger VIII impact areas. The Ranger VIII analyses were not published at the time of this study.

3.1.2 Topography

3.1.2.1 Slopes. Quantitative data on slopes have been provided in the ELMS model in order that lunar vehicle studies can be based on a standard representative lunar surface profile. The percentage of total traverse distance covered by slopes of different degrees are listed in Table 3-1.

Table 3.1 is based on data in ELMS (Ref 8, Figure 4-1 and Table 4-1). The assigned values for engineering properties of soils were taken from ELMS (Table 4-1).

Although a specific traverse on the lunar sufrace will have a specific distribution of slopes and slope lengths, the ELMS model is used to predict a representative surface profile. The percent distance covered and the frequency of occurrence of all slopes in any specific region is independent of length of traverse. Distribution of positive and negative slopes was found to be approximately equal.

These assumptions and the quantitative slope data presented in the ELMS are used in the present study, with the modification that the maximum slope required for the present vehicle study is 15^{o}. In the ELMS model, slopes greater than 15^{o} constitute only 2.5% of the total traverse distance.

The slopes on the lunar surface in a marial region are those associated with ridges and mounds (positive elements) and with craters and possibly crevasses (negative elements). Craters are discussed separately below, because of their importance in shaping the terrain at all scales.

Ridges in the Ranger photograph area are shown on RLC 3 of the Air Force ACIC series at the scale of 1:100,000.

The irregular ridges in this area are roughly parallel and in an echelon arrangement. The shortest is about 15 km (10 miles) long; widths are irregular, ranging up to 3 km (2 miles). According to Kuiper (Ref 6, p. 70) the narrowest ridge element is about 50 m (160 feet) wide, 500 m (1600 feet) long, and about 10 m (30 feet) high. Shoemaker (Reference 12, p. 110) describes sharply defined branches that extend short distances off the main ridges. This gives a braided appearance in plan view. Some branches of cross ridges as short as 300 m (1,000 feet) in length are 50 m (160 feet) or less in width and have local slopes on their flanks approaching 20^{o}. Locally the ridges are sharp in comparison with the rounded rims of most small craters nearby.

Two kinds of mounds were identified by Shoemaker (Ref. 12, p. 110-113) in the most detailed photographs. Gentle, irregular, elongate mounds, with many superimposed, small craters are 5-15 m (15-50 feet) wide, separated by narrow, winding, shallow depressions. The relief probably does not exceed a few meters, and the slopes appear to be less than 10^{o}. Another type of mound about 5 m (15 feet) long and 3 m (10 feet) wide, with a 1 m (3 feet) diameter crater in the summit, looks more like a crater with a greatly exaggerated rim than a mound.

More rugged terrain will be found at the borders of the maria and in isolated patches of highlands that project above the marial surface. It is not expected that either spacecraft landings or vehicle sorties would be made in the highland areas in early exploration stages.

3.1.2.2 Walls. Steep walls, comparable to the lunar "Straight Wall," were not reported by the Ranger photograph interpreters, nor in ELMS. Therefore, there is no basis for predicting that vehicle sorties on the maria will be restricted by walls.

3.1.2.3 Crevasses. Crevasses have not been definitely recognized in the Ranger VII photographs. Urey (Ref. 14, p. 145) cites "Cracks of considerable length" that give

him the impression there may be crevasses below which are bridged over with surficial material. Shoemaker (Ref. 12, p. 108) observed scarps within several craters that may be considered evidence of slumping. In the absence of definite information, any abrupt slopes or very deeply shadowed areas should be avoided. The mental picture of narrow crevasses in competent rock that might be crossable by a vehicle apparently does not apply to the lunar surface in the maria.

3.1.2.4 Craters. At all scales, craters are the dominant features on the lunar surface, and the process of cratering is the principal agent of erosion and filling in of pre-existing craters.

Frequency and Size

Data available on both the size and frequency distribution of craters in a lunar area are functions of the scale of the photograph in which they are viewed. Large craters are relatively widely spaced. Crater frequency increases with decrease in crater size down to the limit of resolution of the photograph. The Ranger photography shows craters down to less than a meter in diameter. In the photograph showing greatest detail, the general background has a rough appearance (which can be amplified by enhancing) that indicates still smaller craters near the limits of resolution. Craters are so closely spaced that the smallest craters are abundantly distributed over the larger ones (Reference 4, p. 8).

Crater density should vary with the geologic age of specific maria. The crater density discussion in this report is based on Ranger VII observations. Other maria of different geologic ages may differ, depending on the length of time each has been subject to bombardment by meteoritic and secondary materials (impact ejecta).

Crater density is significantly different in ray areas and in inter-ray areas. The Ranger VII impact area is a region crossed by rays. The Experimenter Team reported (Ref. 4, p. 8) that, of area mainly within a ray, more than 50% was occupied by craters, as compared with 20% in areas outside the rays. The most detailed of the Lunar Ranger Chart series shows a ray area (see Figure 3-1).

The size range of craters in the Mare Cognitum area is shown to scale on the Air Force ACIC series of charts (Ref. 2). On the 1:1,000,000 scale chart (RLC 1), four craters are shown in the overall area of Ranger photography that have diameters between 12 and 18 km (7-1/2 to 11 miles) and depths, from rim to floor, ranging from 750 to 2130 m (2500-7000 feet). Within the area of effective coverage at the 1:100,000 scale, the largest crater is 1-1/2 km (about 1 mile) in diameter and the deepest crater is 200 m (650 feet) deep. Within the area of effective coverage at 1:10,000 (RLC 4), the largest crater is about 375 m (1200 feet) across and 60 m (200 feet) deep. In the area of 1:1,000 coverage (RLC 5) (see Figure 3-2) the largest distinct crater shown is about 30 m (100 feet) across and 5 m (16 feet) deep.

Types of Craters

Deep circular craters are conspicuous features of the lunar surface. These craters have remarkably uniform shape through a large range in size - in the Ranger VII area from 62 km (38 miles) in diameter down to 2 m (6 feet). Characteristically these craters have distinct, smooth, raised rims of near uniform height (Ref. 12, 76-81). Inner walls are also smooth, uniform and steep with average slope between 30° and 35°. Craters with diameters greater than 7 km (4.4 miles) have relatively smooth, level, circular floors. Some craters are surrounded by bright halos or rays, others are not. Deep circular crater distribution appears to be random at all scales and, though conspicuous, they occupy a very small percentage of the maria surface. In part of the Ranger VII area, relatively deep craters from 400 to 900 m (1300-3000 feet) in diameter closely resemble the typical large deep circular craters except for the lack of well-developed rims. Vehicle traverses should avoid all deep craters by detouring.

As increasing detail can be seen on the lunar surface, elongate shallow craters are found in all sizes from 3 km (nearly 2 miles) to 1 m (3 feet) in length. These craters are shallow, with low irregular rims or no rims. Many of them appear to be composite, formed of 2, 3 or even 4 craters merged together (see Figures 3-1 and 3-2).

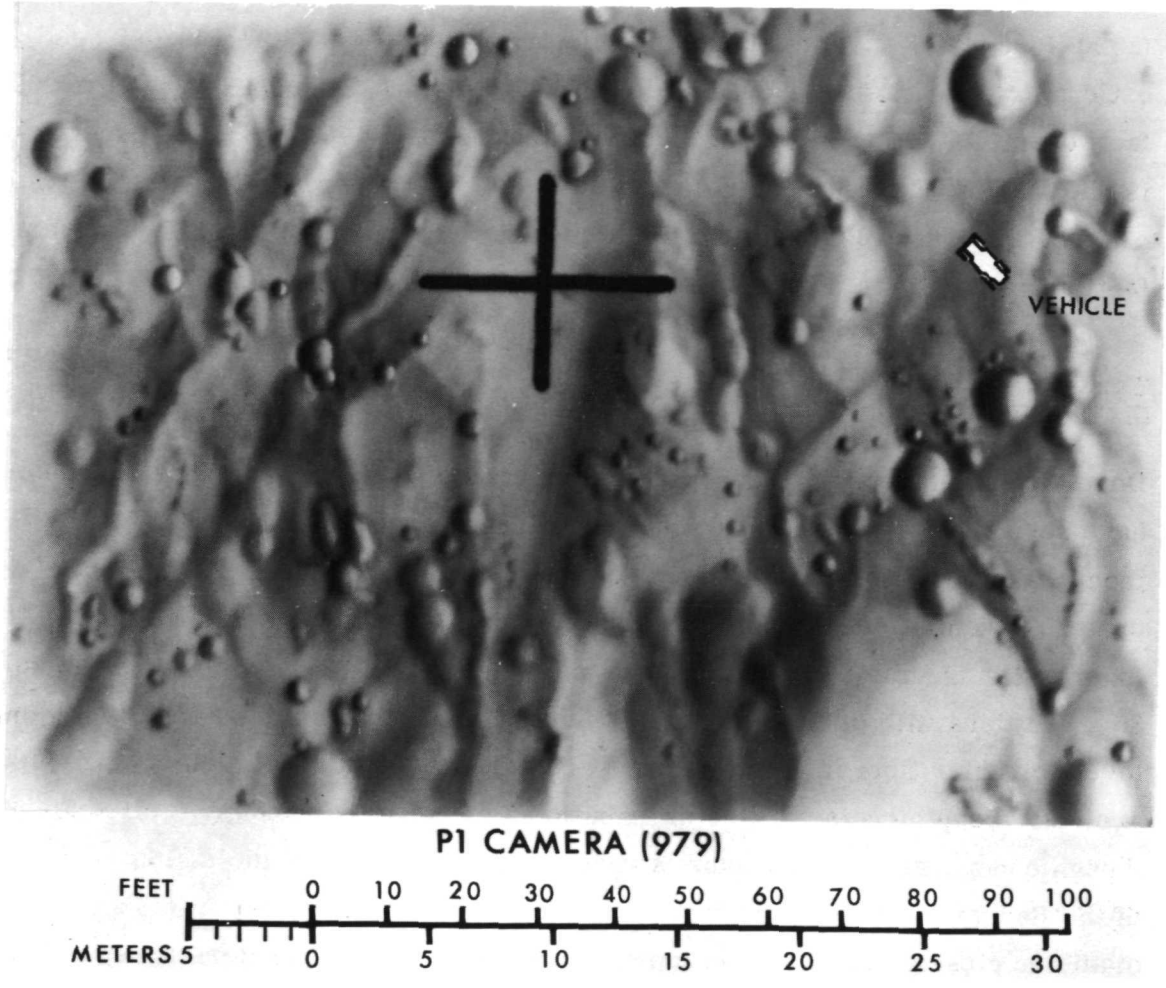

Figure 3-1. Map from P1 Camera - Ranger VII - Lunar Charts

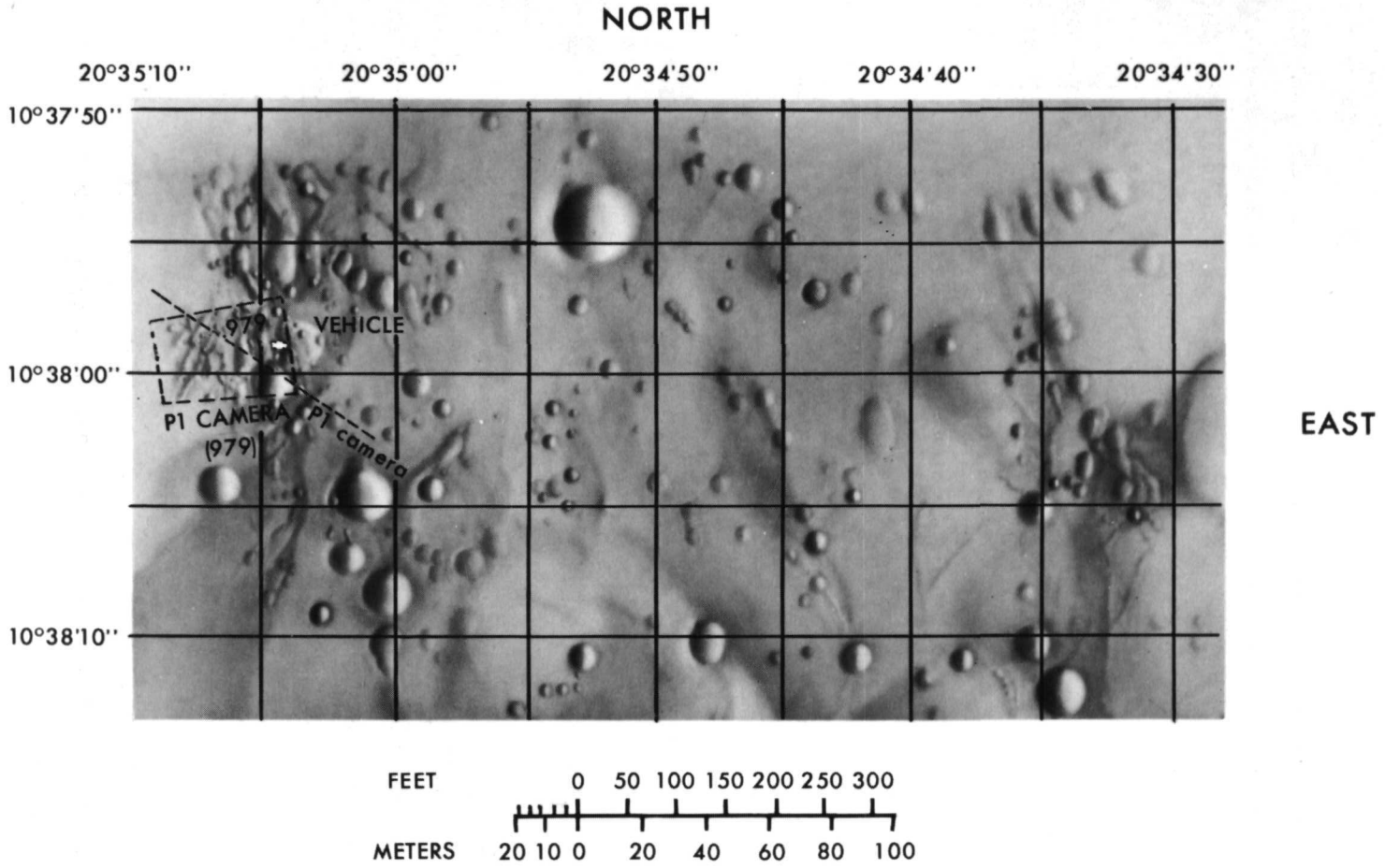

Figure 3-2. Ranger VII - Lunar Chart 5 - Sclae 1:1,000

At diameters less than 300 m (1000 feet) a type of shallow circular crater predominates. These craters are circular in plan but have low rounded rims and are shallower than the deep circular craters. This third type exhibits a complete sequence of crater forms down to craters so shallow and with such rounded rims as to be barely discernible.

A fourth type of crater is a new type discovered in the Ranger records - shallow depressions and dimple craters (Ref. 4, p. 10; Ref. 6, p. 50; Ref. 12, p. 108; Ref. 14, p. 143). The few unusual craters of this type are about 100 m (328 feet) across, with low, broadly rounded brims and rounded bottoms. In some of these craters the walls seem to steepen slightly, forming a funnel-shaped pit at the center. Only a few of these craters were seen. It is important that a vehicle operator avoid such craters because of the possibility that they may be susceptible of collapse. These areas may be recognized by their deeply shadowed centers.

Ranger photograph A-199 (see Figure 3-3) shows several types of craters.

3.1.2.5 Protuberances and Rocks. The scarcity of small surface bumps or isolated protuberances has been pointed out by all the Ranger VII experimenters (Ref. 4, p. 8). At least half a dozen craters have rock-like masses on their floors (Ref. 6, p. 50-51) which have been variously interpreted as remnants of impacting masses, as extrusive igneous masses (Ref. 6, p. 50), or as the result of slumping or landslide (Ref. 12, p. 108). The crater with the clearest evidence of rocklike protuberances is shown in Figure 3-3.

If the terrain of the Ranger VII area is typical of potential mare landing sites, a vehicle on the lunar surface would not need to lengthen its path appreciably to detour around boulders or protuberances greater than about 1 m (3 feet) in diameter. The rocklike masses that were identified lie within relatively deep craters that would be avoided by vehicles because of excessive slope.

Data are not yet available for predicting the number and size of smaller rocks below the limit of resolution of the Ranger photographs that would be obstacles to the passage

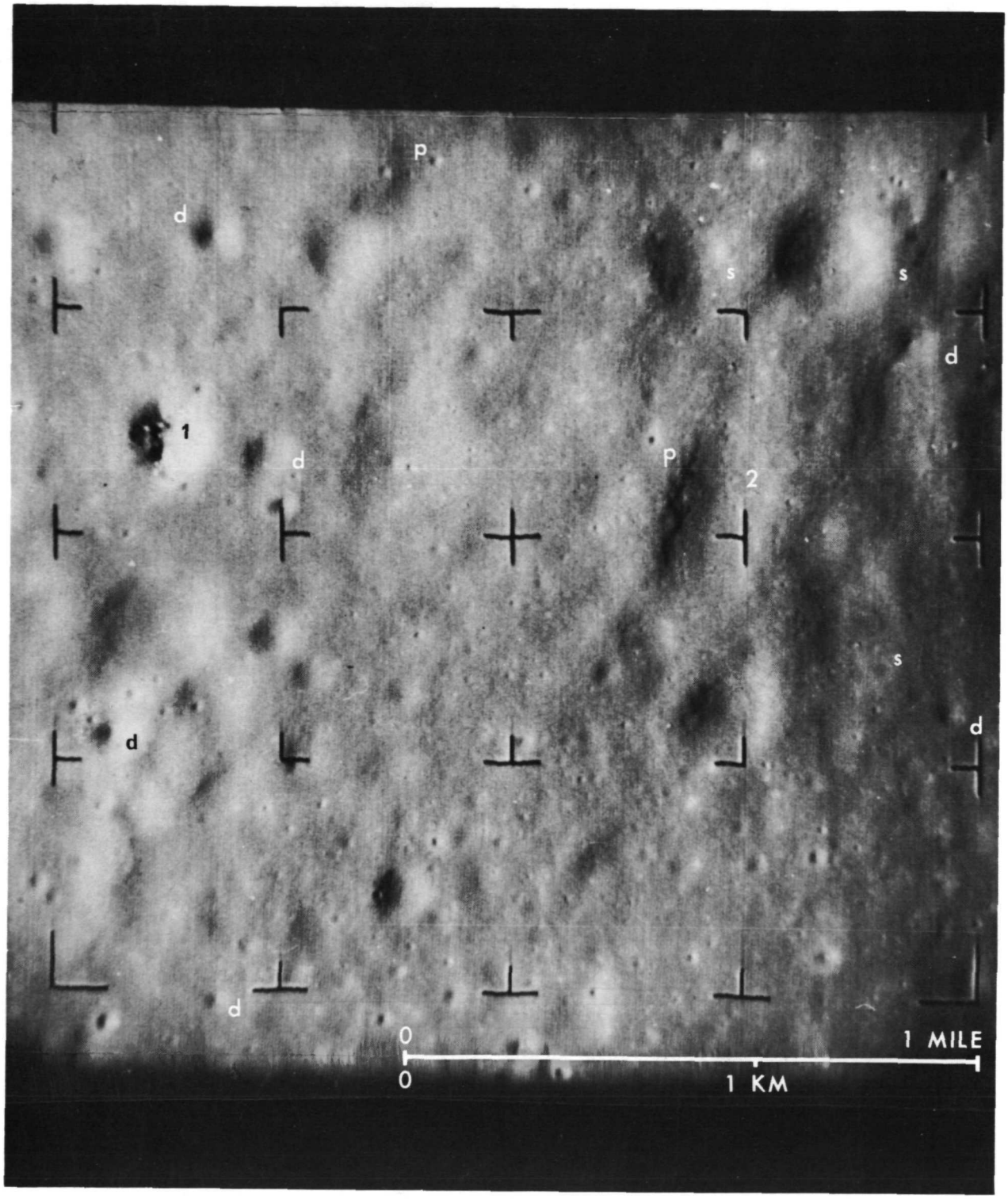

Figure 3-3. Ranger VII Photograph - A Camera, Photo 199

of vehicle wheels. In the "Additional Guidelines for the Army Vehicle Modification Study" (transmitted from NASA, 12 January 1966), under paragraph 2b, obstacle heights of 2.5-5.0 cm (1-2 inches) were suggested for use in estimates of multiple obstacle negotiation, though no guidelines were proposed for frequency of occurrence of obstacles.

3.1.3 Trafficability

3.1.3.1 Soil Description. Most of the debris on the lunar surface is composed of fragments of the rock that made up the original mare surface. The meteoritic material from outer space that impacts the mare surface constitutes only a minor component of the debris. Secondary impact of local particles that are set in motion by the primary meteoritic impacts provides the bulk of the debris. The chemical and mineralogic composition of the rock fragments is not known.

Beneath a thin veneer of finely pulverized rock powder (perhaps a few mm thick) the debris is probably composed of silt, sand, gravel, and cobble-size particles of angular shape. The average grain size is expected to increase with depth. Near the base of the debris, fragments may be several centimeters in diameter.

The thickness of the debris layer varies from a few tens of meters down to 1 mm, being thickest on the floors of the oldest and largest craters, and thin or absent along walls of very young craters that have cut through the debris layer. Between craters less than 100 m (328 feet) in diameter, the average thickness of the debris layer is probably between 1/2 and 1 m (1.64 - 3.28 feet). Also, it is highly probable that the underlying rock surface has considerable local relief.

In ray areas (see Figure 3-1) a layer of coarsely crushed rock may overlay the debris (Ref. 12, p. 132). The ray material appears to be essentially unconsolidated, probably similar to a mixture of dry sand and angular gravel.

3.1.3.2 Engineering Properties

General Statement

In the absence of direct information on the engineering properties of lunar surface materials, the following values for soil properties required for estimating vehicle performance are assigned. These values are presented in the ELMS model (Ref. 8, p 4-13), slightly modified in paragraph 2(d) of "Additional Guidelines for the Army Vehicle Modification Study" transmitted by NASA, 12 January 1966. The ELMS model, which was made to establish a baseline for determining vehicle requirements and evaluating the performance capabilities of proposed designs, was provided by NASA (Paragraph 5.1 of Work Statement).

Density

In the absence of actual data, interpretations by Shoemaker (Ref. 12, p. 131-132) are useful in estimating the density characteristics of lunar materials. These interpretations are backed up with experience based on cratering experiments. The following observations apply to a typical local area between rays on Mare Cognitum:

- The surface layer, a few mm thick, is a fragile open network of loosely stacked, very fine grains. The porosity is on the order of 90%.
- In the underlying debris, grain size probably averages less than a millimeter. Porosity decreases rapidly with depth, probably to less than 50% at depths of a few tens of centimeters.

Angle of Internal Friction

The assigned value of 32° for the angle of friction (ϕ) of lunar surface materials is a conservative value. For terrestrial dry sand, representative value of ϕ are as follows (Reference 13, p. 82).

	Round Grains Uniform	Angular Grains, Well-Graded
Loose	28.5°	34°
Dense	35°	46°

Lunar soil particles are not expected to be well-rounded nor of uniform size, and their ϕ values may well be greater than 32°.

Sinkage

Sinkage values for given soil conditions are directly related to values of soil deformation modulus, angle of internal friction, cohesion, and to wheel loading as applied. In the present study, such data are presented as given values (Table 3-2). Using these data and accepting soil cohesion as zero, absolute sinkage, both static and dynamic may be computed for lunar and terrestrial counterparts. In the case of static sinkage, a direct or straight line relationship exists between terrestrial sinkage and lunar sinkage in soils of similar properties which is directly proportional to equal footing area and a change to 1/6 gravity. Sinkage during vehicular motion (dynamic) is mildly complicated by the inclusion of forward compression as well as vertical compression. With equated soil values, a homogeneous soil and zero soil cohesion, terrestrial sinkage and lunar sinkage can be related on a first order basis.

As an example, the following is given:
where,

- Coefficient of cohesion (c) = 0
- Modulus of soil deformation due to cohesion (kc) = 0
- Angle of internal friction (ϕ) = 32°
- Modulus of soil deformation due to friction ($K\phi$) = 0.50
- Stratification induced factor, dimensionless (n) = 0.50
- Applied pressure (p) earth, (p^1) moon
- Sinkage (Z) earth, (Z^1) moon
- Area of footing, terrestrial and lunar = b

Formula:

- $p = (kc/b) + k\phi)Z^n$

  $p = (o/b + 0.5)Z^{\theta.5}$

  $p = 0.5\ Z^{\cdot 5}$

  $p^2 = 0.25\ Z$

  $Z = 4P^2$

- $p^1 = P/6$, therefore

  $Z^1 = 4\ (p/6)^2 = 4P^2/36$

  $Z^1 = P2/9$

  $Z^1 = \frac{Z}{36}$ moon sinkage $= \frac{1}{36}$ earth sinkage

Table 3-2

ENGINEERING PROPERTIES ASSIGNED FOR LUNAR MARIAL SOIL

	Kø	ø	n	c	Kc	
1.	0.05	20°	1.0	0	0	Assigned in 12 Jan "Additional Guidelines" 2(d) for use in drawbar-pull vs weight ratios for "worst case" to provide indication of vehicle capability-limitation range.
2.	0.5	32°	0.5	0	0	Given in ELMS for soils on slopes from 0° to 4°. Also specified for drawbar-pull vs weight ratios.
3.	1.0	32°	0.75	0	0	Given in ELMS for soils on slopes 5° to 7-1/2°.
4.	3.0	32°	1.0	0	0	Given in ELMS for soils on slopes 10° to 20°. Also specified for drawbar-pull vs weight ratios.

Kø - Modulus of soil deformation due to frictional ingredients of soil $(lb/inch)^{n+2}$

ø - Angle of friction (between soil grains), degrees

n - A dimensionless factor reflecting stratification of soil

c - Coefficient of soil cohesion, psi

Kc - Modulus of soil deformation due to cohesion ingredients of soil $(lb/inch)^{n+1}$

3.1.4 Detours

Time required for point-to-point vehicle travel will be increased above that estimated for straight-line distances by the need to make detours. Detours will be required to avoid the steep slopes of the few deep craters, to find low slope angles for crossing ridges, to avoid obstacles and potentially hazardous areas such as "dimple" craters.

Air Force Ranger VII Lunar Chart 5 was analyzed to derive an estimate of the average excess distance that may be required to include detours. On the map showing effective coverage at 1:1,000 scale, 10 random traverse lines were drawn. A map measurer was used to find the difference between the straight line distances and the lengths of traverses that detoured around the craters shown on the chart. (To be conservative, detours were made around craters than could probably be crossed by the vehicle in addition to the steep-sloped craters.) From the comparisons made on the 1:1,000 scale chart (Figure 3-2), the average excess distance required by detouring along the 10 lines is 6.8 percent, (ranging from 0 percent to 12 percent).

To check this estimate, which seems low, analysis was made of the small map, scale 1:350, that covers the area of the last photograph from the P1 camera (Figure 3-1). Although the area covered is very small - 48 by 33 meters (157 by 109 feet), the scale of this map reveals the greatest amount of detail of the available lunar maps, and it includes craters smaller than are shown at the 1:1,000 scale. Detours around features shown at this scale require an average increase in distance traveled of 23.7 percent (ranging from 12 to 38 percent) increase over straight-line paths.

The area covered by the last P1 camera photograph happens to be within a ray area, and the relief is more rugged than in marial areas not covered by rays. Rays occupy a relatively small part of most marial areas, however, and the relative percentages must be weighted.

An additional factor to consider is the probable need of detours to avoid obstacles too large to drive over but too small to show in Ranger photographs. Although quantitative evidence is not available, the detour allowance should provide obstacle avoidance.

Thus, an average detour allowance of 20 percent is suggested for distances to be travelled by a vehicle in excess of straight line distances. This figure takes into consideration the lack of "vehicle-scale" detail on the 1:1,000 map, and the fact that the area shown on the more detailed map covers an area typical of only a small part of the lunar maria surface areas, and it includes a safety factor for obstacle avoidance.

3.2 Terrestrial Terrain Analog

3.2.1 Analog Area Discussion

The Yuma Proving Ground near Yuma, Arizona, has been the terrestrial surface area selected for analogous comparison purposes for two reasons. These are that (1) the M-274 vehicle received extensive field testing on these grounds and (2) desert terrain and soil materials characteristics most closely resemble the accepted lunar soil criteria (See Figure 3-4). Specific terrain features and soil properties encountered are discussed below. Comparison analysis of lunar and terrestrial terrain and soil values are discussed under paragraph 3.1.3.

3.2.2 Topography

3.2.2.1 Slopes. The proving grounds are characterized by a low rolling topography. Dry washes are found but occur infrequently. Slopes vary from very flat up to 30°. Most often slopes vary from horizontal to 20° with the majority below 15°.

3.2.2.2 Walls. Implied in this term are very steep slopes. In the proving grounds these occur at the limiting borders of the washes. Composed of water-incised soil banks, they vary in height from a few inches to several feet. The majority are below

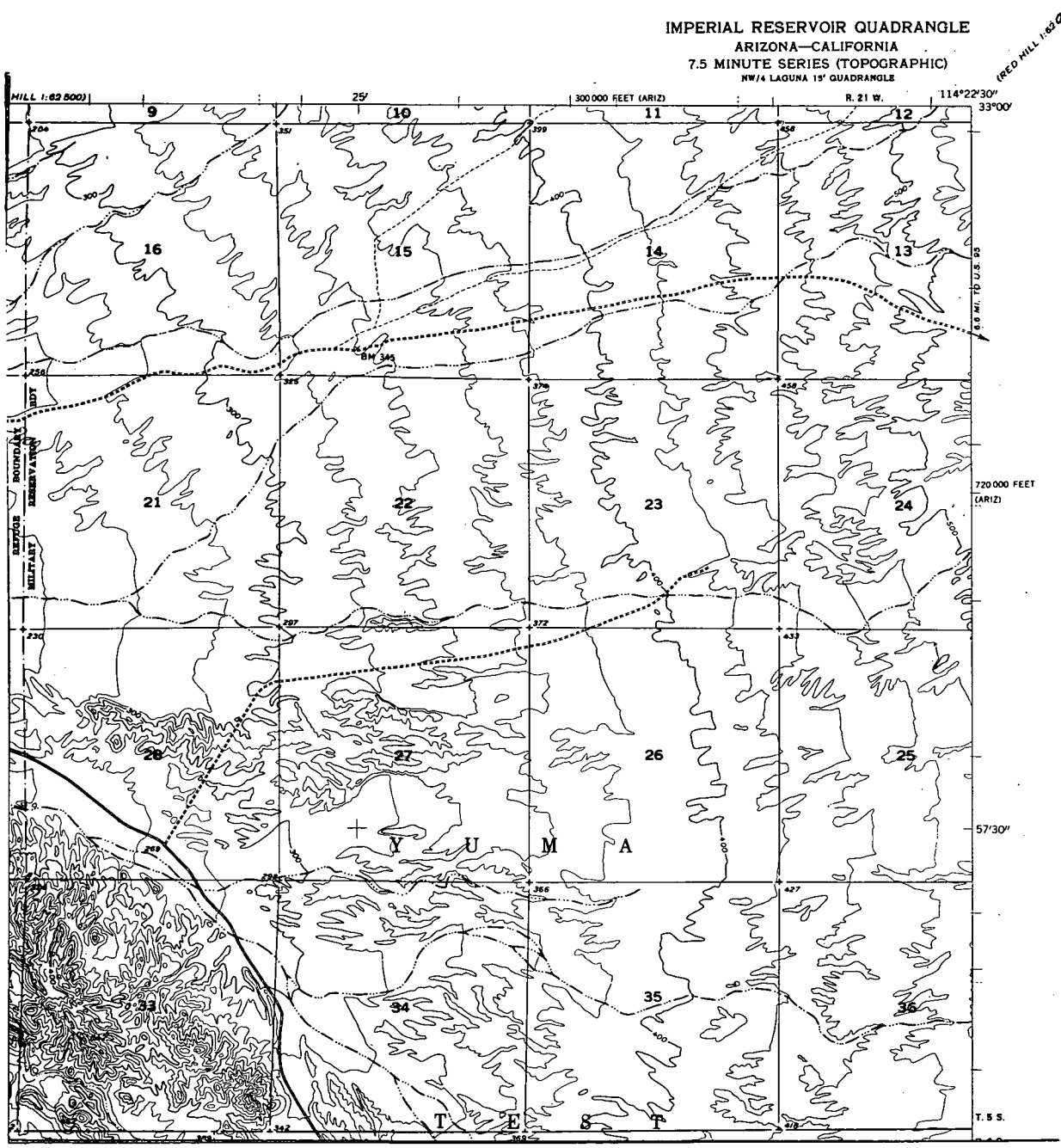

SECTIONS ARE ONE MILE SQUARE, APPROXIMATELY; CONTOUR INTERVAL 20 FEET

Figure 3-4. Typical Map - Area of Yuma Proving Ground

twelve inches. Steep-angled walls tend to retain their character due to the infrequency of rainfall or water flow. However, the soil crumbles or sloughs easily under wheel loading.

3.2.2.3 Crevasses. Defined as long but relatively narrow voids in the surface material, such features usually require high strength, rocklike materials both for genesis and retention. Neither characteristic is typical of the proving ground. The closest any surface phenomena come to resembling such a feature in this selected area is in narrow reaches of the washes. Characterizing features are low walls, shallow bottoms and short length.

3.2.2.4 Craters. This feature is defined as basins having raised rims with the central depression resting significantly below the surrounding average terrain elevation. No naturally occurring blast craters are characteristic of the proving ground. However, the rolling nature of the terrain allows for reasonable simulation of real craters. This can be accomplished by utilizing two features, (1) traverse across closely spaced parallel or near parallel ridges or (2) traverse across circular depressions created in the windblown sand soils.

3.2.2.5 Protuberances. Protuberances are defined as large or small, generally isolated, high density obstacles to vehicular movement. On the average, few such occur on the proving ground because of the geologic origin of the materials which were brought in and deposited by river flow deposition. In selected areas, sand removal by wind action has concentrated cobbles and gravel at the surface, a phenomena known as "desert pavement". However, where the proving grounds vehicle test areas border on hilly rock exposures such features can be found. In these areas vehicular traffic can circumnavigate such objects either with ease or with only moderate detours. Only outside the selected analogous area are obstacles a serious terrain phenomena.

3.2.3 Trafficability

3.2.3.1 Soil Description. Soil varies between the gross values of sandy silty gravel and sand with low admixture of silt and gravel fragments (Ref 10). Laboratory soil analyses show: (1) Sp, 98% sand, 2% fines, (2) Gp, 62% sand, 31% gravel, 7% fines. Sand-sized particles are rounded to semi-rounded. Gravel is angular to semirounded. Fines are mostly silt. During summer months (test period) water content of surface soil was less than 5%.

3.2.3.2 Engineering Properties (1) (3) (9) (16).

- Average undisturbed density: 1682 kg/m^3 (105 lbs/ft^3)
- Wheel track density (same soil): 1906 kg/m^3 (119 lbs/ft^3)
- Estimated angle of internal friction: 30° - 45°
- Sinkage:

This soil reaction is related both to the observed soil values and to (1) tire size (7.50 x 10); (2) tire pressures (12, 10 and 8 psi); (3) and total vehicle load (1900 lbs). Test records indicate that at minimum density 1281 kg/m^3 (80 lbs/ft^3) and all slopes above 5°, 5.08 cm (2 inches) of sinkage would occur before forward movement would occur. Sinkage on slopes below 5° did not cause significant change in vehicle operation and was not recorded.

- Slippage

Defined as tire rotation in excess of surface speed, slippage was found to be related to tire pressure, power applied, selected minimum soil density (1281 kilogram/$meter^3$ or 80 lb/ft^3) and to road speed.

Slippage varied as follows:

Tire Pressure	Gear Ratio	Slippage Variation		Speed Range
552 mb* (8 psi)				
	1st low	77 to 9%		1.45-6.60 km/hr (0.9-4.1 mph)
	2nd low	15 to 6%	as compared to	4.67-10.5 km/hr (2.9-6.5 mph)
	1st high	15 to 12%		4.83-8.69 km/hr (3.0-5.4 mph)
690 mb (10 psi)				
	1st low	76 to 6%		1.45-6.60 km/hr (0.9-4.1 mph)
	2nd low	28 to 14%	as compared to	4.02-9.81 km/hr (2.5-6.1 mph)
	1st high	18 to 13%		4.83-8.64 km/hr (3.0-5.7 mph)
827 mb (12 psi)				
	1st low	80 to 9%		1.93-7.72 km/hr (1.2-4.8 mph)
	2nd low	29 to 10%	as compared to	3.54-10.3 km/hr (2.2-6.4 mph)
	1st high	19 to 13%		4.83-8.64 km/hr (3.0-5.7 mph)

*millibar

3.3 Terrain Comparison

3.3.1 Introduction

The purpose of comparing the concept of lunar terrain with its selected terrestrial analog is to make use of the terrestrial testing and experience record of the army vehicles, whose potential lunar capabilities are being evaluated in this study. In order to do this, the terrestrial analog selected was chosen from a test area for the Mule vehicle which has many characteristics of lunar terrain.

The topography and the engineering properties of soils that influence vehicle mobility are comparable, item by item, for the two environments. Based on analysis

of the degree of similarity, or dissimilarity, of the significant features, an evaluation is made of the degrees of applicability of terrestrial experience to prediction of lunar vehicle capability.

3.3.2 Topography

3.3.2.1 Slopes. In a large part of the Yuma Proving Ground the topography is gentle and the relief is low, comparable with that of the lunar terrain model. The two landscapes probably differ greatly in their general aspect because the lunar terrain has been sculptured by random cratering which creates circular effects and softened by the covering debris, whereas the Yuma landscape retains the more angular outlines characteristic of surfaces that are developed on horizontally stratified deposits. Terrestrial terrain is shaped by the processes of rock weathering, erosion, and deposition, through the action of water flow and wind. The results of these processes are lacking on the moon which has neither an atmosphere nor a hydrosphere. Regardless of their genesis, the slopes in the two regions are comparable quantitatively. Traverses with the slopes specified for the lunar model (Table 3-1) can be laid out on the Yuma Proving Grounds. Steeper slopes are also found at the Yuma Station, so the range of slopes at the terrestrial analog not only covers, but appreciably exceeds, the range of slopes to be expected on the lunar landing area.

3.3.2.2. Walls. The walls that have been reported in some lunar areas are not expected to be encountered in the marial landing areas. Neither would there be low walls in the lunar landscape like those described at the Yuma test site, because the moon has no streams to erode channels in the debris. Therefore, the question of how steep or how high a wall can be ascended or descended is not critical for the present study. If, contrary to expectation, a wall should be encountered on the lunar traverse, the wall will have to be detoured, thus limiting the total area that can be explored.

3.3.2.2 Crevasses. Because the presence of crevasses implies a hard rock surface, crevasses are not considered in the present study. In both the lunar surface model and the Yuma test area the surface and shallow subsurface materials are fragmented and particulate.

3.3.2.4 Craters. Craters present the major problem in matching lunar and terrestrial terrain models. Impact craters are the dominant topographic feature on the moon and they are entirely missing from the Army vehicle test areas. However, wind or water eroded depressions on the Proving Grounds have slopes similar to those of the very shallow, nearly obliterated craters on the marial lunar surface. Intermediate slopes of crater walls are duplicated in the terrestrial analog area by slopes of ridges. Craters with steep slopes and craters whose bottoms cannot be clearly seen by the vehicle driver should be avoided by detouring.

3.3.2.5 Protuberances. The lunar terrain model and the comparable part of the Yuma Proving Grounds are alike in the scarcity of boulders or rock protuberances.

3.3.3 Trafficability

3.3.3.1 Soil Description. In both the lunar surface model and the selected terrestrial analog, the surface material is particulate. The size gradation of the two materials are similar, according to the best estimates of the lunar debris gradation. In the Yuma Proving Ground area, the sand-size particles are rounded to semirounded, and the coarser fragments are angular to semirounded. Lunar materials have been reworked, particularly the surface layers, by continuous impact, but the degree of rounding should be much less owing to the lack of abrasion by wind and water transportation.

The greatest difference between lunar and terrestrial soils of similar particle size and gradation is the complete lack of pore pressure which is such an important factor in determining the engineering properties of soils. Also, the lack of gas or liquid films on soil particles in the ultra-low pressure environment of the moon may result in some degree of inter-particle adhesion, particularly of small particles.

A factor to be considered in regard to the subject of soil particle adhesion is the possibility of equalizing cohesive properties in the lunar soil as compared to those operative in the terrestrial soil. As stated, some degree of lunar soil particle

adhesion may occur due to vacuum welding. In the terrestrial soil, a similar effect occurs which is related to the properties of the natural water film adhering to the individual soil particle. Such adhered water is the essential reason for cohesion observed in a typical soil mass and is present even in soils considered as "dry, cohesionless." In comparing the hypothetical moistureless lunar soil and a typical "dry" sand, it is probable that the soil mass cohesion for both soils is similar in absolute magnitude.

3.3.3.2 Engineering Properties. A comparison of engineering properties for the two soil types selected may best commence with a brief resume' of their assumed similarities. They are both granular; largely devoid of moisture; predominantly containing angular particles; and for their gravity field, moderate to high in porosity and having low to zero cohesion. Also, disregarding their respective gravitational fields, each will probably react similarly to pressure, particularly confining pressure, i.e., at any given density, compacting pressure similarly applied will result in similar resultant higher densities.

Engineering properties showing dissimilarities can be related to mode of formation. In the case of the lunar soil, less soil layering and consequent abrupt vertical change in density can be expected than in the terrestrial analog. Natural in-place densities, a reflection of gravitational differences and depositional modes, will be significantly lower in the undisturbed lunar soil. The convenient assumption of zero cohesion removes the necessity of a discussion based on mineralogic differences. Finally, those fines sized below a 200-mesh sieve are of significant shape difference. Terrestrial soil fines tend to be flake-like, a reflection of their secondary mineral origin. Lunar fines, reflecting their primary mineral crystal habit, will tend to be non-flakey, angular in shape. Dependent on the individual soil-fines content, the equivalent terrestrial soil will exhibit properties showing tendencies toward a lower soil strength. This is a reflection partly of certain mineralogic constituency (slipperiness) and partly of dynamic orientation of flakey grains in parallel or near-parallel to the direction of externally applied pressure.

3.3.4 Conclusion

Though the lunar landscape will not look like the Yuma Proving Grounds to a vehicle driver, the slopes to be negotiated by the vehicle and the materials over which the vehicle must pass are believed to be similar insofar as they affect vehicle mobility. (See Figs. 3-5 thru 3-8.)

Impact craters, which are dominant features on the moon, are lacking on the terrestrial analog test area. The slopes that the vehicle will be required to traverse, however, in crossing most craters are duplicated on the test area. Deep craters with steep walls are relatively few and lunar traverses can avoid them by detouring. Steep walls, crevasses, and rocky protuberances are not believed to be characteristic of marial lunar areas nor of the part of the Yuma test area that has been selected for the terrestrial analog.

In composition, the assumed surface lunar soils and the soils at the Yuma Proving Grounds have much in common. Both are particulate materials, with sand-sized particles predominating and with varying amounts of gravel and silt. Both soils are dry. A significant difference is the pulverized rock powder that may cover the lunar surface but this very fine material is believed to be a veneer over coarser granular material. The granular particles on the lunar surface are less rounded and not as well sorted as the particles of the terrestrial analog soils.

Until the engineering properties of lunar soils can be observed and measured, truly valid comparisons cannot be made. To allow for the factors of lunar versus terrestrial soil behavior that cannot be compared at the present state of knowledge, the assigned soil values are conservative with appreciable margins of safety.

The known and assumed properties of terrestrial and lunar soils, respectively, will probably impart a similar reaction to cross-country vehicle movement, as a direct line function of the gravitational differences. There is, in this assumption, an acceptance of the influence of the stated soil differences as minor factors, i.e., not introducing major differences in soil reaction to trafficability.

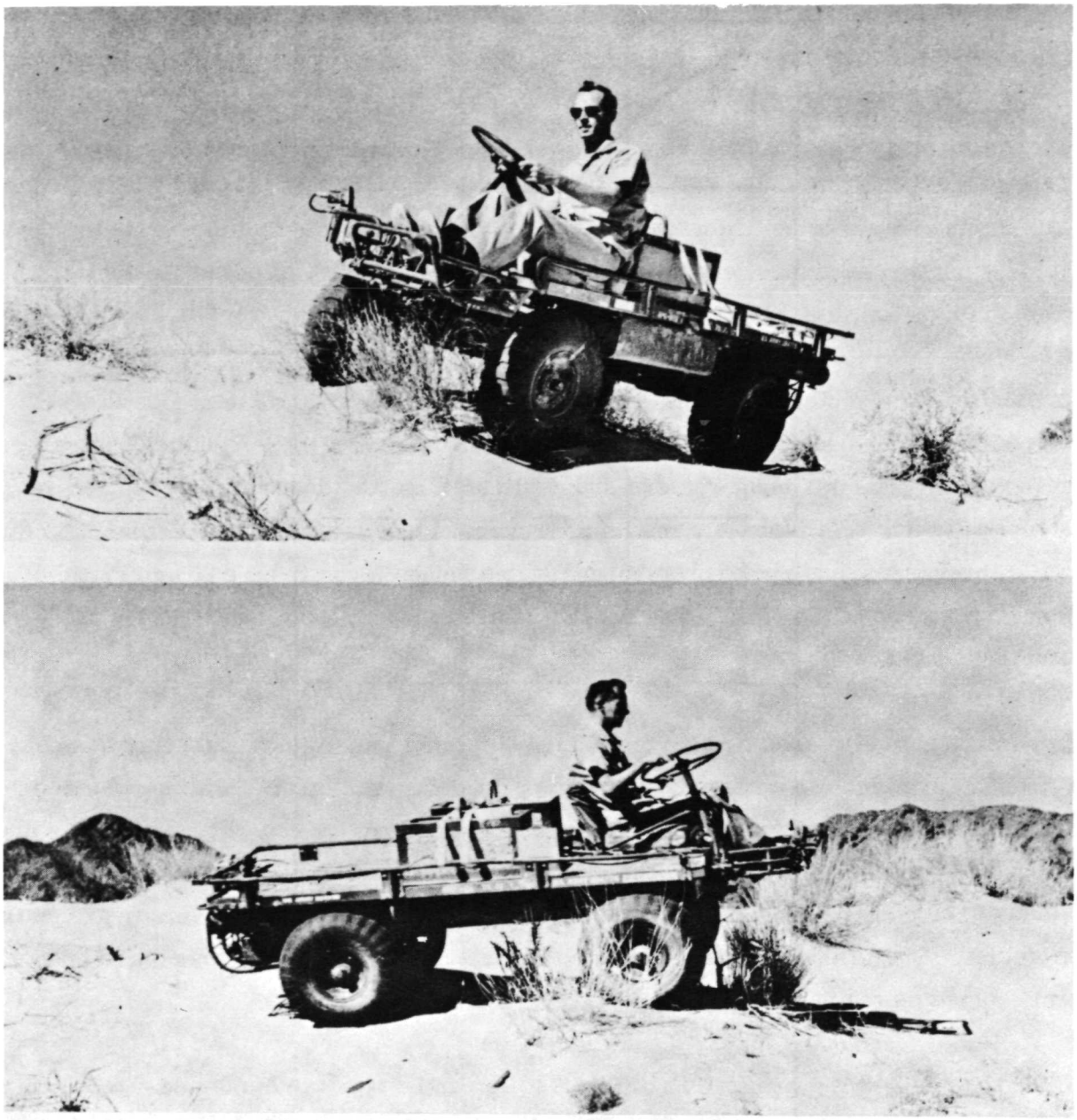

TYPICAL OPERATION OVER SAND PLAINS

YUMA PROVING GROUNDS -- M274 TEST OPERATIONS

Figure 3-5. Yuma Proving Grounds - M-274 Test - Sand

Figure 3-6. Yuma Proving Grounds - M-274 Test - Stoney Desert

Figure 3-7. Yuma Proving Grounds - M-274 Test - Dry Washes

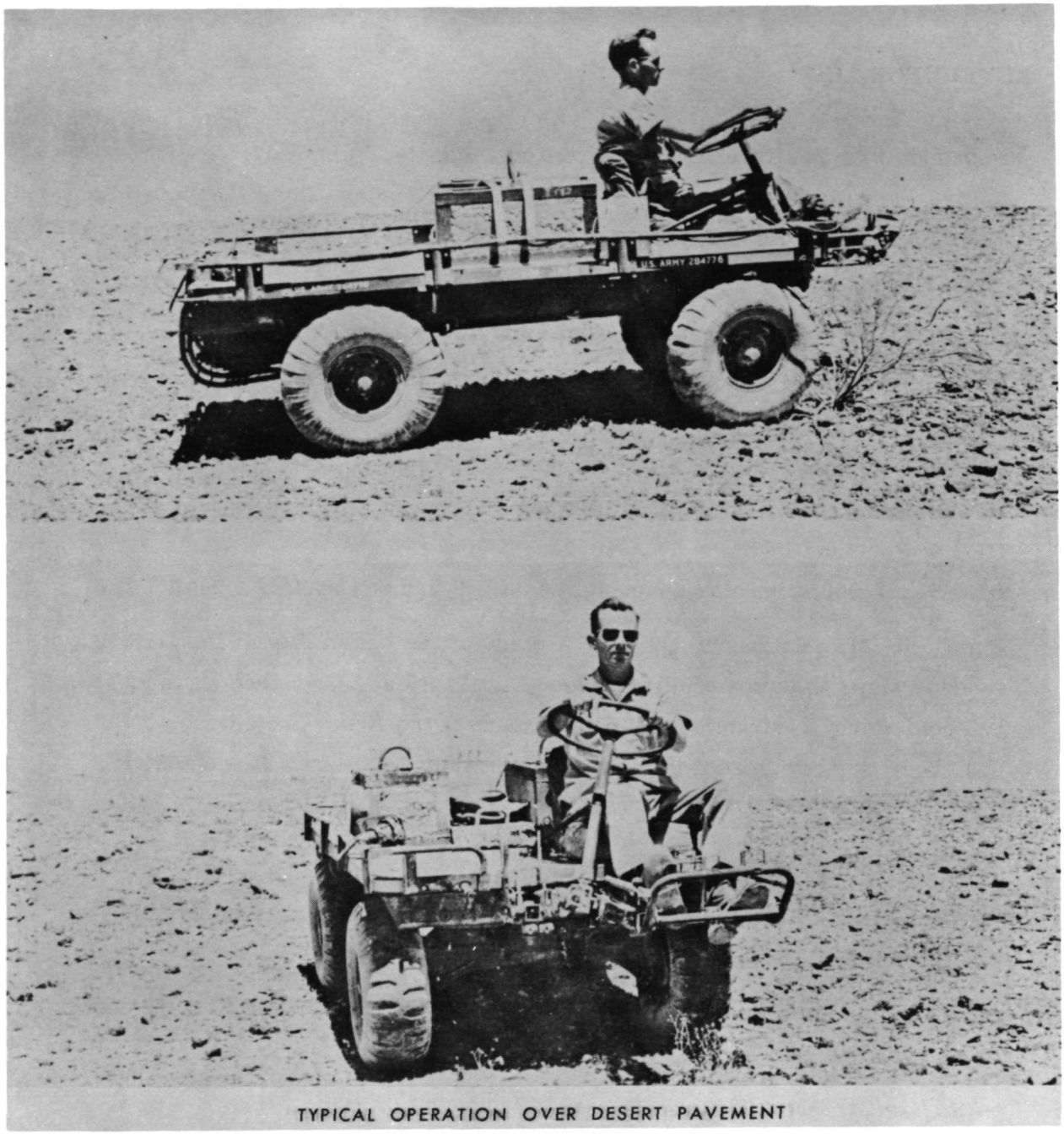

TYPICAL OPERATION OVER DESERT PAVEMENT

Figure 3-8. Yuma Proving Grounds - M-274 Test - Desert Pavement

3.4 REFERENCE LIST

3-1 Aberdeen Proving Ground, Ordnance Test Activity, Yuma, Arizona, "Automotive Test Division Report on Desert Test of Carrier, Light Weapons Infantry, 1/2 ton, M-274," Report No. OTA/IT-5065/2, ASTIA-AD226 902, September 1959.

3-2 U. S. Air Force, "Aeronautical Chart and Information Center," Ranger VII Lunar Charts," RLC 1 through 5, dated 1964:

RLC 1	Mare Cognitum	1:1,000,000
RLC 2	Guericke	1: 500,000
RLC 3	Bonpland H.	1: 100,000
RLC 4	Bonpland PQC	1: 10,000

RLC 5 1:1,000 and areas covered by last 2 P camera photographs at 1:350

3-3 Bunch, H. M., Robinson, C. G., "A Study of the Feasibility of Developing Overlay Maps to Indicate Performance Capabilities of Ordnance Equipment In Selected World Environments," Department of the Army Project No. 598-09-004, Southwestern Research Institute, San Antonio, Texas, June 1962.

3-4 Experimenter Team for Ranger VII, "Preview of Scientific Results: NASA-JPL," Technical Report 32-700, 1965

3-5 Heacock, R. L. 1965, "Introduction: NASA-JPL," Technical Report No. 32-700.

3-6 Kuiper, G. P., "Interpretation of Ranger VII Records," NASA JPL Technical Report No. 32-700, 1965.

3-7 NASA, Jet Propulsion Lab, "Ranger VII," 1964 and 1965:

Part I Photographs (Camera "A" series; Camera "B" series, Camera "P" series).

Part II Experimenters' Analyses and Interpretations, Technical Report No. 32-700 (Individual contributions are listed under the authors' names).

3-8 NASA, John F. Kennedy Space Center, "Engineering Lunar Model Surface (ELMS), Launch Support Engineering Division, Future Studies Branch, TR-83-D, by Masor, R. L. McCombs, W. M. and Cramblit, D. C., 1964.

3-9 Office, Chief of Ordance, Technical Information Report 11-2-1A1 (3), "Development of 1/2 ton 4 x 4 Infantry Light Weapons Carrier M-274 XM 274 Mechanical Mule," April 1960.

3-10 Shamburger, J. H., Waterways Experiment Station, Leighty, R., Cold Region Research & Engineering Laboratories, Army Material Command (data informally obtained), "Soils Data" (In-place density and solid gradation curves) on Yuma Proving Ground courses for Project Otter (Overland Train Terrain Evaluation Research), January 1966.

3-11 Schurmeier, H. M., Heacock, R. L., and Wolte, A. E., "The Ranger Missions to the Moon," Scientific American, Volume 214, No. 1, p.52-67, 1966.

3-12 Shoemaker, E. M., "Preliminary Analysis of the Fine Structure of the Lunar Surface," NASA-JPL Technical Report No. 32-700, 1965. (p. 75-134)

3-13 Terzaghi, Karl and Peck, R. B., "Soil Mechanics and Engineering Practice," John Wiley, New York, 1948.

3-14 Urey, H. C., "Observations on the Ranger VII Photographs," NASA-JPL Technical Report No. 32-700, 1965. (p. 135-148)

3-15 Whitaker, E. A. "Further Observations on the Ranger VII Records," NASA-JPL Technical Report No. 32-700, 1965. (p. 149-154)

3-16 Yuma Proving Grounds Report 4030, Report of USATECOM Project No. 1-3-4090-70, "Product Improvement Test of Truck Platform, Utility, 1/2 ton, 4 x 4, M-274 (274A1) with A042 Engine Under All Season Desert Conditions," DDC-44-369, July 1964.

GLOSSARY

DEFINITION OF TERMS

AAP	Apollo Applications Program (formerly AES-Apollo Extension System). A concept for continuing exploration of the Moon and near-earth space through maximum utilization of the existing Apollo hardware.
Bekker Soil Values	Expressions of soil characteristics in parametric values utilized to determine soil-vehicle relationships in evaluation of a vehicle's mobility in soils by methods proposed by M. G. Bekker in numerous publications.
CM	The Apollo Command Module
Constraint	A general guideline which must be followed in the study.
Criteria	Complete instructions for the conduct of a task.
ELMS	Engineering Lunar Model Surface. A document prepared by NASA-MSFC which defines a relationship between lunar surface soil characteristics and surface slopes. It also establishes a distribution of soil characteristics and slopes with distance for traverses on the maria surfaces.
LEM	The Lunar Excursion Module of the Apollo program.
LEM/S	The Lunar Excursion Module modified into a shelter-laboratory consisting of a modified LEM ascent stage delivered unmanned to the lunar surface by a modified version of the LEM descent stage.
LEM-Taxi	A modified version of the LEM which is used to transport two astronauts to and from the lunar surface in conjunction with AAP mission.
LSSM	Local Scientific Survey Module. A surface roving vehicle designated to furnish transportation and power for carrying and emplacing scientific experiment packages.
Lunar Flying Vehicle	LFV—or "lunar hopper" is a system designated to act as an abort capability from a surface vehicle or a transportation adjunct vehicle.

MTBF	Mean Time Before Failure. Utilized in derivation of cumulative test times necessary to demonstrate reliability.
Mission	Those experiments specified to be performed at a particular location within a designated time period.
Mobility System	A roving vehicle or a flying vehicle or a combination of vehicles to provide transportation on or over the lunar surface for one or more astronauts and experiment package cargo.
Module	A discrete embodiment of all or a portion of the equipment required for performance of a specified function.
Payload	The aggregate of equipment and supplies to be delivered by a hardware transportation unit.
PLSS	Portable Life Support System, personal life support pack utilized by astronaut in space suit.
Radiator	Exchanger for rejecting excess heat by means of radiation to space.
Radius	Maximum radial distance for LEM/S permitted on a vehicle traverse.
Sink	A body (deep space) utilized for the disposal of heat in a thermodynamic process.
Structure	Refers to the vehicle chassis and structural frame.
Super Insulation	Multilayer insulation, such as Linde SI-44 which consists of alternate layers of aluminim foil and submicron glass fiber paper (35-70 alternate layers) with intervening spaces evacuated of atmosphere to a low order of pressure.
Traverse	An excursion over the lunar surface in a vehicle for the purpose of conducting scientific experiments or of emplacing scientific packages on the lunar surface.

SYMBOLS AND UNITS

$\mathring{A}$	Angstroms, unit of length, equal to 10^{-10} meters.

A	Area, square meters or square centimeters.
Bar	Unit of pressure, 10^5 newtons/meter^2
C	Calorie, unit of thermal energy, see J, below.
C_p	Specific heat, such that
	C_p J expresses the proper MKS units of Joules per kilogram.
c	Coefficient of soil cohension, lbs-force/in^2.
D	Diameter, meters or centrimeters.
d	Infinitesimal differential operator
E	Energy, Joules or watt hours.
erg	Unit of energy, 10^7 ergs equals one joule.
e.v.	Electron-volt, unit of energy, 6.24×10^{18} ev equals one joule.
$^\circ$F	Degrees Fahrenheit.
g	Acceleration due to gravity.
J	Mechanical equivalent of heat, 4186 joules per kilogram calorie.
Joules	Unit of energy (MKS) or newton-meter.
$^\circ$K	Degrees Kelvin.
K_c, k_c	Modulus of soil deformation governed by cohensive character of soil (lbs-force)/(inch)$^{n+1}$.
$K\phi$, $k\phi$	Modulus of soil deformation governed by internal frictional character of soil (lbs-force)/(inch) $^{n+2}$
Kg	Kilogram, basic MKS unit of mass.
km	Kilometer, unit of distance, 1,000 meters.
L	Length, meters or centimeters.

M	Mass, kilograms or grams.
$\dot{M}$	Time derivative of mass, mass rate per unit time, kilograms per second.
m	Meter, basic MKS unit of length.
n	Exponent parameter governed by soil characteristic, applied to sinkage in sinkage-soil load function, stated to reflect soil stratification, see Bekker Soil Values.
n	Newton, MKS unit for force.
p	Pressure, bars.
Q	Energy content, joules
$\dot{Q}$	Time derivative of energy or power, joules/second or watts.
r	Radius, in meters or centimeters.
s	Distance, in meters.
T	Temperature, absolute scale, in degrees K (or as stated).
t	Time, seconds, minutes, or hours.
v	Velocity, meters/sec or kilometers/sec.
w	Mass flow rate, kilograms/second
z	Deformation of soil, in the Bekker Soil Values, expressed as inches.
α , a	Alpha, absorptivity of solar radiation, decimal fraction of incident radiation absorbed at body temperature.
ϵ , e	Epsilon, emissitivity, decimal fraction of theoretical black body radiation radiated at body temperature.
η	Eta, efficiency.
θ	Theta, angle between normal to a surface illuminated by solar radiation and the incident propagation path.

μ	Mu, viscosity, poise or centipoise.
π	Pi, the number of radians in 360 degrees of arc.
ρ	Rho, density, kilograms per cubic meter, or grams per cubic centimeter.
σ	Sigma, Stefan-Boltzmann constant, 5.71×10^{8} watts/m^2 $^{\circ}K^4$
ϕ	Phi, angle of internal friction, in non-cohensive soils generally regarded as equivalent to angle of repose.
ϕ	Phi, flux, solar radiation flux, watts per square meter.
ϕ_s	Incident solar radiation flux.
ϕ_r	Reflected solar incident radiation flux.
Ψ	Psi, fluid transport modulus.